Author's Response

Dear Dr. Jack Middelburg,
thank you very much for taking our manuscript into further consideration for publication in Biogeosciences.

We have carefully revised our manuscript following your suggestions and we include below:

- our point-by-point answers to the two Referees including the detailed discussion of the major and minor comments, and (marked in color) the actual modifications made on the manuscript for each point;
- a marked-up version of the manuscript.

We look forward to your response.
Best regards,
Elisa Lovecchio

Answer to Referee #1

We thank Referee nr.1 for the time spent on reviewing our manuscript and for his/her thoughtful comments that have helped us to better understand the role of our small detritus pool and the sensitivity of our results with regard to our treatment of organic matter. This will improve the quality of our manuscript. We include below our detailed answers to all the raised questions/comments.

Answers to Major comments

Major Comment nr.1:
The NPZD model is very simple which is not a problem by itself. It performs enough well to be suitable for that study. This is quite clearly shown in the validation section of the paper. However, according to me, it lacks a critical reservoir especially concerning the objectives of that study: DOC or more precisely semi-labile and semi-refractory DOC. Concentrations of semi-labile DOC range from typically 20 to 40 umol/L in the upper ocean (Hansell et al., 2009; Hansell and Carlson, 2014). Its lifetime is also quite long and ranges from weeks to years which makes it possible for that pool to be transported far away from its production region. It has been shown to potentially play an important role in the subtropical gyres (e.g., Roussenov et al., 2006; Torres-Valdés et al., 2009). In the present study, this pool is omitted and thus, a potentially large contribution to the lateral export of organic carbon is not represented. This needs at least to be discussed in the discussion section.

Answer to MC1:
As correctly stated by this reviewer, our NPZD model does not include an explicit DOC pool, which at first sight could be considered as a serious shortcoming given the potentially substantial contribution of DOC to the lateral transport of organic carbon. However, our model includes, in addition to the standard pool of fast sinking (large) particulate organic carbon (Large Detritus, LDet), also a pool of very slowly sinking particles (Small Detritus, SDet). Given its sinking speed of 1 m day^{-1} SDet represents essentially a suspended POC pool. Thus, this pool has some similarity to a (semi-refractory) DOC, particularly regarding its susceptibility to being subject to strong lateral transport. The important difference is that SDet coagulates to LDet, while this is not the case for DOC, i.e., SDet has a somewhat shorter lifetime in the surface ocean than the semi-refractory DOC. At the same time, the rate of production of DOC is likely smaller than that of SDet, since most of the organic matter produced in the surface ocean is routed first through SDet, while this is not the case for DOC. Thus, while we are clearly not representing DOC in our model simulations, we do not expect the explicit consideration of DOC to completely change our results. Or in other words, we would argue that the impact of this shortcoming is smaller than possibly inferred at first sight.

In order to explore the potential impacts of our lack of consideration of DOC more quantitatively, we ran a sensitivity study where we altered the behavior of SDet to become like DOC. Specifically, we set the sinking speed of the SDet pool to zero, i.e., $w_{SD}=0$, and reduced the coagulation time scale t_{coag} to 2/5 of its baseline value to mimic as closely as possible a dissolved organic carbon pool. No

adjustments were made to the parameterization of the LDet pool to compensate for the strong reduction in the routing of organic carbon toward this pool. This sensitivity study thus needs to be considered as an extreme scenario - i.e., is meant to explore the potential contribution of DOC rather than an attempt to quantify it in detail. We spun up the model with the new biological parameters from year 24 of the baseline run (6 years of spinup) and used years 30-35 for the analysis, as we did for the baseline run.

The results of this sensitivity simulation (see Figures MC1-1-3 below) suggests that a dissolved pool of organic carbon would tend to intensify the lateral fluxes of organic carbon in the euphotic layer and stimulate the local recycling of organic matter, increasing both primary production and heterotrophic activity in the near-surface layer, but not alter net community production in a major manner. These apparently contradictory conclusions can be rationalized by our modifications resulting in a substantial increase in the average lifetime of SDet. Rather than becoming subject to sinking and coagulation, SDet now remains in the surface ocean, increasing the standing stock of POC there substantially, which increases also the offshore transport. However, due to the reduced reactivity of SDet resulting in a longer lifetime, the net horizontal divergence of SDet remains roughly the same, even though the transport is larger and reaching further out into the open North Atlantic. The roughly unchanged horizontal divergence of organic matter transport implies a roughly unchanged net community production as well. Thus, for the key question at hand, i.e., can the offshore transport fuel net heterotrophic conditions in the offshore regions of the Canary CS, the answer essentially remains unchanged.

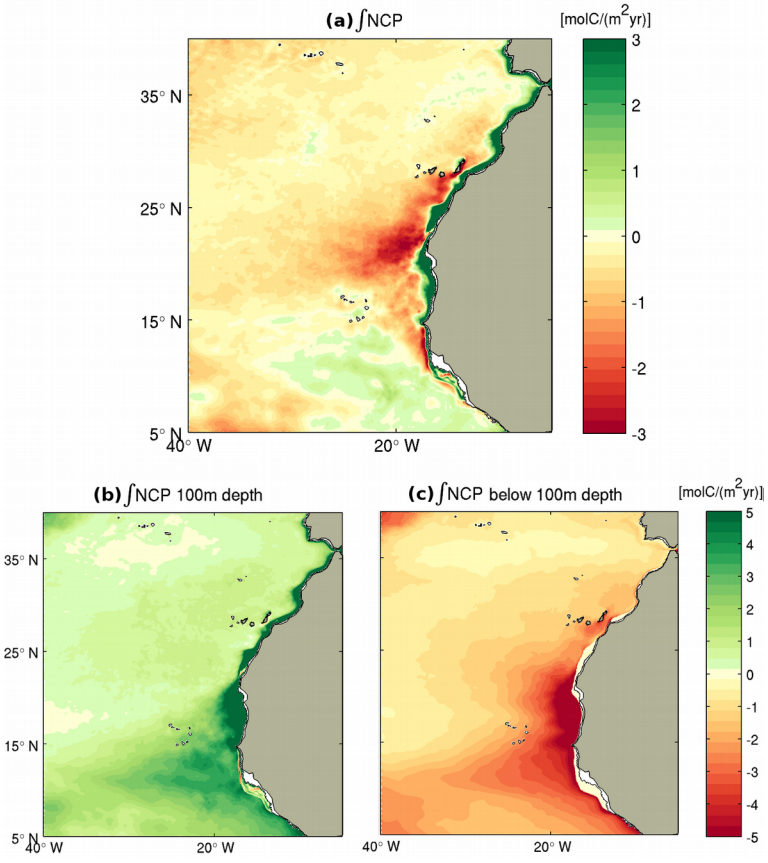

Figure MC1-1: Map of Community Production including sediment remineralization in the sensitivity study with reduced sinking and coagulation of SDet: (a) vertically integrated in the whole watercolumn; (b) vertically integrated in the first 100m depth; (c) vertically integrated below 100m depth. Compare to Figure 6 in the main text.

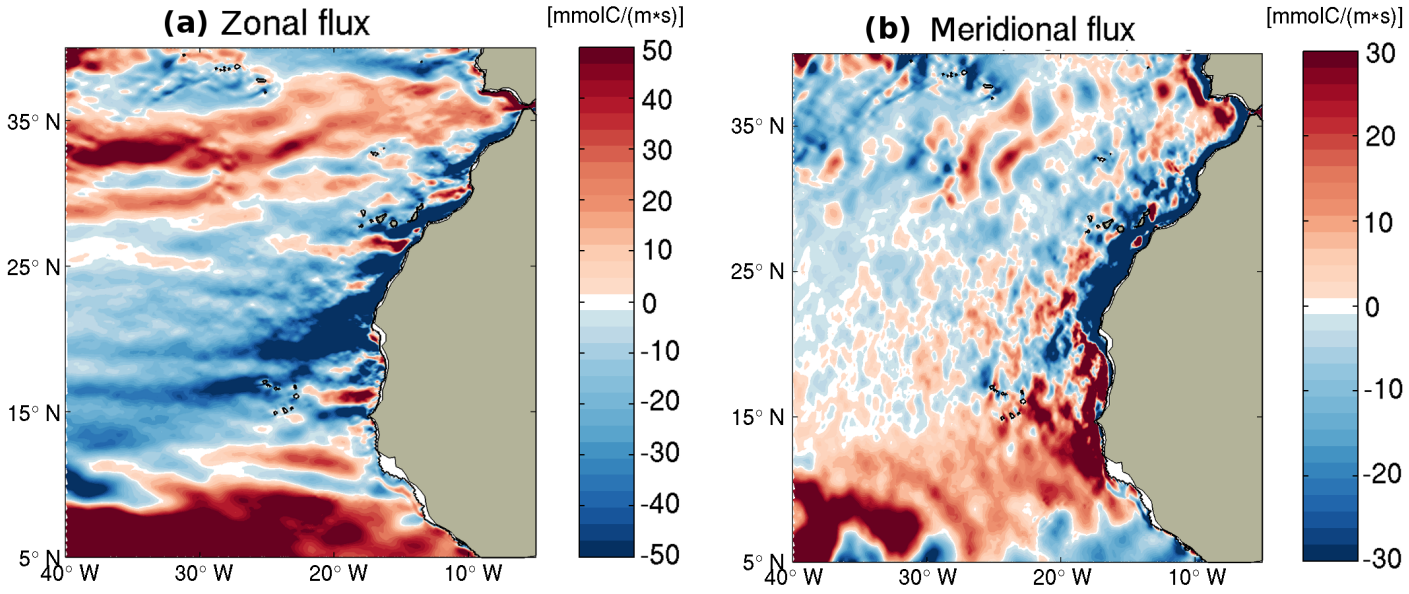

Figure MC1-2: Map of horizontal transport of POC in the sensitivity case with a non-sinking and very slowly aggregating SDet pool. (a) zonal transport of total POC in the top 100 m. (b) as (a), but for the meridional transport. Contrast this to Figure 11 in the main text.

In response to this comment:

- We have mentioned this model limitation and its potential implications directly in the Abstract (p.1, ll.18-21):

> "Our modeled offshore transport of organic carbon is likely a lower bound estimate due to our lack of full consideration of the contribution of dissolved organic carbon and that of particulate organic carbon stemming from the resuspension of sediments. But even in the absence of these contributions, our results emphasize the fundamental role of the lateral redistribution of the organic carbon for the maintenance of the heterotrophic activity in the open sea."

- We have modified our manuscript in order to refer to our modeled total organic carbon explicitly as Particulate Organic Carbon POC.
In particular, we have added the next passage in the Methods section (pag.6 ll.2-6):

> "As the model does not include an explicit DOC pool, our modeled total organic carbon corresponds to POC only. However, the small detritus, given its very small sinking speed, behaves essentially as a suspended POC pool, i.e., shares many similarities to DOC. To assess the possible implications of our neglecting DOC, we run a sensitivity experiment where we turned the small detritus pool into essentially DOC by setting its sinking velocity to zero and by reducing it coagulation rate."

- We have divided the Discussion section into two subsections (namely “Implications and comparison with previous work” and “Limitation and caveats”) and in the latter subsection we have introduced a new paragraph to examine the potential contribution of DOC to the lateral redistribution of organic carbon, based on the suggested literature and on the results our sensitivity experiment (p.29 l.14 – p.30 l.4):

> “Regarding DOC, the pool that matters is that of semi-labile DOC as it has a life time of beyond a few days, implying that it can be transported substantial distances before it gets remineralized. As a result, it has the potential to enhance our modeled lateral export of organic carbon. This is especially the case since DOC is readily produced in the surface ocean and contributes also substantially to the export of organic matter from the near-surface ocean (Hansell, 2002; Arístegui et al., 2002; Hansell et al., 2009; Hansell and Carlson, 2015), in particular in subtropical regions such as the North Atlantic gyre (Torres-Valdés et al., 2009; Roussenov et al., 2006). Even though DOC is not explicitly modeled, the small detritus, with its sinking speed of w_{SD} =1 m day^{-1} , represents essentially a suspended POC pool with some similarity to a semi-refractory DOC, particularly regarding its susceptibility to lateral transport. But differing from DOC, the small detritus coagulates to large detritus resulting in a shorter lifetime than DOC in the surface ocean. At the same time, the rate of production of DOC is likely smaller than that of the small detritus, likely leading to a situation where the small detrital pool likely has a behavior that is rather close to that of DOC. Thus, we would argue that the impact of our shortcoming of not representing the dynamics of DOC explicitly is smaller than possibly inferred at first sight. In order to explore more quantitatively the potential impacts of our lack of explicit consideration of DOC, we ran a sensitivity study, in which we set the vertical sinking of the small detritus, w_{SD}, to zero and reduced the coagulation time scale for small detritus to 40% of its baseline value. No adjustments were made to the parameterization of the large detritus. This sensitivity study needs to be considered as an extreme scenario - i.e., it is meant to explore the potential contribution of DOC rather than an attempt to quantify it in detail. We spun up the model with the new biological parameters from year 24 of the baseline run (6 years of spinup) and used years 30-35 for the analysis, as for the baseline run. The results show, as expected, an intensification of the lateral fluxes of organic carbon in the euphotic layer. The standing stock of suspended POC increases about twofold, largely due to its longer average lifetime in the surface ocean, stimulating the local recycling of organic matter. This increases both primary production and heterotrophic activity in the near-surface layer, leaving the NCP pattern basically unchanged and preserving the net autotrophy of the near-surface waters. In fact, even though the lateral transport of small detritus is much larger in this sensitivity study and reaching further out into the open North Atlantic, the net horizontal divergence of the lateral flux remains roughly the same. Thus, for the key question at hand, i.e., can the offshore transport fuel net heterotrophic conditions in the offshore regions of the Canary CS, the answer essentially remains the same.”

Major Comment nr.2:
In this study, the importance of mesoscale features is emphasized several times but never clearly quantified. It would have been nice to have such a quantification. I would suggest two possible means to do that: 1) to perform a classical separation technique between the mean and eddy components of the transport; 2) to perform a simulation in which the non linear terms in the Navier-Stokes equations for momentum are cancelled such as in Gruber et al. (2011). Otherwise, any discussion of the effect of the mesoscale circulation remains quite speculative and qualitative.

Answer to MC2:
We agree with Referee nr.1 that mesoscale processes play an important role for the lateral redistribution of organic carbon in the region and that their contribution needs to be discussed more quantitatively. However, we are of the opinion that a full in-depth analysis goes well beyond the scope of this paper, which is already quite detailed and long. Our preferred strategy is to leave this aspect to a second, dedicated publication that focuses exclusively on the role of mesoscale processes for the long-range transport of organic carbon in the region. This follow-up study will include an analysis of the decomposition of the fluxes into their mean and turbulent components, some sensitivity studies and a study of the influence of mesoscale eddies on the offshore transport and transformation of organic matter.

- For this present paper we have strengthened the discussion of the mesoscale contribution with more concrete references to previous literature such as Arístegui et al. (2009), Gabric et al. (1993), Fischer et al. (2009), Álvarez-Salgado and Arístegui (2015). We have also added in the present paper a reference to the follow-up study that we are currently working on (p.26 l.20-22):

> "Further insights into the special role of mesoscale activity in the lateral redistribution of organic carbon in the CanUS and a quantification of this component of the transport will be provided in detail in a dedicated publication."

<u>Answers to Detailed comments</u>

DC1: Page 2, line 1 - *"resuspension of bottom sediments and can create ... " I guess something is missing in this sentence.*
Thank you. We have corrected it to: "resuspension of bottom sediments can create..."

DC2: Page 4, line 33 - *In the list of state variables that are listed, you should add O2.*
Thank you, we have added the variable (p.5, ll.1-3):

"An additional four state variables have been added to reflect the cycling of carbon and oxygen, namely dissolved inorganic carbon (DIC), alkalinity, mineral $CaCO_3$ and dissolved oxygen (O_2) (Hauri et al., 2013; Turi et al., 2014; Lachkar and Gruber, 2013)."

DC3: Page 5, lines 11-12 - *Phytoplankton can coagulate with small POC to form large POC. Is it also the case for small POC with small POC?*
Yes, thank you. We have added the smallPOC-smallPOC coagulation in the text (p.5, ll.12-13):
"Coagulation of phytoplankton with small detritus as well as coagulation of small detritus with small detritus also forms large detritus..."

DC4: Page 7, lines 28-33 - *You should refer to figure 3 to illustrate the different regions.*
Thanks for the suggestion. We have added a reference to Figure 3 (p.8 ll.14-15):
"The lateral extension of the full CanUS boxes and of the subregional boxes is presented in Figure 3 together with the pattern of the modeled currents."

DC5: Page 10, lines 8-13 - *Almost everywhere, except near Cape Blanc, high values of Chlorophyll are too narrow and too much trapped near the coast. As mentionned by the authors, this bias is especially strong in the Southern part of the CanUS domain.*
Yes, we acknowledge the limitation of the modeled surface Chlorophyll. However, along the whole northern coastline from 32°N down to Cape Blanc (21°N), surface Chlorophyll is not narrower than in the satellite product. Below Cape Blanc, Chlorophyll is underestimated at the surface due to a deepening of the chlorophyll maximum, as discussed in pages 10 and 11.

DC6: Page 11, lines 1-6 - *The authors here discuss the characteristics of the modeled sub-surface maximum of Chl (DCM) and they refer to Figure B2. This is not always easy to see from Figure B2. The most obvious bias that emerges from the figure is the too high values of Chl at depth below 50m. Otherwise, it is hard to quantify from that plot the depth of the DCM in the model and in the data.*
We take note of this comment. In response, we have added a short description of the figure in the caption (p.35, Figure B2):
"Evaluation of the modeled annual mean Chlorophyll (CHL) by subregion and by depth for the first 500km offshore as defined by the first two budget analysis boxes, see Figure 4. The spread of the dots is maximum for the southern subregion, in which modeled CHL is too low at small depths and too high at large depths."

DC7: Page 17, lines 3-6 - *For sure in the interior of the ocean, the contribution of small POC to the vertical sinking flux of organic matter should drop very quickly with depth. A figure showing the contribution of the different pools of organic matter to total organic carbon would be nice.*
We have added a plot of the mean vertical profiles of the four pools of modeled organic carbon in the CanUS in the appendix of the paper as Figure B6, p.38. The plot is here visible as visible in the following Figure DC7-1.

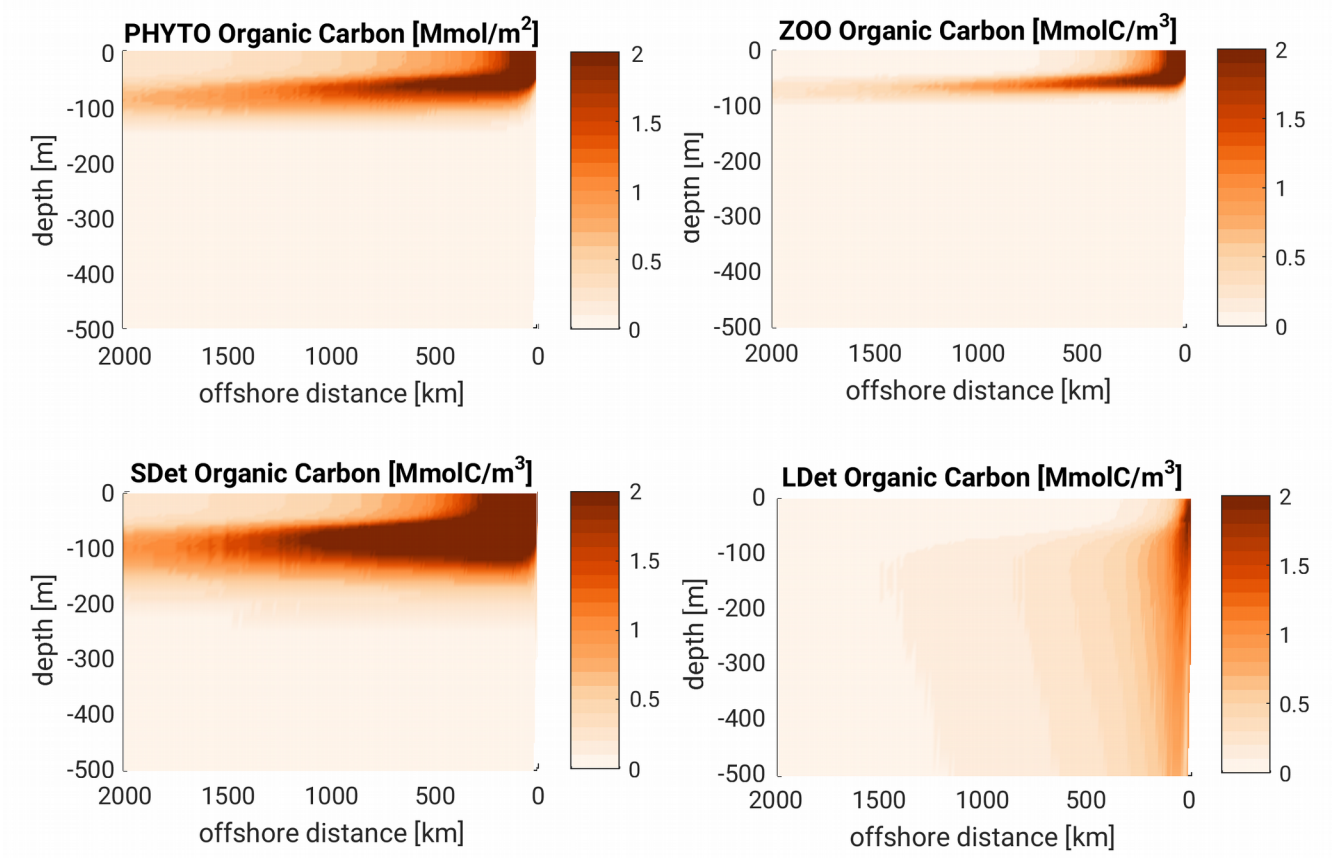

Figure DC7-1: Mean vertical offshore sections of the organic carbon components in mmolC/m^3; x-axis:offshore distance [km], y-axis: depth [m]

DC8: Page 18, Figure 9 - *The fluxes in the different boxes are not balanced (the imbalance is however small). Is it because the model is not fully at steady state or because of the internal variability related to the mesoscale activity?*

We have added a passage in our Methods section to explain the reasons of the lack of closure of our budget fluxes (p.7 ll.33 – p.8 l.2):

"In our analysis we disregarded the contribution of the horizontal and vertical mixing associated with the background diffusivity. We also used a fixed depth for the sigma layers that define the box boundaries, disregarding their vertical oscillations. Both approximations can result in small residuals in the budget analysis."

DC9: Page 18, lines 1-6 - *The DeltaE diagnostics is interesting. It accounts for two processes that can increase the export without changing the NCP: 1) The organic matter that is being transported laterally and that sinks out of the upper ocean increases the export and thus DeltaE. 2) The organic matter that is being transported laterally and that remineralizes in the upper box. This stimulates the biological activity which produces more organic matter which is sinks out of the upper ocean. In that case, NCP is not changed (the increase in PP compensates for the remineralization of the laterally supplied organic carbon) and export is increased which increases DeltaE. This two mechanisms should*

be explained here, especially because in the discussion section it is shown that the second process dominates.
We thank Referee nr.1 for his/her comment. In the end, we have decided to maintain the (extended) discussion of these two possible mechanisms in the Discussion section, “Implications and comparison with previous work” subsection.

DC10: Page 20, line 22 *"and quantify the contribute of the different zonal bands ..." I guess it should be contribution*
Thanks. We have corrected it as suggested.

DC11: Page 22, line 25 *"and quickly channel water ..." It should be channel.*
Thanks. We have corrected it as suggested.

DC12: Page 24, line 8 *"becomes particularly important the offshore waters" Some words are missing here.*
Thanks, we have corrected it to (p.25, ll.6-7):
“Among these vertical components, the advective+mixing vertical export becomes particularly important in the offshore waters.”

DC13: Page 25, lines 18-20 - *The splitting between the contribution of the mean flow and of the eddy transport is not really clear here. See my second major concern above.*
As anticipated in our previous answer to MC2, we plan to illustrate in detail and detangle the mean and mesoscale contributions to the transport in a dedicated publication, currently in preparation. We have added references to: Arístegui et al. (2009), Gabric et al. (1993), Fischer et al. (2009).

Answer to Referee #2, Josep L. Pelegrí

We thank Dr. Josep L. Pelegrí for his careful review of our manuscript and for his thoughtful comments that will surely help to improve its quality. We tried to address all his comments and we include below a detailed answer to all the questions.

Answers to Major comments

Major comment nr.1:
(1) Evaluation of the model's performance
This is a very critical aspect and the authors dedicate a significantly long section, including an appendix, to evaluate the performance of the model. They compare the numerical output with observations using different datasets: the near-surface seasonal circulation as inferred from surface drifters; the annual-mean sea surface height, sea surface temperature (SST) and sea surface salinity; the annual-mean mixed layer depth (MLD); the annual-mean surface chlorophyll; and the annual-mean and seasonal-mean net primary production (NPP).
I value this effort very much but, honestly, at the end of the Evaluation section I have important doubts on how good the model's performance is. Throughout this section the authors recognize the existence of substantial differences between model and field data, and also talk about model bias.

Answer to MC1:
As stated by Dr. Pelegrí, we have invested quite some effort to carefully evaluate many aspects of our model. As a result, we feel that we are well aware of its strengths and its limitations. While there are clearly some issues, the results of our model evaluation are in line with most state of the art models – in many respects the fidelity of the model simulated fields is even better than that of most models. However, it is clear that models are never perfect, so the question we have to answer is to what degree biases and other types of errors will affect the results and the conclusions drawn from them. Our overall assessment is that, despite the biases, that the performance of our model is more than adequate to answer the main scientific question regarding the magnitude and the importance of the long-range lateral fluxes of organic carbon. Thanks to the information provided by a detailed model comparison with observations, we are also able to discuss in the paper how our results are affected by the observed biases, especially in the southern subregion of the Canary Upwelling System (CanUS), where we see the largest and most relevant differences from the observations. We address the different elements of this first main comment in sequence:

A) *In Figure 2 they show the spatial distribution of model-data differences for several surface fields. The differences are not negligible at all, as clearly seen by the range of values in the mean fields and the differences, e.g. SST (range of values is 12◦ C and range in deviations is 4◦C) and MLD (range of valuesis 100 m and range in deviations is 60 m).*

The SST biases are clearly significant but actually quite a bit smaller than implied by Dr. Pelegrí's comment, i.e., ±2°C. The SST plot (Figure 2b) shows that differences between model and observations

lay in the interval [-0.75ºC,1ºC] in the large majority of the domain, with a large fraction of this bias having a range of only ±0.5ºC. Larger differences are confined to a very narrow coastal band. The region located south of Cape Blanc has the extensive bias. But also here, the (positive) bias has a range of only [0.5ºC,0.75ºC]. This warm bias is accompanied by a positive bias in salinity of about 0.5 (Figure 2c), leading to a near complete compensating with respect to their impact on density. Overall, we consider these biases to be small relative to the spatial and temporal variations. They are also too small to affect substantially primary production or the lateral export of organic carbon. Therefore we expect that these SST and salinity biases have a minor impact on our study. In response to this comment, we will discuss the SST and salinity biases and their impact on the study more explicitly.

The biases in the mixed layer depth are likely more relevant for our study. As highlighted by Dr. Pelegrí, while the modeled distribution agrees overall reasonably well with the observed one based on Argo-floats, our modeled MLD shows sharper gradients than the observed pattern resulting in rather large differences in the northern nearshore and the central offshore region. This could be a true bias of our model, but we also note that the Argo DT-0.2 MLD product was gridded on a relatively low-resolution 2ºx2º grid and that it has a rather limited coverage in the nearshore areas. As a result this product may not be able to properly capture strong gradients and overly smooth distribution relative to reality in regions with strong variations, such as ours. Given our MLD bias structure, it is feasible that some fraction of it could be attributed to biases in the Argo-based product.

In response to this comment, we have extended our discussion of the model biases in the Results and Discussion sections with a more in depth analysis.

- In particular, to be more precise in the discussion of our biases we have modified the Evaluation section as follows (p.8, l.30 – p.10, l.7):

> "Despite the stratus cloud correction, the modeled SSTs are still a bit too warm in the southern sector of the CanUS. However, differences between model and observations are limited to the interval [-0.75°C,1°C] over the large majority of the domain, with a large fraction of this bias having a range of only ±0.5°C. Larger differences are confined to a very narrow coastal band. The model also captures the observed Sea Surface Salinity (SSS, Figure 2c) well; relevant negative differences are only observed in the southern CanUS, in connection with the warm SST bias, resulting in a compensation of the density. Overall, we consider these biases to be small relative to the spatial and temporal variations, therefore we expect these SST and SSS biases to have a minor impact on the conclusions of our study.
> The modeled annual mean Mixed Layer Depth (MLD, Figure 2d) is consistent with the general pattern of the Argo-based MLD product, even tough the modeled pattern has sharper gradients. Deeper than observed values of the MLD are visible in the northern sector of the CanUS and in the nearshore waters of the southern sector of the CanUS. It is worth noting that the Argo dataset was generated on a relatively low resolution grid, i.e., 2°x 2°, and thus is likely underestimating lateral gradients. In addition, the float coverage in Eastern Boundary Current system is relatively low, owing to the strong currents and the offshore transport, making the

> Argo-based MLD product vulnerable for biases in these regions. Nevertheless, some of the differences are likely real, as they appear also in other products. This is particularly the case for the overestimation of MLD in the nearshore region of the southern CanUS and in the long strip extending southwestward from the Canary Island, possibly due to biases in the position of the large-scale currents as evidenced by the differences in SSH (Figure 2a)."

- We have also divided the Discussion section into two subsections (namely "Implications and comparison with previous work" and "Limitation and caveats") and in the latter subsection we have created a dedicated paragraph in which we discuss the potential consequences of our biases in the model evaluation (p.30 l.27 – p.31 l.5):

> "We also need to assess the potential impact of the physical/biogeochemical biases that we diagnosed in the Evaluation section. In the northern CanS our model overestimates the MLD depth; however our modeled MLD shows a meridional gradient that has the same trend as the observed one, with an extremely shallow mixed layer in the southern region below the Cape Verde front and deeper mixed layer in the north. This suggests that, even though we may potentially overestimate vertical mixing in the northern CanUS, this subregion would still be expected to be the only one in which this process is relevant. In the southern CanUS, our model shows a weaker than observed circulation and a deeper than observed chlorophyll and NPP maximum, which may lead to an underestimation of the lateral transport and therefore of the net heterotrophy of the water column. Both a shoaling of the biological production towards the surface characterized by more intense currents and an intensification of the circulation can in fact result in the strengthening of the lateral zonal and meridional organic carbon fluxes. However, an increase of the offshore zonal fluxes in the southern subregion could favor a more heterotrophic water column only if accompanied by an increase of the divergence of the flux, resulting in a substantial accumulation of organic carbon compared to the local production. In the meridional direction, an intensification of the alongshore Mauritanian current may instead increase the influx of organic carbon from the south into the Cape Verde frontal zone, fueling even further the deep respiration in the already strongly heterotrophic central CanUS."

B) *I particularly miss a comparison between the depth distribution of the modelled and observed particulate organic carbon (POC), which is of capital importance for this study. The seasonal results (Figure 5) show very large differences, possibly too large.*

We agree with Dr. Pelegrí regarding the necessity of having a comparison of modeled and observed POC and we thank him for this suggestion. To this end, we have conducted an evaluation of the modeled POC using 2 datasets: 1) the MODIS satellite estimate of surface POC (S-POC in the diagram); 2) the cruise POC measurements from AMT, ANT and Geotraces in the upper 200 m (POC in the diagram) located in the 0km-2000km offshore range of our analysis domain. Most of the in-situ data were collected in fall, especially in October, often in the far offshore region of our domain (cf. Figure MC1-1).

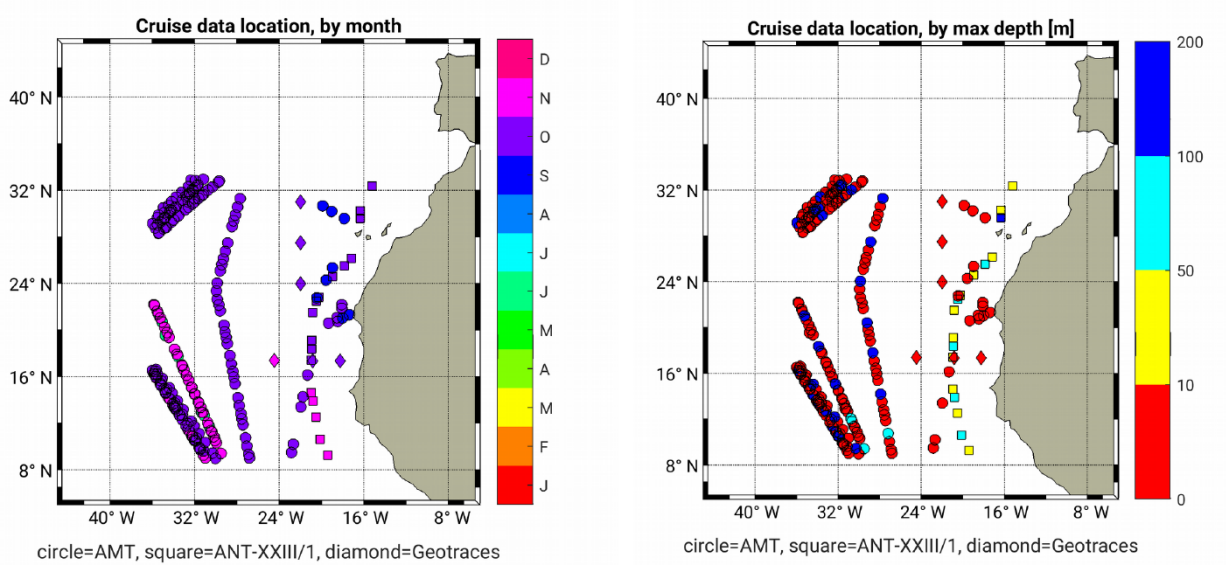

Figure MC1-1: Retrieved cruise POC measurements in the region of analysis corresponding to the Budget Analysis boxes. Data points are colored by sampling month and by maximum depth of the measurement. Circles=AMT (15-23), Squares=ANT, Diamonds=Geotraces.

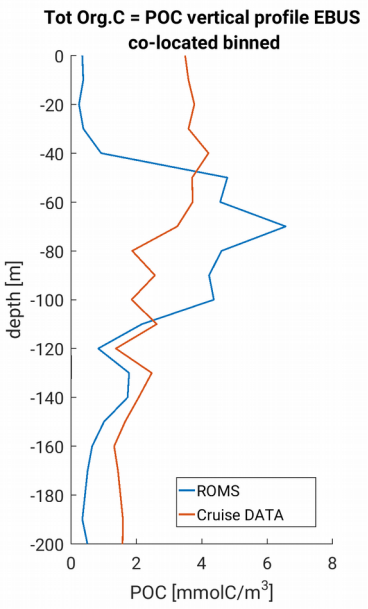

Modeled POC and data were co-located in space and time using a daily ROMS climatology for the same 6 years. As visible from the resulting plot (Figure MC1-2), the magnitude of modeled and observed POC is the same and the vertically-integrated POC in the first 100m also corresponds. Due to our coastally-confined production (largely discussed in the model evaluation) combined with the fact that cruise data are mostly located offshore, and due to the deepening of the chlorophyll maximum in the southern productive subregion, we observe a deeper-than-expected POC maximum in the model. As also discussed in the paper, this may mean that if anything our model may underestimate the offshore transport in the CanUS (and especially in its southern sector), therefore implying that the already large magnitude of the offshore transport that we find may be a low estimate.

Figure MC1-2: mean POC profile in the CanUS compared to cruise data, from co-located POC, binned in depth to 10m depth intervals.

In response to this comment:

- We have added a comparison between the mean profiles of modeled and observed POC using cruise data, combining Figures MC1-1 and MC1-2 into Figure B3 in the Appendix of the manuscript, p.36.

- We have included a comparison with cruise and satellite POC in the annual mean Taylor diagram (Figure B4 of the manuscript, here visible as Figure MC1-3), both based on satellite estimates and on in situ measurements, p.36 and a comparison with satellite POC in the seasonal Taylor diagrams (Figure B5 in the manuscript, here visible as Figure MC1-4) p.37.

- We have introduced a paragraph dedicated to the evaluation of modeled POC in the Evaluation section (p.12 ll.19-29):

> "Modeled Particulate Organic Carbon (POC) concentrations have annual mean values between 5 mmolC/m^3 and over 20 mmolC/m^3 in the first 100m depth of the very productive shelf areas laying therefore in the range of in situ observations (Alonso-González et al., 2009; Arístegui et al., 2003; Santana-Falcón et al., 2016; Fischer et al., 2009). Concentrations decline in the offshore direction with a pattern similar to that of NPP and have maximum values located between 20 m depth in the shelf area and 70 m depth offshore. The modeled POC compares well to the limited in situ data (see Appendix B: Supplementary figures, Figure B3) especially with regard to the vertically-integrated stocks in the first 100m. However, due to our coastally-confined production combined with the fact that cruise data were mostly collected offshore, and due to the deepening of the chlorophyll maximum in the southern productive subregion, we observe a deeper-than-expected POC maximum in the model, in agreement with the vertical bias in CHL. Due to the absence of sediment resuspension and of a mechanism of disaggregation of the large detrital particles in the model, deep peaks of POC such as those present in Alonso-González et al. (2009) and Álvarez-Salgado and Arístegui (2015) are not observed in the annual mean modeled POC concentration."

- In the caption of Figure 7 from the manuscript, p.16, we have highlighted that the plot already presents the mean vertical profile of POC for the whole Canary Upwelling System.

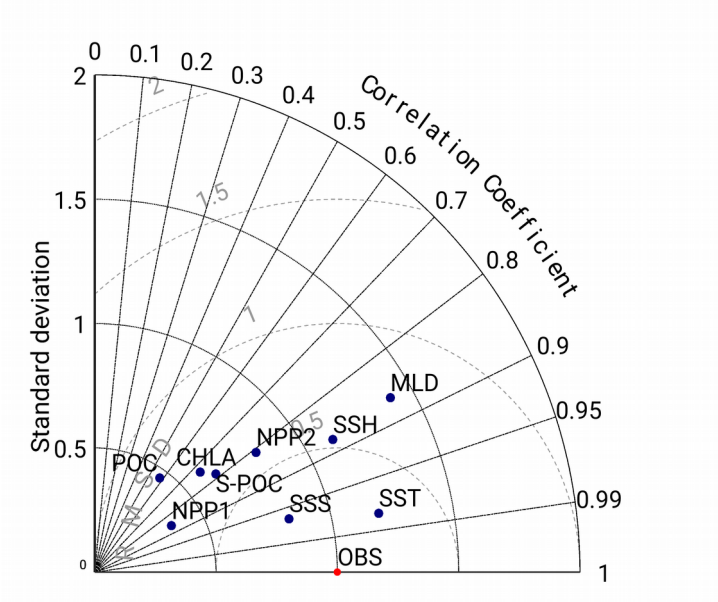

Figure MC1-3: Annual mean Taylor diagram including:
1) an evaluation of surface particulate organic carbon (**S-POC**) using SeaWiFS satellite estimates;
2) a comparison with depth profiles of **POC** from cruise data through co-location of ROMS output in space and time.

For an additional discussion of the implications of having a shallower POC distribution we refer also to our answer to Anonymous Referee 1, in which we discuss the results of some sensitivity studies in terms of both transport and impact on NCP.

C) *The authors end this section referring to a Taylor diagram presented in Appendix B (Figure B3), concluding that there is a "good correlation between the modelled and observed fields both in the annual and in the seasonal means." They show the Taylor diagram for the annual-mean results and for the mean of the seasonal results. The authors argue that the Taylor diagram shows results comparable to other studies for upwelling systems. Rather than comparing with other studies, it would be better to look at the statistics and discuss whether the results are convincing or not. For the annual-mean, for example, SST, CHLA and MLD respectively have a (normalized) standard deviation of about 1.2, 0.6 and 1.4, and a (normalized) root-mean-square difference of 0.3, 0.7 and 0.8. The authors should discuss whether these values are reasonable or not.*

Following Dr. Pelegrí's comment, we have modified the description of our annual mean Taylor diagram in the Evaluation section in order to be more specific and we also have included the discussion of the new seasonal Taylor diagrams (see also point D of the Answers to MC1). The paragraph was modified as follows (p.14 ll.15-30):

> "As visible from the Taylor Diagrams (Appendix B: Supplementary figures, Figure B4 and Figure B5) the agreement between the pattern of the physical and biological variables of interest is also confirmed by the good correlation between modeled and observed fields for both the annual and the seasonal means. All the variables have a correlation of 0.7 or higher with the observations in the annual mean (except cruise data POC) and 0.68 or higher in the seasonal. In the annual mean, the values of the normalized standard deviations are particularly high for annual mean MLD (1.5), which is, as discussed above, due to a combination of too low variations in the Argo-based observational product and overestimation of the MLD variations by the model. Low values of the normalized standard deviations (STD) are observed for surface POC (0.65), CHL (0.6) and for net primary production (NPP1) (0.35), the latter corresponding to NPP from the SeaWiFS VGPM product. This is likely due to the weaker intensity of the modeled blooms. Interestingly, if modeled NPP is compared to the SeaWiFS CbPM product (NPP2), the normalized STD increases to 0.75, reflecting the rather large uncertainties in the NPP inferred from observations. In the annual mean, values of correlation and normalized STD for MLD, SST and CHL are comparable to those presented for the CanUS in the ROMS+NPZD study by Lachkar and Gruber (2011), despite the the boundaries of our grid being much further away, and therefore providing much less constraints on the modeled physics and biology in the region of interest. When compared to studies that used ROMS+NPZD in other upwelling systems such as the California Upwelling System (Gruber et al. (2011), whole domain), our Taylor diagram shows a slightly worse correlation and comparable normalized STD of surface CHL in the annual mean but a better seasonal representation, while modeled NPP has comparable performances."

D) *I am particularly confused by Figure B3b: how is this calculated, just an average mean? What is the meaning? Wouldn't it be much better to show all four seasonal diagrams? It would also help to include, as supplementary materials, diagrams for each subregion.*

The Taylor diagram in Figure B3b is calculated as the simple mean of the seasonal Taylor diagrams. As suggested by Dr. Pelegrí, we have decided to substitute this figure, and explicitly include in the appendix of the paper the four seasonal Taylor diagrams (Figure B5 of the Appendix in the manuscript, p.37), here visible in Figure MC1-4. We have now included surface POC (S-POC) compared against the SeaWiFS satellite estimates also in these diagrams.

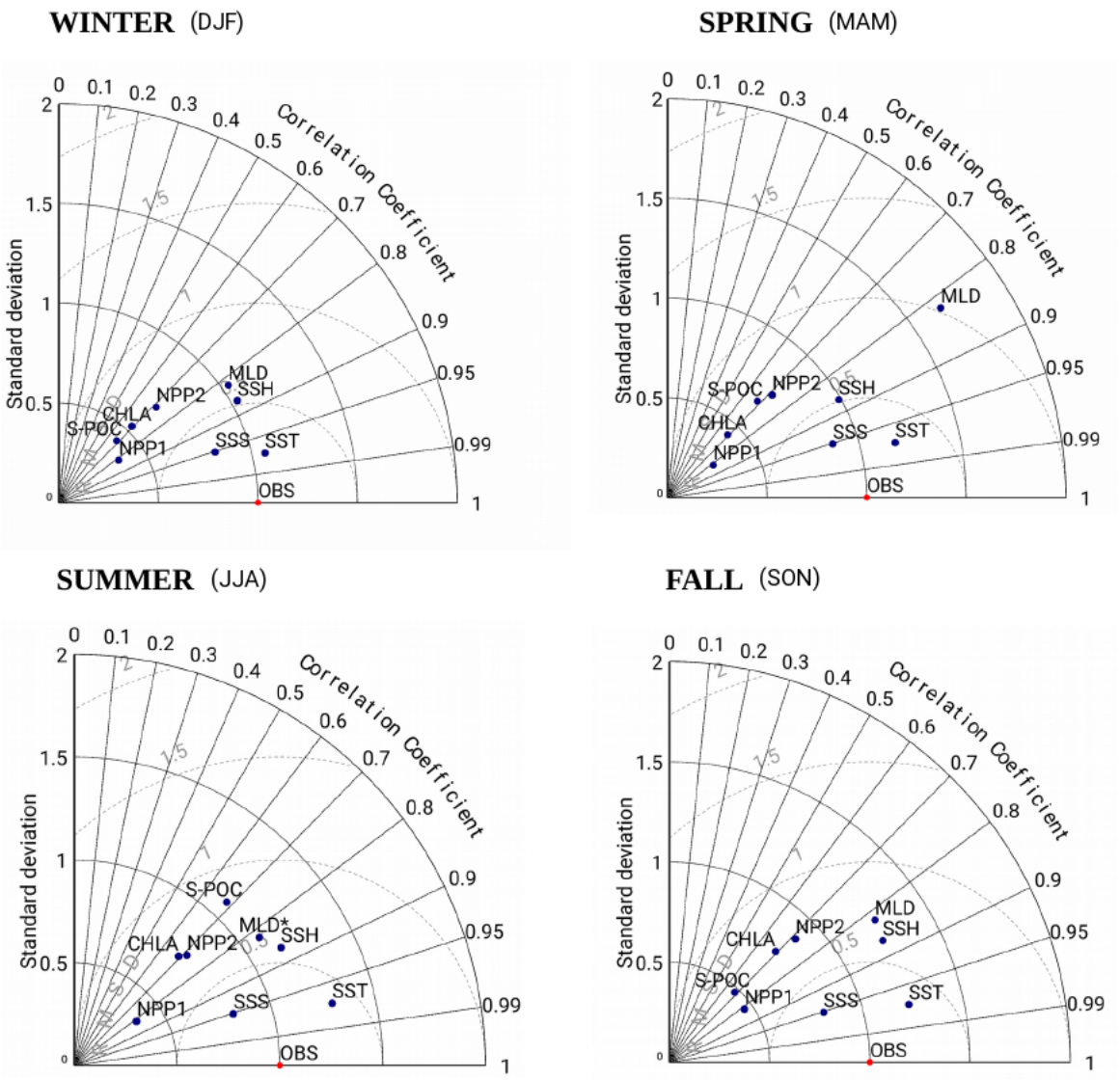

Figure MC1-4: Seasonal Taylor diagrams, including surface particulate organic carbon (S-POC) through a comparison with SeaWiFS satellite product estimate. In the Summer diagram MLD was rescaled to MLD*=MLD/2. The summer MLD_{STD} is therefore 2 times as big as the one represented in the plot, while the correlation remains unchanged.

Major comment nr.2:

(2) Latitudinal partition of the domain

A) *In several places of the Introduction and Discussion the authors recognize that the Cape Verde frontal zone is a natural boundary between the subtropical and tropical domains. Nevertheless, for most of their analysis on latitudinal variability they use a partition in three areas or subregions, as shown in Figure 3b, which is not properly justified. I imagine this is done as an attempt to grasp the character of the meridionally convergent region near Cape Blanc but, as it is clear from the velocity fields in Figures 3 and 5, this is not correct. In my opinion only the southern subregion would comprise an area with approximately coherent dynamics. My suggestion here is to use four subregions of different size: the northern one (25- 32◦ N) would correspond to an area with substantial mesoscalar activity, with eddies and filaments generated both south of the Canary Archipelago and at the upwelling front; the second area would represent the permanent and intense central upwelling region (21-25◦ N); the third are would concentrate on the convergent region immediately south of Cape Blanc, which is the root of the Cape Blanc giant filament (about 17-21◦ N, though these limits change with longitude); the southern area (9.5-17◦ N) would correspond to the tropical region. Right now most of the discussion is either on the results for the latitudinal-average picture or (to a lesser degree) for the three proposed regularly-spaced subregions. With this alternative partition, the paper would certainly become much more informative.*

B) *I value very much the authors' efforts to provide bulk figures for the entire region but I think that plotting these results may be very misleading. For example, the data in Figure 8 suggests that the zonal flux of organic carbon is more intense than meridional one. I doubt this very much: in my opinion this is only an artefact that the latitudinal average tends to cancel the contributions of the southward Canary Upwelling Current and northward Mauritania Current and Poleward Undercurrent (please see references below regarding the main currents in the CanUS). My suggestion is to produce fewer plots on the results for the entire region (Figure 9 is fine but some other plots may be replaced by tables) and instead show what is happening in each area: the CanUS is so large that it surely deserves a closer view for each subregion.*

Answer to MC2:

A) We agree with Dr. Pelegrí that other choices for the subregional Budget Analysis domain were also possible. Our partition serves to quantify both the alongshore convergence of particulate organic carbon from both north and south of Cape Blanc and the subsequent intense offshore flow that takes place along the Cape Verde front. The use of wide domains allows us to have a more robust measure of the fluxes in a region of high mesoscale variability. This partition also avoids us to place boundaries in critical regions such as around the Cape Verde convergence; placing boundaries in such flux-intense regions would make the results of our budget analysis very sensitive to the exact latitude of the boundary.

However, we have considered the latitudinal partition proposed by Dr. Pelegrí, and repeated our analysis on his proposed domains, as shown in Figure MC2-1. The changes basically consists in a sub-division of the central domain into two smaller zonal bands. Our northern and southern zonal bands

already satisfied Dr. Pelegrí's definitions, corresponding to a northern subregion rich in mesoscale activity (now only displaced by half degree) and a southern tropical subregion. The results of the new budget analysis are displayed in Figure MC2-2. As expected, northern and southern subregions are characterized by the same pattern of fluxes as those presented in the paper, since moving the southern boundary of the northern subregion by half a degree north does not affect the budget. The central subregion is split in a "central north" and "central south" zonal bands (green and orange lines). The impact of the offshore flux in these two zonal bands is very similar (Figure MC2-2, panel b). The flow of the Cape Verde front crosses the boundary between the "central north" and "central south" zonal band at about 1000km offshore, adding to the offshore flux in the "central south" subregion at this distance from the coast. However, this effect is an artifact generated by the split of the front in two segments. It thus does not add much to our understanding of the magnitude or the impact of the long-range offshore flux at these latitudes. As regard to the alongshore fluxes, we find that dividing the central subregion in two zonal bands does not clarify the source of the organic carbon that is exported offshore along the Cape Verde front. In fact, while before we could clearly identify the central subregion as a region of alongshore convergence of the organic carbon, now the budget for the "central north" and "central south" subregions depends strongly on the exact location of the intermediate boundary and the exact pathway of the Canary and Mauritanian currents near Cape Blanc. For example, in the 0km-100km offshore range, the "central north" subregion still exports southward more carbon than what it receives from its northern boundary, resulting in a net alongshore export to the "central south" subregion. In contrast, in the 100km-500km offshore range of the "central north" subregion a local recirculation of the carbon from the "central south" zonal band is visible in the meridional fluxes plot of Figure 11 of the paper. This recirculation induces a large net influx of organic carbon in the "central north" subregion. All these effects strongly depend on the exact location of the intermediate boundary in this region of intense flux convergence. As a consequence, we believe that the use of just one large central subregion for the budget analysis is more appropriate for our main purpose of understanding the magnitude and possibly the sources of the lateral offshore flux of organic carbon in the CanUS.

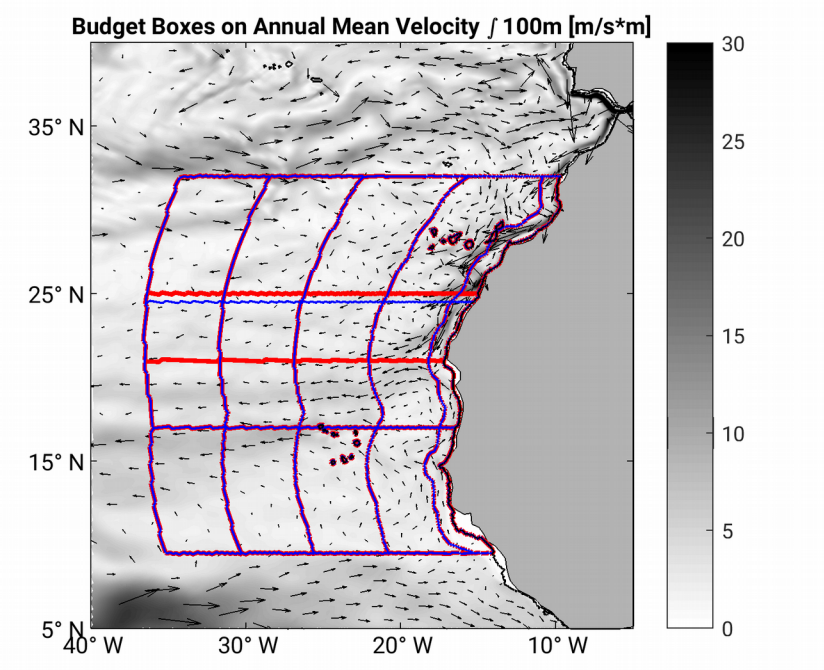

Figure MC1-1: Comparison between the latitudinal domains proposed by Dr. Pelegrí (red lines) and the domains used in the paper (blue lines).

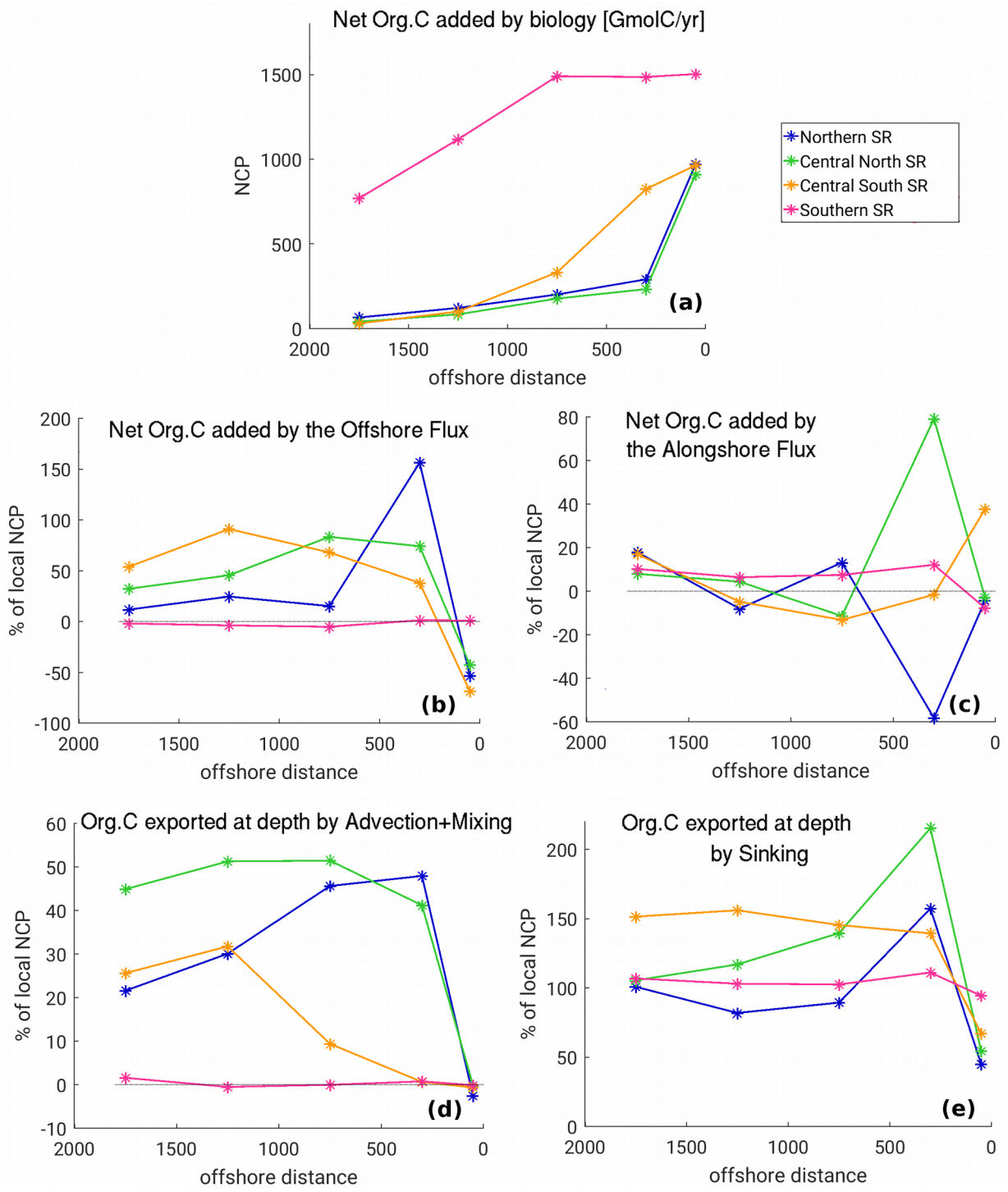

Figure MC1-2: Budget analysis results based on the subregions proposed by Dr. Pelegrí. Trends of NCP and impact of the organic carbon fluxes (divergence of the flux / NCP) by subregion.

In response to this comment we have decided to explicitly illustrate the reasons behind our choice of the zonal partition of the domain into three subregions. This passage was added to the Methods section (p. 8, ll.9-14):

> "To highlight the different roles of the three fundamental zonal bands in the CanUS, we divided the EBUS into three subregions (Southern, Central, Northern), maintaining for each subregion the same five offshore domains as for the previous analysis and considering only the euphotic layer (0 m -100 m). Subregional boundaries were placed at 17°N and 24.5°N. This allows us to distinguish between three regimes of circulation and production of the CanUS: a northern subregion dominated by coastal upwelling and coastal filaments, a southern tropical subregion, and a central subregion where the Canary and Mauritanian Currents converge to form the Cape Verde front (Pelegrí and Peña-Izquierdo, 2015)."

B) We thank Dr. Pelegrí for this comment, and we agree with him on the fact that alongshore fluxes are locally more intense than the offshore fluxes in the nearshore. We also agree that, since Figure 8b shows the meridional fluxes averaged over the whole CanUS, the contribution of the northward and southward alongshore currents mostly cancel each other.

To address this comment, we have modified the text as follows (p.18, ll.1-6):

> "The lateral meridional flux (Figure 8b) shows a complex alternation of northward and southward fluxes, emerging from the integration of the meridional transport across a wide meridional band. Even though this flux is weaker than the zonal flux, this does not imply the absence of substantial alongshore currents within the domain. In fact, many of these currents get averaged out by the meridional integration. Despite this, the intense southward flowing Canary Current is still visible as a negative signature of the mean meridional flux near the coast. Northward fluxes, probably linked to an influx from the organic carbon-rich near equatorial region, are dominant further offshore."

In general, we still believe that an in depth discussion of the bulk fluxes is very relevant for our purpose of quantifying the overall magnitude of the lateral fluxes from the North African coast on the North Atlantic gyre.

For this reason, we have decided to keep the original bulk figures.

Major comment nr.3:

(3) Upwelling of coastal and offshore inorganic nutrients

The coastal upwelling region is a source of inorganic nutrients to the surface layers in the coastal transition zone that are later exported offshore (e.g. Pelegrí et al., 2006; Pastor et al., 2008, 2013). Such a flux of inorganic nutrients is a prime element in the offshore net primary production and the sign of the NCP north of Cape Blanc. However, this issue is not mentioned in the manuscript until the Discussion. The subject is important enough to deserve careful attention when examining the sources and sinks for NPP, it is the difference between new production using the subsurface load of inorganic nutrients or production after remineralization.

The offshore waters in the southern subregion are also largely affected by the presence of upward Ekman pumping, i.e. offshore upwelling resulting from positive wind-stress curl. Again this is an important aspect in the dynamics and NPP balance of this subregion, which is again acknowledged very late in the manuscript and only partly discussed.

The model could be used to assess these different contributions. Perhaps this was not the objective of the authors, which is fine, but then the potential relevance of the upwelling and transport of inorganic nutrients on the NPP and NCP within the entire region should be properly discussed since early in the manuscript.

We agree with Dr. Pelegrí on the importance of including a discussion of sources and sinks of nutrients in the region.

- For this reason we have included in the paper a figure showing the lateral and vertical fluxes of inorganic nutrients (Figure B7 p. 39 of the manuscript, here Figure MC3-1).

- The figure was used in the Results section to better explain the pattern of NCP in the CanUS region, as follows (p.21, ll.5-11):

> "In the euphotic layer the pattern of production changes with latitude transitioning from a sharp offshore NCP gradient in the northern CanUS to an wide offshore extent of high NCP in the southern CanUS. These gradients can be explained by the pattern of the nutrients fluxes (see Appendix B: Supplementary figures, Figure B7). In the northern CanUS, nutrients are in fact mostly provided by coastal upwelling, while the positive signature of the wind-stress curl in the southern CanUS favors Ekman pumping of nutrients also offshore (Figure B7c). Intense production in the surroundings of Cape Blanc is likely due to the convergence of the alongshore nutrient fluxes (Figure B7b), in agreement with Auger et al. (2016) and Pastor et al. (2013)."

- The figure was also recalled in the Discussion in the context of the discussion of the two possible patterns of production and recycling that maintain the long-range offshore transport (p.27, ll.22-23):

> Further, the inorganic nutrients fluxes (see Appendix B: Supplementary figures, Figure B7) are of sufficient magnitude to refuel new growth of organic matter to replace that part that is lost by sinking.

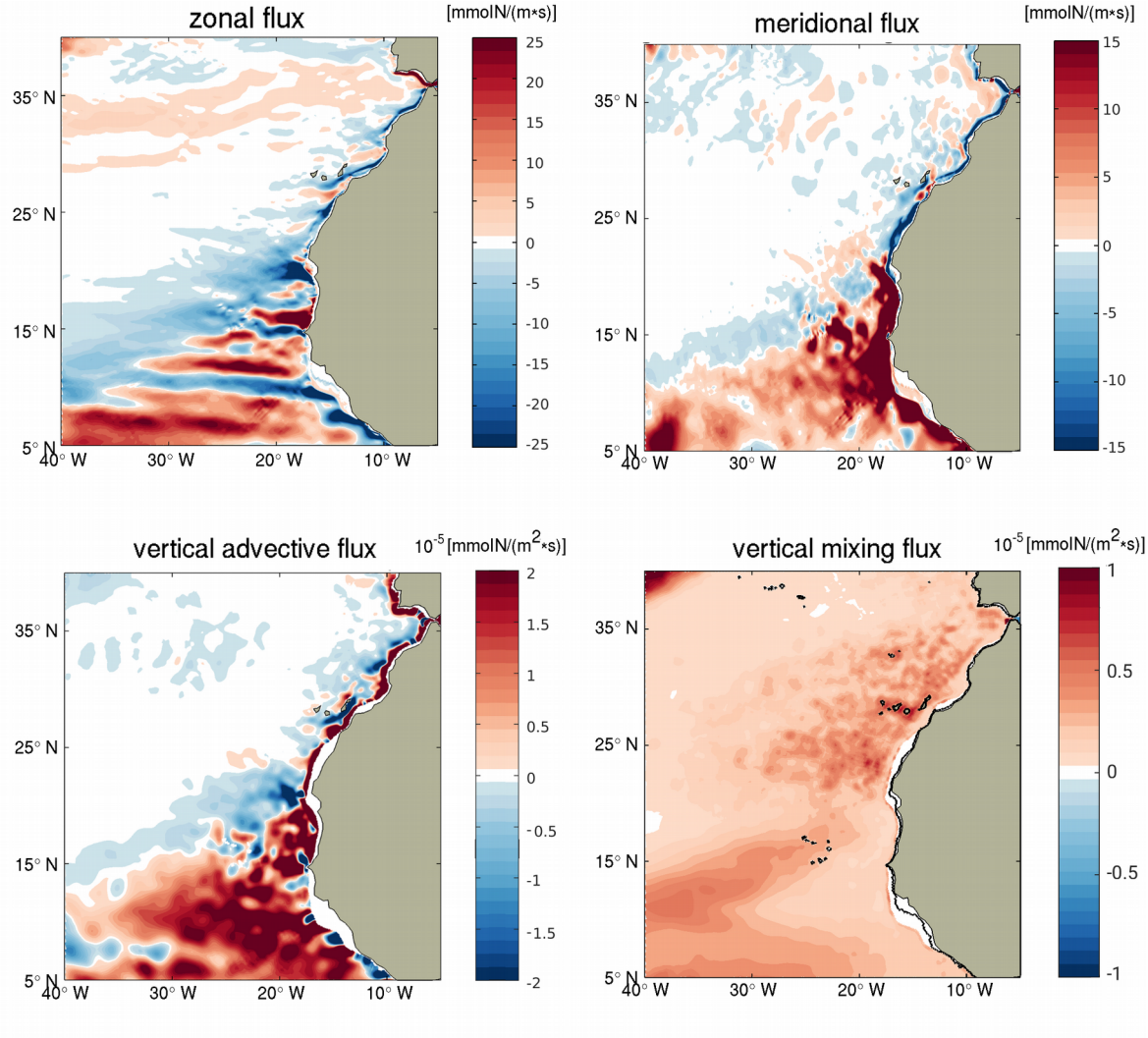

Figure MC3-1: Inorganic Nitrogen fluxes in the first 100m. Horizontal fluxes were integrated in the first 100m, while vertical fluxes were sliced at 100m depth.

Answers to Minor comments

(4) p 1, l 10: *divergence or convergence?*
The divergence is negative, which means flow is convergent.

(5) p 2, l 11: *replace "and can create" by "can create."*
Thank you, it was a typo. We have corrected it as suggested.

(6) p 2, l 15: *"Arístegui."*
Thank you, it was a typo. We have corrected it as suggested.

(7) p 3, l 5: *other relevant references are Pelegrí et al. (2006) and Pastor et al. (2013).*
Thank you for your suggestion. We have added the references in the text.

(8) p 3, l 24: *also Pastor et al. (2013).*
Thank you, we have added the reference in the text.

(9) section on Methods: *how does the model calculate the vertical velocity?*
The vertical velocity is computed through integration of the mass-conservation equation of an incompressible fluid ($\vec{\nabla} \cdot \vec{u} = 0$) from the ocean floor upwards. For detail about the equations solved by ROMS and its numerical solution technique we refer to Shchepetkin and McWilliams (2005) and the ROMS Wiki (https://www.myroms.org/wiki/Equations_of_Motion).

(10) caption of Figure 1: *Gran Canaria is cited in the caption but not located in the map.*
Thank you for the suggestion, we have marked the island of Gran Canaria in the picture with the letter "G", and we have recalled it in the caption.

(11) p 10, l 10-13: *please clarify.*
We have modified the passage as follows (p.11, ll.5-8):

> "Less well captured is the surface CHL in the productive southern sector of the CanUS, where the model substantially underestimates CHL at the surface. This is also the region where the model is biased too warm and salty, and where the modeled MLD exceeds the expected near-zero value, suggesting that this low surface CHL is primarily consequence of our physical biases in circulation and vertical stratification."

(12) caption of Figure 4: *VGPM is first mentioned here but it is defined nowhere in the manuscript.*
The used SeaWiFS VGPM product is described in detail in Table A3 (Appendix) among the products used for the Model evaluation.

(13) p 12, l 21-24: *asides the Canary Current and the Mauritanian Current you should also probably refer to the Canary Upwelling Current (associated to the coastal upwelling jet) and the Poleward Undercurrent (please see references below).*
Thank you. We have added these currents in our description as follows (p.10 ll.13-16):

> "Between the CC and the African coast, an intense and narrow Canary Upwelling Current (CUC) flows southward along the shelf (Mason et al., 2011). A poleward undercurrent (not shown) flows along the whole North African coast with its core typically centered at 200 m - 300m depth (Pelegrí and Benazzouz, 2015)."

(14) p 12, l 31-32: *". . . NPP is a better measure than chlorophyll for evaluating. . ."*
Thank you, we have corrected the sentence as suggested.

(15) p 13, l 1: *Pastor et al. (2013) is probably a better reference.*
Thank you for your suggestion, we have added this reference.

(16) caption Figure 6: *panel b also includes sediment remineralization?*
Yes, all panels include remineralization. We have adjusted the caption in order to make this clear.

(17) p 18, l 3-5: *are you using two different definitions for excess export?*
No, ΔE is always defined as ΔE= vertical export – NCP.
To avoid confusion we have substituted the symbol Δ (previously used in Figure 9) with ΔE both in the plot and in the caption. We have also adapted the legend of Figure 10 in line with this choice.

(18) p 20, l 1-2: *here and elsewhere it is best to not refer to lines, they should be defined in the figure's caption or legend (otherwise you would have to define them everywhere).*
Thank you for your suggestion. However, we have decided to maintain the references to the lines to ease the reading of the manuscript.

(19) p 20, l 27 and 33: *"north of the Cape Verde front. . ."*
Thank you for your suggestion, we have corrected this error throughout the whole manuscript.

(20) p 22, l 2: *". . .south of Cape Blanc."*
Thank you for your suggestion, we have corrected this error throughout the whole manuscript.

(21) *please revise caption of Figure 12.*
Thank you for highlighting this typo, we have revised the caption.

(22) Figure 13: *I suggest that you also show the meridional fluxes.*
Thank you for your suggestion. However, due to the length of the manuscript and to the fact that the vertical slices of the mean meridional fluxes do not add any substantial information that cannot be

inferred from the 2D plot of the meridional fluxes (Figure 11b), we have decided not to include this plot.

(23) caption Figure 13: *"vertical" rather than "vertcal."*
Thank you. We have corrected the typo as suggested.

(24) p 24, l 14: *"(Figure 13)."*
Thank you. We have corrected the typo as suggested.

(25) p 25, l 6-8: *this is likely an artefact of the SW-NE orientation of the coast.*
Thank you for your suggestion. We have explored this question, also observing some animations of the organic carbon concentration from the model output. However, we are still not sure that the inclination of the coastline can result in an onshore flux in the open waters of the northern CanUS. Instead, we clearly see the organic carbon being transported eastward by the Azores current at the northern boundary of the CanUS domain. As a consequence, we think that this current is responsible for the positive signature of the zonal flux in the northern subregion.

(26) p 25, l 10 and 15: *please include references.*
Thank you, we have added the following references: Arístegui et al. (2009), Gabric et al. (1993), Fischer et al. (2009).

(27) p 27, l 8: *see also Pastor et al. (2013).*
Thank you for your helpful suggestion. We have added this reference in the text.

(28) p 28, l 7: *"these."*
Thank you, we have corrected it as suggested.

(29) p 28, l 10-18: *usage of so many conditionals raises doubts on the reader.*
Thank you, we have revised the paragraph.

(30) p 28, l 27: *remove "from Section 4.1."*
Thank you, we have removed it.

(31) p 28, l 28: *is this the right way to cite a figure within a reference?*
We have modified the reference as follows (p.28, ll.34-35):
"The spatial pattern of modeled near-surface autotrophy (Figure 6b) agrees with the calculated global distribution of NCP (Williams et al., 2013, Figure 1), ..."

(32) p 29, l 3: *here and elsewhere separate numbers from units, i.e. "2000 km" rather than "2000km."*
Thank you, we have corrected it throughout the whole manuscript.

(33) p 29, l 16-17: *please revise writing.*
Thank you. We have revised the Conclusions as a whole.

(34) additional references: *asides those mentioned above, there are other works that would help better describe the circulation patterns in the CanUS, such as Mason et al.(2011), Peña-Izquierdo et al. (2012, 2015), Pelegrí and Peña-Izquierdo (2015), Pelegrí and Benazzouz (2015).*
Thank you for the valuable suggestions, we have included these references in the manuscript.

On the long-range offshore transport of organic carbon from the Canary Upwelling System to the open North Atlantic

Elisa Lovecchio[1], Nicolas Gruber[1], Matthias Münnich[1], and Zouhair Lachkar[2]

[1]ETH-Zürich, Universitätstrasse 16, 8092 Zürich, Switzerland

[2]Center for Prototype Climate Modeling, New York University Abu Dhabi, Abu Dhabi, UAE

Correspondence to: Elisa Lovecchio (elisa.lovecchio@usys.ethz.ch)

Abstract. A compilation of measurements of Net Community Production (NCP) in the upper waters of the eastern subtropical North Atlantic had suggested net heterotrophic conditions, purportedly supported by the lateral export of organic carbon from the adjacent highly productive Canary Upwelling System (CanUS). Here, we quantify and assess this lateral export using the Regional Ocean Modeling System (ROMS) coupled to a Nutrient, Phytoplankton, Zooplankton, and Detritus (NPZD) ecosystem model. We employ a new Atlantic telescopic grid with a strong refinement towards the north-western African shelf to combine an eddy-resolving resolution in the CanUS with a full Atlantic basin perspective. Our climatologically forced simulation reveals an intense offshore flux of organic carbon that transports over the whole CanUS about 19 Tg C yr^{-1} away from the nearshore 100 km, amounting to more than a third of the NCP in this region. The offshore transport extends beyond 1500 km into the subtropical North Atlantic, along the way adding organic carbon to the upper 100 m at rates of between 8% and 34% of the alongshore average NCP as a function of offshore distance. Although the divergence of this lateral export of organic carbon enhances local respiration, the upper 100 m layer in our model remains net autotrophic in the entire eastern subtropical North Atlantic. However, the vertical export of this organic carbon and its subsequent remineralization at depth makes the vertically-integrated NCP strongly negative throughout this region, with the exception of a narrow band on the north-western African shelf. The magnitude and efficiency of the lateral export varies substantially between the different subregions. In particular, the central coast near Cape Blanc is particularly efficient in collecting organic carbon on the shelf and subsequently transporting it offshore. In this central subregion, the offshore transport adds to the upper 100m as much organic carbon as nearly 60% of the local NCP, giving rise to a sharp peak of offshore respiration that extends to the middle of the gyre. Our modeled offshore transport of organic carbon is likely a lower bound estimate due to our lack of full consideration of the contribution of dissolved organic carbon and that of particulate organic carbon stemming from the resuspension of sediments. But even in the absence of these contributions, our results emphasize the fundamental role of the lateral redistribution of the organic carbon for the maintenance of the heterotrophic activity in the open sea.

1 Introduction

Owing to the dominance of the sinking flux of particulate organic carbon (POC), the ocean's biological pump is often simplified to a one-dimensional vertical process, consisting of the production of POC in the euphotic zone, its vertical export by gravitational sinking, and the remineralization of this organic carbon in the aphotic zone (e.g., Sarmiento and Gruber, 2006). Reflecting this simplified view, most biogeochemical models currently used in the context of global climate models consider only the vertical export pathway for POC, thus neglecting its potential lateral transport by horizontal advection and diffusion (e.g., Aumont et al., 2003; Moore et al., 2004; Galbraith et al., 2010; Shigemitsu et al., 2012).

Nevertheless, the horizontal transport of POC can be substantial, even in the presence of vertical sinking speeds ~~of POC~~ of 10 m day^{-1} or more. This is especially the case in places characterized by high lateral advective velocities (Helmke et al., 2005) and the presence of upward vertical transports that can help to maintain high organic matter concentrations in the upper ocean against its gravitational sinking (Plattner et al., 2005). In addition, resuspension of bottom sediments ~~and~~ can create nepheloid layers that can transport POC over hundreds of kilometers (Ohde et al., 2015; Inthorn et al., 2006a; Falkowski et al., 1994). A further important contribution to the lateral transport of organic carbon is that of dissolved organic carbon (DOC), estimated to account for 20 % of the export to depth and for about 10 % of the respiration rates in the deep ocean (Hansell, 2002; Arístegui et al., 2002; Ducklow et al., 2001). As a consequence of these transport processes, the different organic carbon pools get redistributed laterally from regions of excess production to regions of intense remineralization and burial, giving rise to a complex three-dimensional pattern of organic carbon cycling.

Such a lateral connection between organic carbon sources and sinks in the marine environment is at the heart of a long-standing controversy regarding the net metabolic state of the upper ocean in the oligotrophic subtropical gyres (Williams et al., 2013; Duarte et al., 2013; Ducklow and Doney, 2013). Based on a compilation of data from bottle-incubations that measure the net changes of oxygen over time, Duarte and Agustí (1998) and Del Giorgio and Duarte (2002) had suggested that oligotrophic systems, and particularly the near-surface layer in the center of the subtropical gyres tend to be heterotrophic. They suggested, although without any quantification, that this net heterotrophy is sustained by organic carbon that is supplied laterally to the center of the gyres from the adjacent more productive regions. This claim has fueled an intense debate, ranging from a discussion of the suitability of oxygen incubation experiments to assess the metabolic state of the ocean, to the question of whether it is actually possible to supply such a large amount of organic carbon through lateral processes (Williams et al., 2013; Duarte et al., 2013; Ducklow and Doney, 2013).

A key role in this debate is ~~played~~ taken by the Eastern Boundary Upwelling Systems (EBUS), as these very productive continental margins (Chavez and Messié, 2009; Carr, 2002) are straddling the oligotrophic subtropical gyres. They thus may provide the source of the organic carbon that fuels the purportedly heterotrophic conditions in the latter regions (Liu et al., 2010; Walsh, 1991). In fact, with most of the NCP measurements indicating net heterotrophic stemming from the eastern subtropical North Atlantic (Duarte et al., 2013), the Canary Upwelling System (CanUS) has been at the center of studies addressing the offshore transport of organic carbon (e.g. Pelegrí et al., 2005).

Located on the eastern side of the North Atlantic Ocean, the CanUS spans the region between the North African Coast ~~between 9°N and 33°N~~ and the adjacent portion of the North Atlantic Gyre between 9°N and 33°N(Váldes and Déniz-González, 2015). A complex circulation pattern determines strong subregional differences in the CanUS in terms of circulation, mesoscale activity, seasonality of upwelling and biology (Arístegui et al., 2009). The high productivity in the CanUS is sustained both by local coastal upwelling and by meridional alongshore advection of nutrients (Carr and Kearns, 2003; Auger et al., 2016), & (Pelegrí et al., 2006; Pastor et al., 2013). Sufficiently long water residence times in the nearshore region, favorable light and temperature conditions also contribute to sustain high levels of production (Lachkar and Gruber, 2011). Dedicated local surveys have demonstrated that the export of coastally produced organic carbon from the CanUS shelf to the open sea can be intense (Pelegrí et al., 2005; Arístegui et al., 2003) and include living organisms (Brochier et al., 2014). On top of the mean Ekman transport, persistent filaments originating on the CanUS shelf have been reported to be able to export up to 50 % of the coastally produced organic matter as far as several hundreds of km offshore (Gabric et al., 1993; Ohde et al., 2015). Due to these fluxes, a substantial amount of coastally produced organic carbon in the CanUS escapes remineralization in the nearshore region and is advected offshore towards the center of the North Atlantic Gyre (Fischer et al., 2009; García-Muñoz et al., 2005) & (Álvarez-Salgado and Arístegui, 2015). Estimates from multiple local surveys indicate that on average about 16 % of the coastal production by phytoplankton is laterally exported to the open sea. The CanUS constitutes therefore a good potential candidate source region for the organic carbon required to fuel the purportedly heterotrophic conditions in the subtropical North Atlantic. However, despite its potential impact on the offshore biological activity (Alonso-González et al., 2009; Álvarez-Salgado et al., 2007), the magnitude and range of the total long-range offshore transport of organic carbon in the CanUS is still poorly quantified.

The quantification of this export is notoriously difficult to achieve through in-situ studies owing to the intermittency of the transport and the importance of eddies, filaments and other turbulent structures(e.g., Peliz et al., 2004; Nagai et al., 2015), providing models an opportunity to fill the gap. These models need to have relatively high resolution, in order to resolve this mesoscale dynamics, forcing most studies to employ regional models instead of global ones. But so far, relatively few high resolution modeling studies have focused on the CanUS compared to other upwelling regions and even fewer have employed a fully coupled biogeochemical model (Auger et al., 2016; Fischer and Karakaş, 2009; Lachkar and Gruber, 2011)& (Pastor et al., 2013).

Most of the ~~conducted work regarding~~ modeling work conducted to assess the lateral redistribution of organic carbon relied on regional configurations of the Regional Ocean Modeling System (ROMS) and tended to focus on sub-aspects of the offshore transport of organic matter, either by focusing on sub-regions, or by focusing on the offshore transport of a subset of constituents. In the most recent study, Auger et al. (2016) used a regional ROMS configuration coupled to the biogeochemical/ecological module PISCES (Pelagic Interactions Scheme for Carbon and Ecosystem Studies) to highlight the important role of the lateral redistribution of nutrients and phytoplankton on the CanUS shelf for determining the complex seasonal pattern of chlorophyll and for the fueling of the persistent Cape Blanc offshore bloom. Despite the specific focus on phytoplankton, their analysis extended the work of previous studies which concentrated on the lateral transport of organic carbon in limited portions of the CanUS. Among these studies, Sangrà et al. (2009) estimated the integrated lateral export and production of organic

carbon in the eddy corridor shed by the Canary Archipelago and its potentially big impact on the region combining a physical ROMS simulation with estimates of carbon concentration in the eddies based on a few eddy surveys. With a ROMS-driven Lagrangian experiment, Brochier et al. (2014) studied the observed biological coupling between the African coast and the Canary Islands in terms of the offshore transport of ichtyoplankton (eggs and larvae of fish) by filaments. With a wider focus area, Fischer and Karakaş (2009) employed a relatively simple Nutrient Phytoplankton Zooplankton and Detritus (NPZD) model coupled to their regional configuration of ROMS to study the role of sinking speeds in the vertical export of organic carbon to the deep ocean in the CanUS. While these studies demonstrated clearly the importance of offshore fluxes in the CanUS, they ~~failed to address the total~~ did not address the long-range transport of organic carbon from the CanUS into the oligotrophic subtropical North Atlantic. This is largely due to the limited offshore dimension of the regional ROMS configurations, with typical offshore extents of a few hundred kilometers only.

Here we overcome this limitation and provide a first comprehensive quantification of the long-range lateral fluxes of organic carbon from the CanUS shelf to the open North Atlantic using a new regional configuration of ROMS. This configuration employs a basin-scale telescopic grid that allows us to model the whole Atlantic basin in a continuous manner, while maintaining a full eddy resolving resolution in the region of study. Thus, this configuration is ideally suited to assess the long-range transport owing to its fully resolving all scales. Furthermore, this permits us to push the lateral boundaries far away from the region of interest, thus avoiding the many challenges and distortions associated with the lateral boundary conditions in regional studies. We couple this physical setup with a NPZD-type ecosystem model that fully resolves the three-dimensional dynamics of the ~~organic carbon redistribution~~ redistribution of POC. In particular, the vertical sinking of the different pools of organic matter is explicitly solved for, permitting us to advect and diffuse POC in the vertical and horizontal directions. ~~Our~~ Even though we are not taking the transport of DOC explicitly into consideration, our results show that the organic carbon offshore flux in the CanUS significantly enhances the carbon availability of the open waters. Substantial subregional differences in the pattern of lateral and vertical fluxes and key pathways for the carbon lateral redistribution are highlighted and discussed in the context of the previous research.

2 Methods

2.1 Model configuration

We employ the UCLA-ETH version of the Regional Ocean Modeling System (ROMS) (Shchepetkin and McWilliams, 2005), coupled with the Nutrient, Phytoplankton, Zooplankton and Detritus (NPZD) biogeochemical ecosystem module of Gruber et al. (2006). ROMS solves the 3D hydrostatic primitive equations of flow on a discretized curvilinear grid, using terrain following vertical coordinates (sigma levels). Surface elevation, barotropic and baroclinic horizontal velocity components, potential temperature and salinity are its prognostic variables. Vertical mixing is parameterized by the K profile parameterization (KPP) scheme (Large et al., 1994).

The NPZD ecosystem module is a nitrogen-based model with two limiting nutrients, i.e., nitrate and ammonium, one class of phytoplankton, one class of zooplankton and two detritus pools, i.e., a small one that sinks very slowly, and a large one

that is subject to more rapid sinking (Gruber et al., 2006). These components plus a dynamic chlorophyll-to-carbon ratio form the seven prognostic variables of the nitrogen component of the model. An additional four state variables have been added to reflect the cycling of carbon and oxygen, namely dissolved inorganic carbon (DIC), alkalinity, ~~and~~ mineral $CaCO_3$ and dissolved oxygen (O_2) (Hauri et al., 2013; Turi et al., 2014; Lachkar and Gruber, 2013). The carbon and oxygen cycles are linked to the nitrogen cycle by fixed stochiometric ratios. Thus, the fluxes of organic carbon diagnosed in our model are actually the fluxes of organic nitrogen multiplied by the C:N ratio assumed in the model, i.e., 117:16.

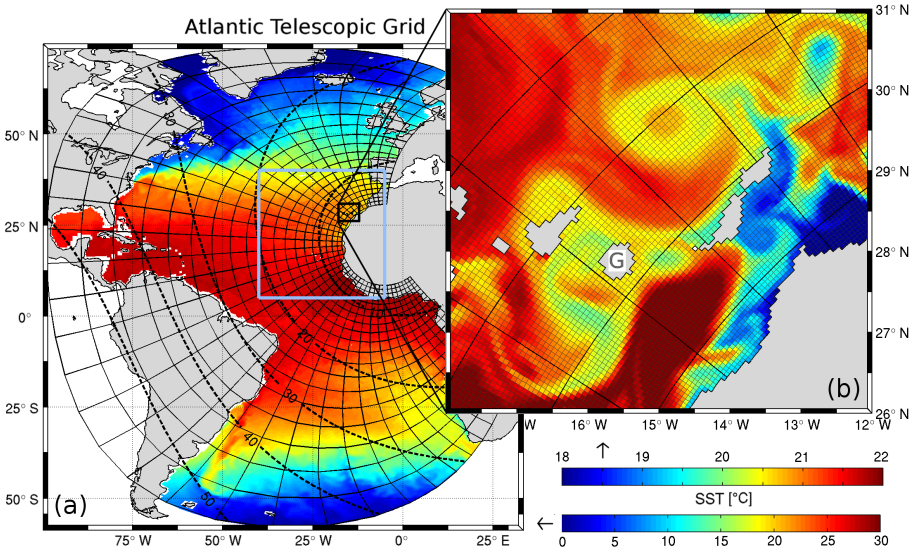

Figure 1. Map of the domain of the Atlantic telescopic grid together with a snapshot of the modeled sea-surface temperature. (a) Map of the full domain. Shown are every 20th grid line. Dashed isolines indicate the resolution of the grid in km. The light blue square highlights the region of interest used for the CanUS plots throughout the whole paper [5°N to 40°N, and -40°E to -5°E]; the black square indicates the region used for the zoomed-in subplot (b) Zoom on the Canary Islands region with actual grid resolution. Every 20th line is plotted thicker, corresponding to the grid lines shown in (a). As a point of reference, the island of Gran Canaria (G) has a diameter of about 45 km.

Particulate organic carbon (POC) in the model, i.e., the sum of phytoplankton, zooplankton, and the two detritus pools, is subject to advection and diffusion in vertical and horizontal directions, as well as explicit vertical sinking (the latter does not apply to zooplankton, however). Sinking velocities for phytoplankton, small detritus and large detritus are 0.5 m day^{-1}, 1 m day^{-1}, 10 m day^{-1}, respectively (see Gruber et al. (2011) for a complete set of parameters). Particulate organic carbon is formed through phytoplankton growth and is lost through zooplankton respiration and the remineralization of the two detrital pools. Within the organic carbon pool, phytoplankton mortality feeds into the small detritus pool, while zooplankton mortality and phytoplankton excretion is routed to both the small and large detritus pools with constant proportions. Coagulation of phytoplankton with small detritus as well as coagulation of small detritus with small detritus also forms large detritus, while no disaggregation is considered in our NPZD model, i.e., large detritus cannot disaggregate back into small detritus. Bacterial remineralization of organic matter is modeled as an implicit process through the definition of constant remineralization rates

and takes place both in the water column and in the sediments. The sediments act as a temporal buffer in our model, receiving the organic matter from the water column, and then slowly remineralizing it back to its inorganic constituents, which are released back immediately to the overlying water column. Neither burial nor sediment resuspension is considered. As the model does not include an explicit DOC pool, our modeled total organic carbon corresponds to POC only. However, the small detritus, given its very small sinking speed, behaves essentially as a suspended POC pool, i.e., shares many similarities to DOC. To assess the possible implications of our neglecting DOC, we run a sensitivity experiment where we turned the small detritus pool into essentially DOC by setting its sinking velocity to zero and by reducing it coagulation rate.

In order to optimally model the long-range transport of organic matter from the CanUS to the open North Atlantic, we employ a newly developed Atlantic telescopic grid (Figure 1) that covers the full Atlantic basin (-60°N to 70°N) while having a strong focus in resolution toward the north-western African coast. This was achieved using a conformal mapping that moves one pole of the ROMS grid over Northwest Africa (4°W, 20°N) and the other over Central Asia (75°E, 37°N). The grid has a dimension of 813 x 397 with a resolution that goes from a full eddy resolving 4.7 km near the African coast to a relatively coarse 50 km in the western South Atlantic and in the Caribbean (Figure 1). Within the CanUS region as defined in our analysis, the resolution ranges between 4.7 km at the coast and 19.5 km. In the vertical, we are considering 42 terrain following (sigma) levels with a surface refinement that allows to have a better vertical resolution in the euphotic layer. We use a new vertically stretched grid that transitions more rapidly from a pure terrain following orientation to a more horizontal orientation in order to reduce spurious mixing in the stratified open ocean.

2.2 Boundary Conditions

The coupled ROMS+NPZD model was run with monthly mean climatological forcing at the surface including the fluxes of heat and freshwater, solar shortwave radiation, wind stress and atmospheric pCO_2. All forcings were derived from ERA-Interim reanalysis (Dee et al., 2011), with the exception of atmospheric pCO_2, which was computed from the GLOBALVIEW marine boundary layer product (GLOBALVIEW-CO_2 (2011), see Landschützer et al. (2014) for details). A detailed description of the data sources used for the forcing is provided in Appendix A: Datasets, Table A1a and Table A1b. We next describe some corrections we had to apply to the forcing.

The ERA-Interim-based shortwave radiation and total heat flux fields have been shown to be biased high in regions of persistent cover with stratocumulus clouds (Brodeau et al., 2010). This is particularly relevant in the southern subregion of the CanUS, where stratocumulus are very pervasive and not well represented in the ERA-Interim ~~reanalyses~~reanalysis. We thus apply corrections to the original ERA-Interim reanalysis fields, taking advantage of the work by the Drakkar community (Dussin et al., 2016). They have already developed corrected forcing fields, i.e., the Drakkar Forcing Sets (DFS) (Dussin et al., 2016) on the basis of the ERA-Interim reanalysis (Brodeau et al., 2010), providing the corrected fields for the downwelling surface ~~shortwave~~ short wave radiation (DSWR) and downwelling surface ~~longwave~~ long wave radiation (DLWR). We thus compute correction masks ourselves, using the difference between the DFS and the uncorrected ERA-Interim data sets as the basis. Concretely, we first computed monthly means of the DFS daily climatology DSWR and DLWR. The monthly climatological means of the same two variables from ERA-Interim for the period were then used as a reference to calculate correction masks

(C) for each month by simply differencing, i.e., $C_{dswr} = ERA_{dswr} - DFS_{dswr}$ and $C_{dlwr} = ERA_{dlwr} - DFS_{dlwr}$. These correction masks were then regridded to our grid and applied to our ERA-Interim-derived monthly climatological mean forcing solar radiation (S) and total heat flux (TH) so that $S' = S - C_{dswr}$ and $TH' = TH - (C_{dlwr} + C_{dswr})$.

Another correction to the forcing regards the regions with sea ice cover at the northern boundary of the domain. Here we account for freshwater and latent heat fluxes associated with sea ice formation and melting by correcting the surface fluxes of the model forcing. An offline correction for the forcing was calculated from the ERA-interim sea ice fraction (c) and NSIDC sea ice drift ($\boldsymbol{u}$) monthly climatologies. Using these two datasets, the corrections to the freshwater flux (F_{fw}) were calculated according to Haumann et al. (2016), but simplified by using monthly mean climatologies, a constant sea ice thickness h_0 = 1.5 m and a sea ice density ρ_{ice}= 910 kg m^{-3}. An analogous equation was used to calculate the correction to the heat flux (F_h), so that: $F_h = \rho_{ice} L \cdot h_0(\partial(Ac)/\partial t + \boldsymbol{\nabla}(Ac\boldsymbol{u}))$ where A is the grid box area, and L the latent heat of fusion of water. The heat flux is constrained throughout the model simulation, so that the surface temperature cannot drop below the freezing temperature (Steele et al., 1989), which prevents strong heat loss in sea ice covered areas.

River runoff in the form of monthly climatological data (Dai et al., 2009) was also added to the freshwater fluxes. River sources were regridded to the closest ocean grid point and spread to a number of adjacent ocean grid points that depends the order of magnitude of the incoming flux to avoid numerical problems.

The model was run with open lateral boundaries at all grid boundaries confined by water, including at the Strait of Gibraltar. These climatological monthly lateral boundary conditions were prepared the same way as in previous studies (Lachkar and Gruber, 2013). A detailed description of the datasets used for the boundary conditions can be found in Appendix A: Datasets, Table A2.

2.3 Simulation and Analysis

The model was initialized to be at rest with temperature, salinity, nitrate, and the inorganic carbon parameters corresponding to the mean climatological value of December and January. The remaining biogeochemical variables were initialized to small non-zero values. The model was then run forward in time for a total of 35 years, using the monthly climatological forcing described above. We use the first ~~30~~ 29 years as spin-up, and undertake our ~~analyses~~ analysis using the last 6 years (years 30 to 35) of the simulation. This permits us to obtain a good representation of the climatological mean state of the CanUS, i.e., to average out the substantial intrinsic variability present in the setup.

To quantify the offshore transport of organic carbon including all its biogeochemical transformations, we undertake a full budget analysis, calculating all fluxes of organic carbon within each grid box and between all adjacent boxes. ~~Physical fluxes~~ The organic carbon budget analysis fluxes include physical fluxes through the boundaries of the boxes ~~include~~ and the integrated biological flux within each box. Physical fluxes include: vertical and horizontal advective fluxes in the three directions, vertical mixing ~~(eddy-diffusive) fluxes~~ fluxes associated with the eddy diffusivity and the vertical sinking flux. ~~Convective mixing was disregarded as it is small.~~ The net biological flux of organic carbon within each box is equivalent to the ~~net community production~~ Net Community Production (NCP), i.e., the net amount of carbon added or removed by biological activity, computed by summing all organic carbon production processes (phytoplankton growth) minus the sum of all processes that convert

organic carbon back to inorganic forms (respiration and remineralization). In our analysis we disregarded the contribution of the horizontal and vertical mixing associated with the background diffusivity. We also used a fixed depth for the sigma layers that define the box boundaries, disregarding their vertical oscillations. Both approximations can result in small residuals in the budget analysis.

For the whole CanUS, defined as the region between 9.5°N and 32°N, we have defined two layers of 3-dimensional large-scale boxes. Each depth layer has a constant thickness of 100 m, very close to the mean depth of the euphotic layer in the CanUS region (98.7 m), so that our analysis spans in total the first 200 m of depth. Each depth layer is subdivided into the same five offshore boxes up to 2000 km distance from the north-west African coast according to the following ranges of distances: (1) 0 to 100 km from the coast, narrow "coastal box" directly influenced by the coastal upwelling; (2) from 100 km to 500 km offshore; (3) from 500 km to 1000 km offshore; (4) from 1000 km to 1500 km offshore; (5) from 1500 km to 2000 km offshore.

To highlight the different roles of the three fundamental zonal bands in the CanUS, we ~~have~~ divided the EBUS into three subregions (Southern, Central, Northern), maintaining for each subregion the same five offshore domains as for the previous analysis and considering only the euphotic layer (0 m -100 m). Subregional boundaries were placed at 17°N and 24.5°N. ~~The subregional box analysis was done for the euphotic layer only (0 m -100 m)~~This allows us to distinguish between three regimes of circulation and production of the CanUS: a northern subregion dominated by coastal upwelling and coastal filaments, a southern tropical subregion, and a central subregion where the Canary and Mauritanian Currents converge to form the Cape Verde front (Pelegrí and Peña-Izquierdo, 2015). The lateral extension of the full CanUS boxes and of the subregional boxes is presented in Figure 3 together with the pattern of the modeled currents.

3 Evaluation

The model represents well the general circulation of the whole Atlantic Basin with a particularly good agreement ~~of~~ between the modeled Sea Surface Height (SSH) ~~with~~ and the observed one (Appendix B: Supplementary figures, Figure B1). ~~This is remarkable given the lateral extension and the stretching of the grid on which ROMS was run.~~ Less well modeled is the SSH in the eastern side of the North Atlantic Gyre and in particular in the Gulf Stream region. Especially problematic is the too ~~late~~ northerly separation of the Gulf Stream from the North American coast, a problem shared with many ocean general circulation models. These deviations are likely connected to our relatively coarse resolution in that part of the domain (Figure 1). But they occur far away from the region of interest, and are thus considered tolerable for the purpose of this study. The SST pattern is also well represented; differences are concentrated in the near equatorial region and are probably connected to a weaker equatorial circulation and a possible residual overestimation of the net heat flux in this region despite the correction we applied to the original forcing.

A zoom on the North-East Atlantic region allows us to evaluate the representation of the variables in our region of study, i.e., the CanUS. Here, modeled annual mean SST (Figure 2a) and SSH (Figure 2b) are well reproduced with a clearly visible signature of low SSH and cold water along the African coast as a result of the Ekman upwelling. Some differences in SSH

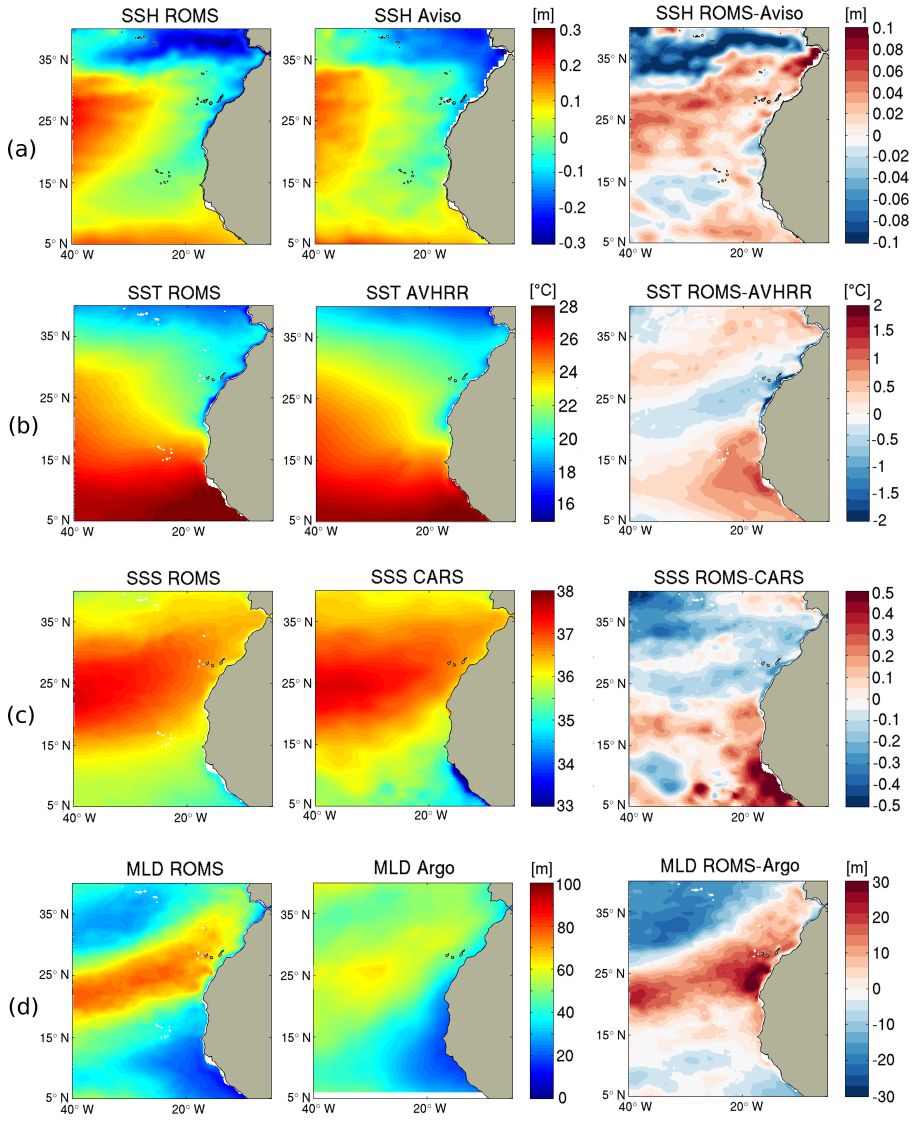

Figure 2. Evaluation of the modeled annual mean fields in the CanUS region. (a) Sea Surface Height (SSH); (b) Sea Surface Temperature (SST); (c) Sea surface Salinity (SSS); (d) Mixed Layer Depth (MLD). Left column: model; Middle column: observations; Left column: difference between model and data. A detailed description of the data used for the evaluation is provided in Appendix A: Datasets, Table A3.

are discernible at the northern boundary owing to the eastward flowing Azores Current being located slightly more south than observed. A slight shift south is also visible at the southern boundary. Despite the stratus cloud correction, the modeled SSTs are still a bit too warm in the southern sector of the CanUS~~, but~~ . However, differences between model and observations ~~rarely exceed~~ are limited to the interval [-0.75°C,1°C~~and the latter are very confined to the nearshore. Modeled~~] over the large majority of the domain, with a large fraction of this bias having a range of only ±0.5°C. Larger differences are confined to

a very narrow coastal band. The model also captures the observed Sea Surface Salinity (SSS, Figure 2c) well~~reproduces the observed fields~~; relevant negative differences are only observed in the southern CanUS, in ~~correspondence to~~ connection with the warm SST bias, ~~with a consequent~~ resulting in a compensation of the density. Overall, we consider these biases to be small relative to the spatial and temporal variations, therefore we expect these SST and SSS biases to have a minor impact on the conclusions of our study.

The modeled annual mean Mixed Layer Depth (MLD, Figure 2d) ~~shows sharper gradients than the observed~~ is consistent with the general pattern of the Argo-based MLD product, even tough the ~~general pattern is consistent with the observations~~modeled pattern has sharper gradients. Deeper than observed values of the MLD are visible in the northern sector of the CanUS and in the nearshore waters of the southern sector of the CanUS. It is ~~also~~ worth noting that the Argo dataset ~~is provided~~ was generated on a relatively low resolution grid, i.e., 2°x 2°, and thus is likely underestimating lateral gradients. In addition, the float coverage in Eastern Boundary Current system is relatively low, owing to the strong currents and the offshore transport, making the Argo-based MLD product vulnerable for biases in these regions. Nevertheless, some of the differences are likely real, as they appear also in other products. This is particularly the case for the overestimation of MLD in the nearshore region of the southern CanUS ~~. Also the general overestimation of MLD by the model along a~~ and in the long strip extending southwestward from the Canary Island~~is likely real, possibly connected to the~~ , possibly due to biases in the position of the large-scale currents as evidenced by the ~~biases~~ differences in SSH (Figure 2a).

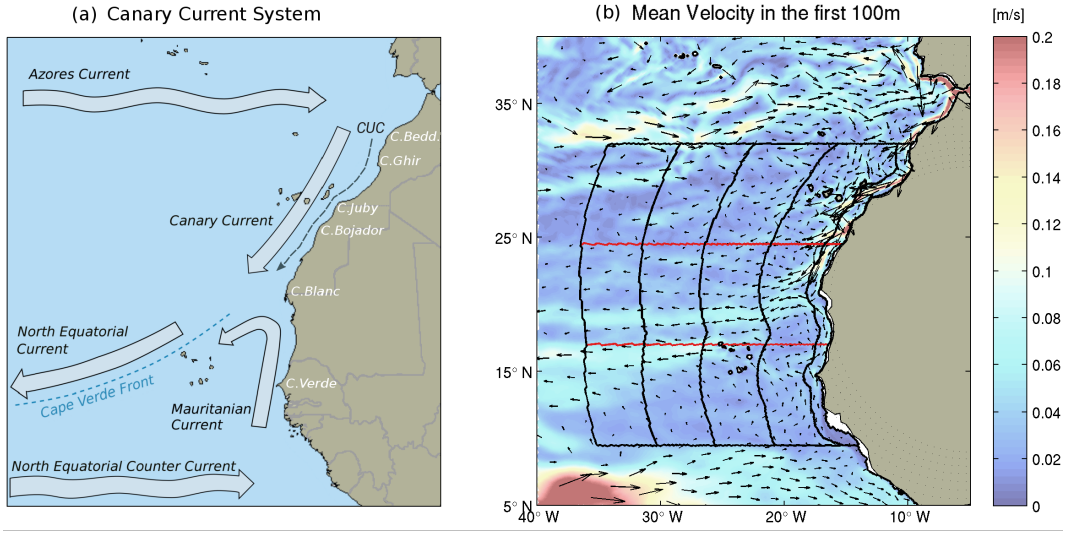

Figure 3. Maps of the circulation of the Canary Current System. (a) Schematic depiction with major currents adapted from Arístegui et al. (2009); (b) Modeled system of currents: vertically averaged flow in the first 100 m depth. Black lines represent the boundaries of the budget analysis regions for the Full CanUS analysis, while red lines indicate the 2 extra subregional boundaries ~~for the subregional budget analysis~~. The Full CanUS covers the region between 32°N and 9.5°N. Subregional boundaries are at 17°N and 24.5°N. From East (African coast) to West boxes span the following ranges of offshore distances: 0 km-100 km, 100 km-500 km, 500 km-1000 km, 1000 km-1500 km, 1500 km-2000 km.

The modeled annual mean circulation averaged over the first 100 m of depth corresponds well to the system of currents described schematically in Mackas et al. (2006) and Arístegui et al. (2009) (Figure 3). The Canary Current System is delimited on the northern edge by the eastward flowing Azores Current and on the southern edge by the eastward flowing North Equatorial Counter Current. Within these boundaries two currents flow in opposite directions along the African coast: the Canary Current (CC) flows southward between Cape Beddouza (33°N) and Cape Blanc (21°N), while the weaker and seasonal Mauritanian ~~current~~ Current (MC) flows northward between 10°N and Cape Blanc (21°N). Between the CC and the African coast, an intense and narrow Canary Upwelling Current (CUC) flows southward along the shelf (Mason et al., 2011). A poleward undercurrent (not shown) flows along the whole North African coast with its core typically centered at 200 m - 300m depth (Pelegrí and Benazzouz, 2015). Next to Cape Blanc, both the ~~Canary Current and the Mauritanian Current~~ CC and the MC detach from the coast and flow offshore forming the Cape Verde frontal zone, a natural boundary for the flow of water masses and tracers in the region. This front divides the region into a northern so-called Moroccan subregion and a southern Mauritanian-Senegalese subregion that differ in both physical circulation and biological activity.

~~The overall~~ The offshore gradients in annual mean sea surface chlorophyll (CHL) are well captured by the model (Figure 4a) ~~. This is especially the case~~ in the northern CanUS, where the absolute values are ~~captured well, even though the model is slightly biased low~~very close to the observations. Less well captured is the surface CHL in the productive southern sector of the CanUS, where the model ~~underestimates the observed surfaceCHL substantially~~substantially underestimates CHL at the surface. This is also the region ~~in which~~ where the model is biased too warm and salty, and where the modeled MLD exceeds the expected near-zero value, suggesting that this low surface CHL ~~bias is real and not simply a result of uncertainties in the satellite retrievals in this region, owing to frequent cloud cover and difficult optical conditions in the water column~~is primarily consequence of our physical biases in circulation and vertical stratification.

Our analysis of the vertical CHL distribution reveals that in the southern CanUS the modeled CHL has a deep maximum located between 20 m and 50 m depth, while little of the CHL is found in the surface layer (see Appendix B: Supplementary figures, Figure B2). The depth of the modeled CHL maximum is deeper than what can be expected for this region, according to local surveys. This deep bias of the chlorophyll maximum, and therefore of production, may be connected to the too deep modeled mixed layer in the surroundings of the Cape Verde Islands, a region in which the observed MLD is very shallow, or to a too fast depletion of the nutrients at the upper edge of the nutricline. This deeper than observed primary production may result in a less intense lateral transport of CHL in this subregion given the decline of the advective currents with depth. This potential limitation will be discussed in depth in throughout the paper.

Modeled vertically integrated chlorophyll (not shown) as well as total annual Net Primary Production (NPP) (Figure 4b), show instead intense biological activity in the southern CanUS, where NPP reaches values higher than in the northern subregion, especially offshore. However, modeled values of NPP are lower than the SeaWiFS VGPM estimates by about 3-fold. Other NPP estimates such as those based on SeaWiFS CbPM and Modis-Aqua VGPM provide substantially lower estimates of primary production that are slightly closer to our modeled values, but the comparison does not substantially change the picture (a detailed descriptions of all the used datasets is provided in Appendix A: Datasets, Table A3). Despite this underestimation, the pattern and the offshore gradient of the modeled NPP agree with the estimates and allow us to discuss the impact of the

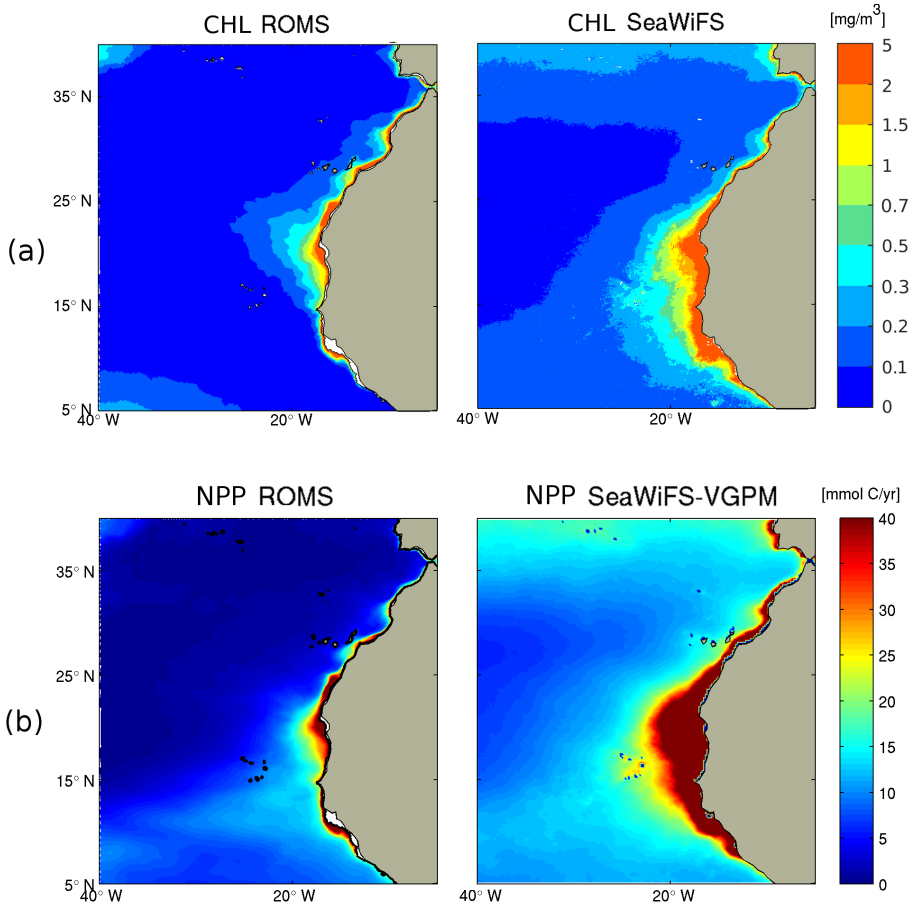

Figure 4. Maps evaluating the modeled chlorophyll and primary production in the CanUS. (a) Comparison of annual mean surface chlorophyll (CHL) between ROMS (left column) and SeaWiFS (right column). (b) Comparison of annual vertically integrated Net Primary Production (NPP) between ROMS (left column) and the VGPM estimate on the basis of the SeaWiFS data (right column). A detailed description of the data used for the evaluation is provided in Appendix A: Datasets, Table A3.

organic carbon fluxes in terms of relative changes in the local carbon availability. A nearly homogeneous 3-fold increase of the modeled NPP would in fact not affect this analysis, even though it would likely change the absolute values of the fluxes of organic carbon that may exceed those found by our study.

Modeled Particulate Organic Carbon (POC) concentrations have annual mean values between 5 mmolC/m^3 and over 20 mmolC/m^3 in the first 100m depth of the very productive shelf areas laying therefore in the range of in situ observations (Alonso-González et al., 2009; Arístegui et al., 2003; Santana-Falcón et al., 2016; Fischer et al., 2009). Concentrations decline in the offshore direction with a pattern similar to that of NPP and have maximum values located between 20 m depth in the shelf area and 70 m depth offshore. The modeled POC compares well to the limited in situ data (see Appendix B: Supplementary figures, Figure B3) especially with regard to the vertically-integrated stocks in the first 100m. However, due

to our coastally-confined production combined with the fact that cruise data were mostly collected offshore, and due to the deepening of the chlorophyll maximum in the southern productive subregion, we observe a deeper-than-expected POC maximum in the model, in agreement with the vertical bias in CHL. Due to the absence of sediment resuspension and of a mechanism of disaggregation of the large detrital particles in the model, deep peaks of POC such as those present in Alonso-González et al. (2009) and Álvarez-Salgado and Arístegui (2015) are not observed in the annual mean modeled POC concentration~~; this limitation and its potential repercussion on the lateral organic carbon transport will be discussed in depth in the Discussion section~~.

A further important evaluation concerns the seasonal cycle, especially since the CanUS is characterized by the most intense seasonal variability among all EBUS (Chavez and Messié, 2009). The first 2 columns of Figure 5 show a comparison between model and observations of the seasonal variations of the circulation in the CanUS averaged in the first 15m, the depth of integration of the drifters. The plot reveals that the modeled CanUS circulation agrees well with the data collected by the drifters on the seasonal scale. As expected, an enhanced offshore flow is visible in summer in the northern Moroccan subregion and in winter and spring in the southern Mauritanian-Senegalese subregion. The alongshore Canary Current is clearly visible in the northern sector of the CanUS. The Mauritanian Current seems to be weaker than observed especially in summer and to a smaller extent in fall. However, the Mauritanian Current is clearly visible in Figure 3b, in which the simulated flow is vertically integrated over the first 100m depth. Vertical sections of the modeled meridional flow (not shown) also show a clear northward flow corresponding to the Mauritanian Current below 10m depth. The modeled Mauritanian current is therefore slightly deeper than observed, possibly due to a deeper MLD observed in the southern CanUS coast (see Figure 2). The seasonality of the Equatorial Counter Current (NECC) is well represented, even though its modeled flow in summer and fall is less intense than in the drifters data. The weaker than observed circulation in the southern sector of the CanUS will be taken into account in the discussion of the model results.

Since we are interested in quantifying the offshore fluxes of organic carbon throughout the upper few hundreds meters, vertically-integrated NPP is a better measure than surface Chlorophyll for evaluating the capacity of our model to reproduce the expected pattern of organic carbon~~than surface Chlorophyll~~. NPP in the CanUS is strongly influenced by the pattern of currents: the Cape Verde Frontal Zone separates a southern area of extended offshore production from a northern subregion ~~characterized by a strong offshore decline in productivity (Arístegui et al., 2009)~~in which productivity declines offshore (Arístegui et al., 2009). Both previous studies and SeaWiFS estimates show that productivity in the northern CanUS is dominated by a summer peak, while productivity in the southern CanUS shows a peaks in late winter and spring (Pelegrí et al., 2005; Pastor et al., 2013). This seasonality and subregional variability is well represented by our model at all latitudes of the CanUS. In both model and observations, the southern Mauritanian-Senegalese subregion is the most productive area of the CanUS and is characterized by a reduced offshore gradient of NPP, while the northern Moroccan subregion is characterized by a sharp offshore gradient of production. The convergence of the coastal currents in the region of Cape Blanc fuels a persistent offshore bloom (Auger et al., 2016) that clearly appears both in the SeaWiFS product and in the model.

As visible from the Taylor Diagrams (Appendix B: Supplementary figures, Figure B4 ~~) the nice~~ and Figure B5) the agreement between the pattern of the physical and biological variables of interest is also confirmed by the good correlation between

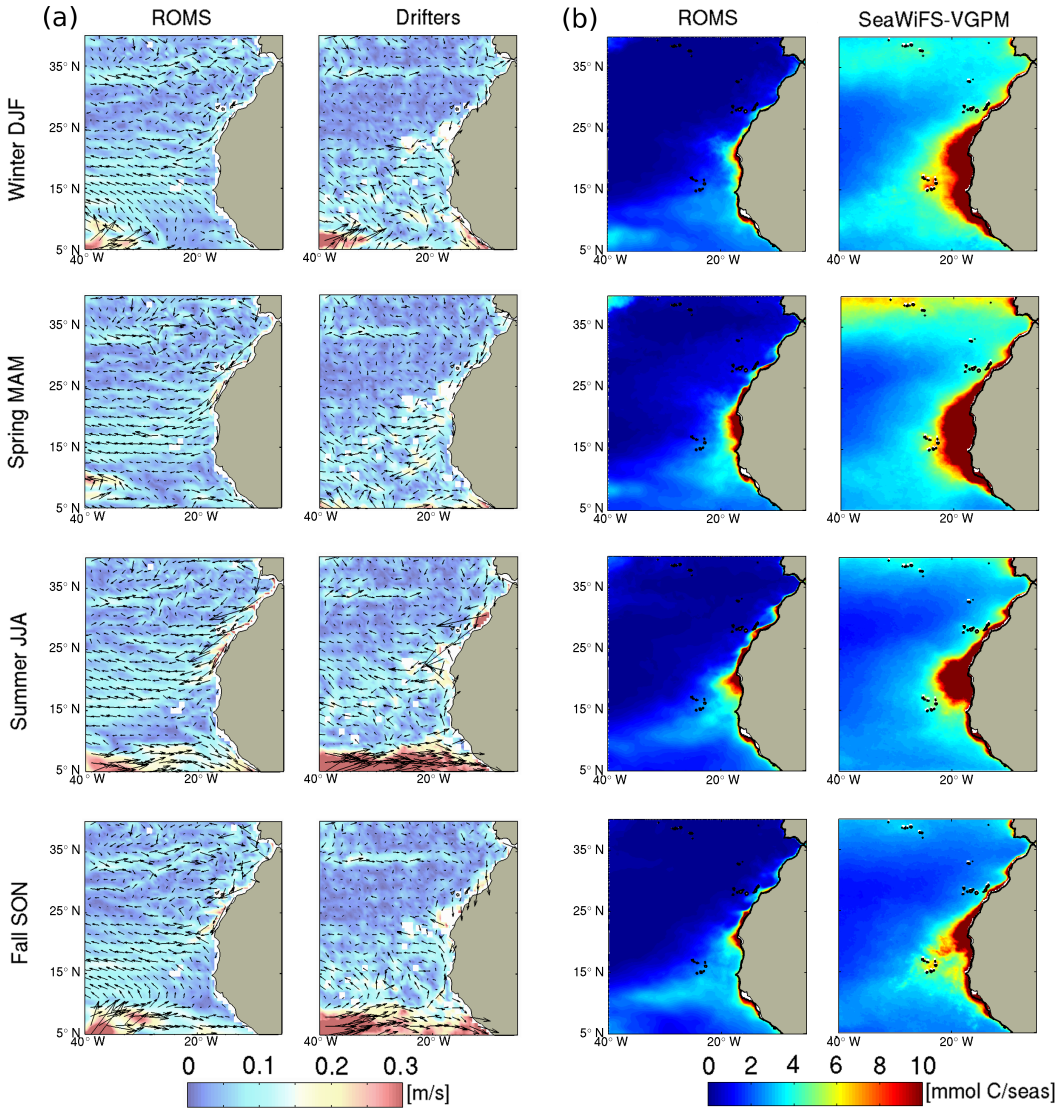

Figure 5. ~~Subplot~~ Panel (a): Circulation in the ~~EBUS~~ CanUS by season. ROMS (left column) and drifters (right column)~~, (Lumpkin and Johnson, 2013)~~]. ROMS output was integrated in the first 15m depth to be comparable with the ~~drifters observations~~drifter data. ~~Subplot~~ Panel (b): Vertically integrated Net Primary Production (NPP) from ROMS (right) and SeaWiFS VGPM estimate. A detailed description of the data used for the evaluation is provided in Appendix A: Datasets, Table A3.

modeled and observed fields ~~both~~ for both the annual and the seasonal means. All the variables have a correlation of 0.7 or higher with the observations in the annual ~~and~~ mean (except cruise data POC) and 0.68 or higher in the seasonal~~means. The annual meanTaylor diagram shows values of correlation and relative standard deviation for~~ . In the annual mean, the values of the normalized standard deviations are particularly high for annual mean MLD (1.5), which is, as discussed above, due to

a combination of too low variations in the Argo-based observational product and overestimation of the MLD variations by the model. Low values of the normalized standard deviations (STD) are observed for surface POC (0.65), CHL (0.6) and for net primary production (NPP1) (0.35), the latter corresponding to NPP from the SeaWiFS VGPM product. This is likely due to the weaker intensity of the modeled blooms. Interestingly, if modeled NPP is compared to the SeaWiFS CbPM product (NPP2), the normalized STD increases to 0.75, reflecting the rather large uncertainties in the NPP inferred from observations . In the annual mean, values of correlation and normalized STD for MLD, SST and CHL are comparable to those presented for the CanUS in the ROMS+NPZD study by Lachkar and Gruber (2011), despite the the boundaries of our grid being much further away, and therefore ~~them~~ providing much less ~~contraints~~ constraints on the modeled physics and biology in the region of interest. When compared to ~~similar studies using~~ studies that used ROMS+NPZD in other upwelling systems such as the California Upwelling System (Gruber et al. (2011), whole domain), our Taylor diagram shows a slightly worse correlation and comparable ~~standard deviation~~ normalized STD of surface CHL in the annual mean but a better seasonal representation, while modeled NPP has comparable performances.

In summary, the evaluation revealed that our modeling system is well suited to investigate the offshore transport of organic matter from the nearshore regions of the CanUS into the North Atlantic. It also showed a couple of shortcomings, especially with regard to our lack of explicit consideration of the role of DOC, and a model biases in a few regions, especially in the southern part of the CanUS. We will investigate and discuss the impact of these shortcomings in the discussion section below.

4 Results

4.1 NCP: Linking sources and sinks of Organic Carbon

The simulation reveals in the long term mean a strong onshore-offshore difference in the vertically integrated NCP, here $\int$NCP, i.e., primary production minus respiration/remineralization integrated from the bottom of the ocean up to the surface including remineralization in the sediments ~~, i.e., $\int$NCP~~ (Figure 6a).

The full water column $\int$NCP is negative across nearly the entire eastern subtropical North Atlantic, while only a narrow strip of less than 100 km along the north-western African coast and a few offshore regions in the southern part of the domain have positive values. This implies that the majority of the region is net heterotrophic, as within each column of water including the sediments more organic matter is being consumed than what is being produced locally. In contrast, the shelf regions of the CanUS are characterized by high levels of organic carbon production that exceed local consumption in the total water column and sediments, leading to a positive $\int$NCP and therefore an excess of organic carbon, which is available for lateral export.

A very different offshore gradient exists if NCP is just integrated over the top 100 m (Figure 6b). Despite the full water column heterotrophy of the offshore waters, the top 100 m of the CanUS have a positive NCP at every latitude and distance from the coast, i.e., are, on average, a net source of organic carbon. In contrast, NCP integrated from 100 m depth downward (Figure 6c) is everywhere negative, i.e., this part of the water column and the underlying sediments are net heterotrophic. Thus, the negative $\int$NCP of the offshore waters (Figure 6a) arises from the excess of respiration at depth over the net production in the overlying surface ocean.

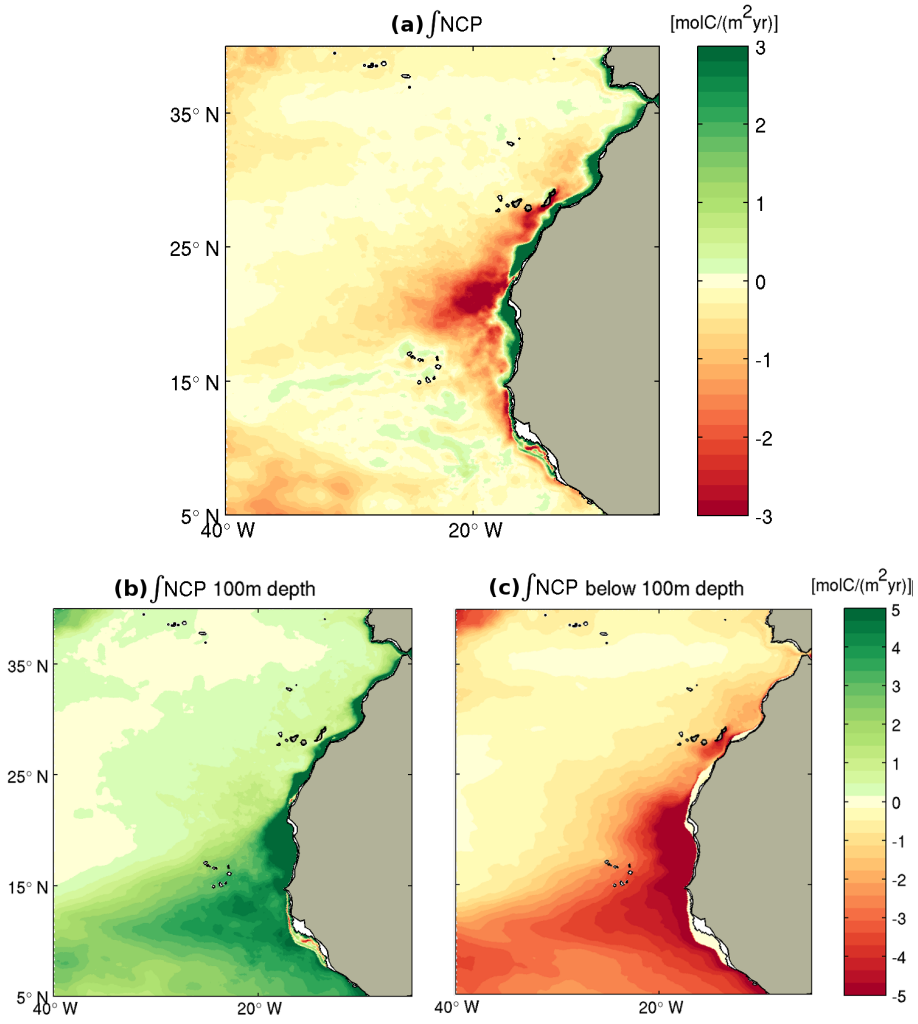

Figure 6. Maps of vertically integrated net community production including sediment remineralization. (a) NCP integrated over the full water column ~~including sediment remineralization~~(∫NCP). This represents the net amount of organic carbon available for lateral redistribution. (b) NCP vertically integrated over the top 100 m only, including sediment remineralization. (c) As (b), for the depth range from 100 m to the bottom. Green indicates positive ∫NCP (net source of organic carbon) while red means negative ∫NCP (net sink of organic carbon).

This switch between positive and negative NCP in the CanUS happens on average at ∼60 m in the nearshore regions deepening to ∼100 m in the offshore region, separating a layer of high net production from a layer of intense net respiration (Figure 7a). This depth corresponds very closely to the euphotic zone depth, here defined by the level at which the light intensity at the surface is attenuated to 1%. Furthermore, this is also just below the depth of the maximum organic carbon concentration (Figure 7b). In the upper 100 m, the majority of this organic carbon stems from small detritus and phytoplankton, while below

that depth and particularly in the nearshore areas, the large particles dominate. The contribution of zooplankton to the total organic carbon pool is substantial, but never dominant (see Appendix B: Supplementary figures, Figure B6).

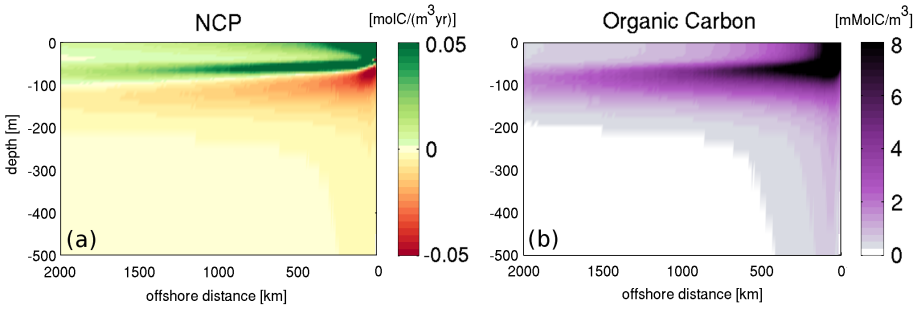

Figure 7. Mean vertical sections of (a) NCP and (b) ~~organic carbon concentration~~ POC in the Canary EBUS, averaged meridionally along lines of equal distance from the coast between 9.5°N and 32°N.

Since there is no substantial accumulation of organic carbon in the long term mean in any of the reservoirs, this onshore-offshore gradient in $\int$NCP requires a ~~substantial~~ considerable amount of organic carbon that is transported from the shelf region into the open subtropical North Atlantic. To understand this complex spatial pattern of autotrophic and heterotrophic activity in the region we next quantify the lateral and vertical fluxes of organic carbon in the CanUS.

4.2 Long-range offshore transport of organic carbon

The dominant nature of the offshore transport of organic carbon from the northwestern African shelf becomes clear by inspecting the annual mean and meridionally averaged section of the zonal flux of organic carbon (Figure 8a). This transport is nearly everywhere negative, indicating a westward, i.e., offshore transport, with the exception of the very nearshore region, where the narrow upwelling cell recirculates the organic carbon back onshore. This offshore flux spans the entire 2000 km range of distances from the coast in the first 200 m of depth, resulting in a continuous displacement of the organic carbon from the nearshore waters to the open sea. Only in the very nearshore region, the narrow upwelling cell causes the zonal flux to recirculate the organic carbon onshore.

~~In the vertical direction, the~~ The intensity of the offshore flux is maximum at the surface, and generally decreases with depth, except for the offshore regions, where a secondary maximum of zonal offshore transport occurs at around 100 m. Below that depth, the transport decreases rapidly and tapers off to very low values below 200 m with the exception of first 500 km from the coast. While the surface maximum of the offshore flux is mainly driven by the intense mean zonal velocity, the intensification of the flux around 100 m in the offshore waters is strongly influenced by the pattern of the organic carbon concentration (Figure 7b).

The lateral meridional flux (Figure 8b) ~~is weaker than the zonal flux and going downward and offshore has~~ shows a complex alternation of northward and southward fluxes~~. In particular~~, emerging from the integration of the meridional transport across a wide meridional band. Even though this flux is weaker than the zonal flux, this does not imply the absence of substantial

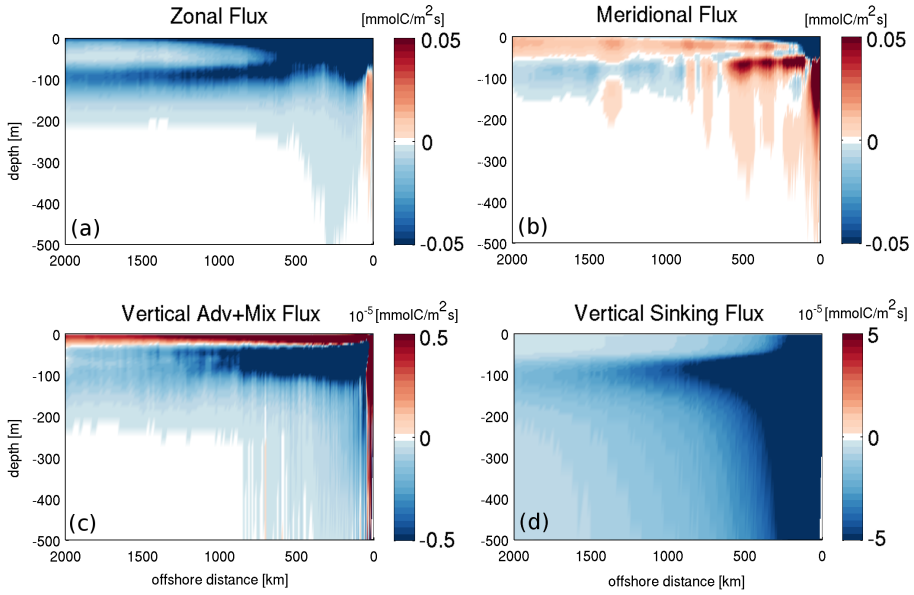

Figure 8. Mean vertical sections of the physical fluxes of organic carbon in the Canary EBUS, averaged meridionally along lines of equal distance from the coast between 9.5°N and 32°N. (a) Zonal flux of organic carbon with positive values indicating eastward (onshore) transport. (b) Meridional flux of organic carbon with positive values indicating northward transport. (c) Sum of vertical advective and mixing (eddy-diffusive) fluxes with positive values meaning upward transport. (d) Vertical sinking flux with negative values indicating downward transport. Note the different scales in the different panels.

alongshore currents within the domain. In fact, many of these get averaged out by the meridional integration. Despite this, the intense southward flowing Canary Current ~~results in~~ is still visible as a negative signature of the mean meridional flux near the coast~~, while northward~~. Northward fluxes, probably linked to an influx from the organic carbon-rich near equatorial region, are dominant further offshore.

The vertical advective and mixing (eddy-diffusive) fluxes (Figure 8c) are overall much weaker than the vertical sinking flux (Figure 8d). The latter, as expected from the fact that we employ constant sinking speeds has a pattern that reflects directly that of the organic carbon concentration (Figure 7b). In contrast, the fact that the vertical advective and mixing fluxes depend on the mean circulation results in a more complex pattern. These fluxes are positive both near the coast in response to the strong upwelling and in the upper first tens of meters where the vertical mixing redistributes the organic carbon against its vertical gradient. Below this shallow layer, subduction and downward mixing are dominant and contribute to the export of organic carbon to depth.

Reflecting the relative contribution of the different pools to the total organic carbon, the fluxes below the first 200 m as well as the vertical sinking flux are dominated by the contribution of the large detritus that reaches deep into the water column declining in concentration in the offshore direction. In the first 200 m, abundant small detritus, phytoplankton and to a smaller extent zooplankton shape the organic carbon fluxes up to the farthest boundary of the analysis domain.

4.3 The organic carbon budget

The annual mean budget ~~for~~ of organic carbon for the upper waters of the whole CanUS highlights the key contribution of the offshore flux to the enhancement of the organic carbon pool and the maintenance of the heterotrophic activity in the open waters (Figure 9a and Figure 10a). In the upper 100 m corresponding roughly to the euphotic layer, the offshore flux is the dominant lateral flux at all distances with a magnitude that always exceeds 10 % of the integrated NCP within the box (Figure 9a). More specifically, at 100 km from the coast the offshore flux of organic carbon transports as much as 1.6 Tmol C yr^{-1} (18.7 Tg C yr^{-1}), a quantity that amounts to more than a third of the integrated NCP in the 0 km-100 km range, i.e. the first coastal box, and to 18 % of the Net Primary Production, NPP_{100km} = 8.6 TmolC yr^{-1}.

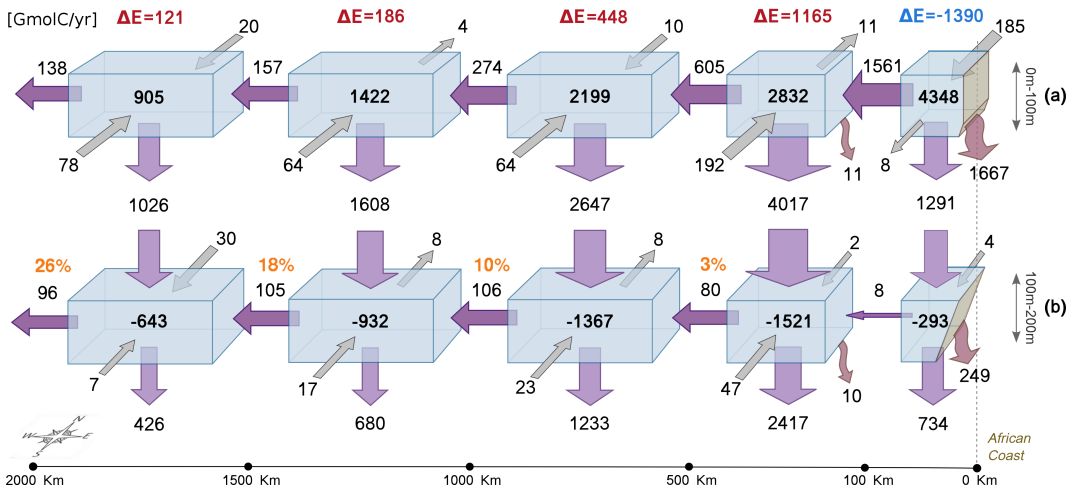

Figure 9. Annual mean Organic carbon budget for CanUS as a whole in units of GmolC yr^{-1} for (a) the top 100 m, and (b) for the 100 m-200 m depth range. The lateral extension of the budget analysis boxes is shown in Figure 3b. The African coast is located on the right edge of the x-axis, with the offshore distance indicated at the bottom. Numbers inside the boxes represent the net biological flux in the volume (integrated NCP). The Arrows between boxes represent physical fluxes with the dimension of the arrows being scaled according to the magnitude of the fluxes. Lateral fluxes are advective, vertical fluxes are divided into fluxes between boxes (straight arrows, advective+mixing+sinking) and sinking fluxes to the sediments (bent arrows). The symbol ~~Δ~~ ΔE = Vertical Export - NCP in (a) is a measure of the excess vertical export in each box with ~~$\Delta > 0$~~ $\Delta E > 0$ indicating that the vertical export exceeds local NCP. The orange percentages in (b) represent the fraction of non-respired influx from above that is exported offshore.

A good measure for the magnitude and impact of the lateral redistribution of organic carbon is the difference between the organic carbon that is produced locally through NCP, and the amount of organic carbon that is exported vertically out of the euphotic zone (here ~~taken as the~~ 100 m). In the absence of any lateral redistribution, this difference, termed excess export, i.e., ΔE = Vertical Export - NCP is zero, while in the case of a strong lateral export of the organic matter, ΔE is negative since less carbon is available for the vertical export at depth. Conversely, if a particular region is importing a large amount of organic carbon through lateral transport and then exporting this carbon to depth, then the excess export ΔE is positive.

The analysis of ΔE as a function of offshore distance reveals that all regions have a positive ΔE with the exception of the nearshore one, whose ΔE is instead negative (Figure 9a). Thus, this supports the notion that the net heterotrophic activity over the whole water column in the offshore direction is fueled by a strong net growth in the very nearshore region of the CanUS. The magnitude of the excess export at depth ΔE ranges between 41 % of NCP in the 100 km-500 km range to 13 % of NCP in the most distant region (orange solid line of Figure 10a) accounting for hundreds to thousands of Gmol of organic carbon per year. This excess export of organic carbon below 100m is explained by the divergence of the lateral fluxes. ~~This divergence~~ In particular, the divergence of the offshore flux (Figure 10a, purple solid line) releases in each region an amount of organic carbon that constitutes between 8 % and 34 % of the local NCP, with the highest value in the 100 km-500 km offshore range, and explains with this organic carbon accumulation from 62 % to 80 % of the excess export at depth in the first 1500km offshore ~~(Figure 10a, purple solid line)~~. In the most distant analysis region (1500 km-2000 km range) the offshore flux divergence drops, resulting in a significant export of organic carbon through the 2000 km offshore boundary and little accumulation; this flux may impact the biological activity even farther in the North Atlantic Gyre.

The alongshore ~~(N-S)~~ lateral fluxes also positively contribute to the total budget with a net influx of organic carbon in the euphotic layer (Figure 9a, blue solid line)). However, the divergence of the alongshore flux exceeds 10 % of the local NCP only in the most distant analysis region ~~(blue solid line of Figure 10a)~~ and represents therefore a minor ~~contribute~~ contribution to the excess export at depth.

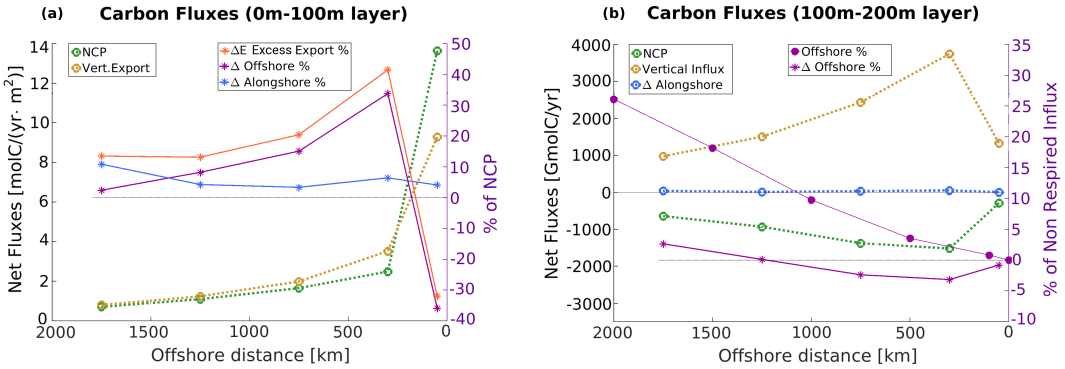

Figure 10. Main flux trends in the CanUS as a function of offshore distance for (a) the top 100 m and (b) for the 100 m-200 m depth range. In both panels: dotted lines refer to the left y-axis, solid lines refer to the right y-axis. Quantities represented by solid lines are expressed as percent of the significant carbon source for the layer, respectively: NCP for the top 100 m in (a), and the non-respired influx of carbon for the 100 m-200 m depth layer in (b). Δ fluxes represent the divergence of the fluxes: net amount of carbon accumulated or removed by the flux in each box. All net fluxes are binned at the center of the box of reference (e.g., fluxes in the 0 km-100 km region are binned to 50 km offshore), except for the offshore flux in panel (b), which refers to the boundaries of the boxes. Note that in panel a, the vertical export is a negative flux and that the yellow dotted line refers to its magnitude, and that ΔE is the excess vertical export as in Figure 9a). In panel b, the non respired influx is computed by summing the vertical influx, the alongshore flux, and NCP.

The fate of the vertically exported carbon in the very biologically active 100 m-200 m depth layer is still strongly influenced by the offshore transport (Figure 9b), except for the nearshore, where the upwelling cell recirculates the organic carbon onshore. The offshore flux intensifies moving away from the coast, reaching its maximum at 1500 km distance from the coast, where its intensity becomes comparable to that of the top 100 m. Given the negative contribution of NCP to the organic carbon budget in this layer, the magnitude and divergence of the offshore flux at this depth can be compared to the non-respired influx of organic carbon, i.e., the amount of incoming carbon that is available in each box after remineralization. The main sources of organic carbon at this depths are the incoming vertical flux from the euphotic layer and to a very small extent the divergence of the lateral alongshore flux (respectively yellow and blue dotted lines of Figure 10b). Therefore, the non-respired influx is defined as the sum of the incoming vertical flux, the divergence of the alongshore flux and the negative NCP.

If we compare the offshore flux at the boundary of the boxes to the non-respired influx in each box we see that the offshore flux moves a substantial amount of the organic carbon available, reaching 26% at 2000 km distance from the shore (purple solid line with circles of Figure 10b). At the same time, due to its intensification in the direction of the open sea, the offshore flux does not release carbon in the boxes as confirmed by its negative divergence up to 1500km offshore distance (purple solid line with stars of Figure 10b and percentages in orange in Figure 9b), but it traps it and transports it even farther toward the open waters. The 100 m-200 m depth layer of the CanUS is therefore still characterized by a significant offshore transport that moves the organic carbon towards the oligotrophic center of the North Atlantic Gyre, furthering water column heterotrophy there.

As the offshore fluxes are small below 200 m (Figure 8a), we omitted them from the plot. In fact, the maximum contribution to the total offshore transport of the water column below 200 m, accounting for a few kilometers of depth, is 12 % reached at 500 km of distance from the shore. This fraction quickly declines offshore to a minimum of only 0.4 % at 2000 km of distance from the shore. Thus, the vast majority of the transport occurs in the top 200 m of the water column in our model.

4.4 Subregional variability of the organic carbon fluxes

Substantial ~~zonal~~ meridional differences in both biological activity and circulation characterize the CanUS and influence the pattern of ~~the~~ vertically integrated NCP (see Figure 6) and the implied lateral organic carbon fluxes ~~. Latitudinal gradients in net primary production and in the distribution of sources and sinks of organic carbon emerge from the plot of vertically integrated NCP (Figure 6~~. In the euphotic layer the pattern of production changes with latitude transitioning from a sharp offshore NCP gradient in the northern CanUS to an wide offshore extent of high NCP in the southern CanUS. These gradients can be explained by the pattern of the nutrients fluxes (see Appendix B: Supplementary figures, Figure B7). In ~~its northern portion, the CanUS is~~ the northern CanUS, nutrients are in fact mostly provided by coastal upwelling, while the positive signature of the wind-stress curl in the southern CanUS favors Ekman pumping of nutrients also offshore (Figure B7c). Intense production in the surroundings of Cape Blanc is likely due to the convergence of the alongshore nutrient fluxes (Figure B7b), in agreement with Auger et al. (2016) and Pastor et al. (2013).

Below 100m, the northern CanUS is characterized by a weak offshore gradient of deep respiration ~~and a~~ which, combined with a sharp offshore gradient of production in the ~~euphotic layer , resulting~~ layer above, results in an extended net water column

heterotrophy in the open waters. In contrast, the southern CanUS is characterized by a widespread vertical correspondence between shallow sources and deep sinks of organic carbon that result in a ~~nearly neutral water column~~ vertically integrated NCP of nearly zero ($\int$NCP$\sim$ 0), with negative values of $\int$NCP confined only between the African shelf and the Cape Verde archipelago. Between these two zonal bands with distinct $\int$NCP signatures, the central CanUS located in the surroundings of Cape Blanc (21°N) and the whole Cape Verde frontal zone are hot-spots for the respiration of the organic carbon. Here, the region of deep intense remineralization extends farther offshore than the area of intense near-surface productivity, resulting in a vast peak of negative $\int$NCP that reaches far into the North Atlantic Gyre. To identify what processes drive the organic carbon redistribution that give rise to these $\int$NCP gradients and quantify the ~~contribute~~ contribution of the different zonal bands to the total transport we analyze in detail the spatial patterns of the physical fluxes of organic carbon.

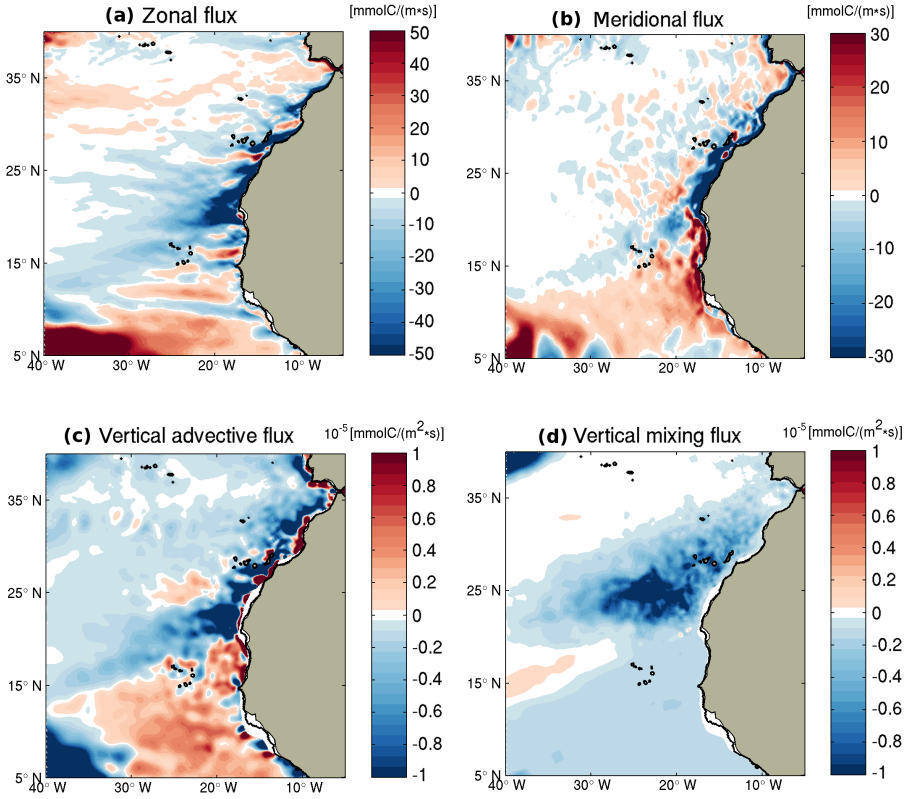

Figure 11. Maps of the organic carbon flux components in the top 100 m corresponding ~~roughly~~ to the euphotic layer in the CanUS. (a) Zonal flux vertically integrated over the top 100 m with positive values indicating eastward (onshore) transport~~.~~; (b) as (a), but for the meridional flux with positive values indicating northward transport~~.~~; (c) vertical advective flux across 100 m with positive values indicating upward transport~~.~~; (d) as (c) but for vertical mixing. Plotted vertical components were smoothed with a 7x7 grid points 2-dimensional filter.

Subregional differences in the organic carbon transport are visible in all of the components of the physical fluxes (Figure 11). Both zonal and meridional fluxes integrated over the top 100 m are clearly influenced by the regional pattern of currents (see

also Figure 3b) and change sign in the proximity of the Cape Verde frontal zone, the crucial boundary between the northern anticyclonic and the southern cyclonic circulation. ~~Above~~ North of the Cape Verde front, the zonal flux is mostly offshore and intensifies moving towards Cape Blanc likely due to both the intense coastal mesoscale activity that culminates at 21°N with the giant Cape Blanc filament and to the formation of the Cape Verde front (Arístegui et al., 2009). South of Cape Blanc, ocean striations appear in the form of alternate onshore and offshore flux bands. The meridional transport converges around Cape Blanc, again with a sharp inversion of sign that reflects the direction of flow of the Canary Current and the Mauritanian Current.

The 100 m horizontal section of the vertical advective transport of organic carbon reflects the signature of the wind stress curl that is negative north of the Cape Verde front and positive to the south. As a consequence, the highest values of advective export at depth are found in the northern regions of low offshore production, while vertical advective export of organic carbon is not favored in the very productive southern subregion. As for the offshore transport, also the vertical advective export in the northern CanUS sector and on the Cape Verde frontal zone is likely enhanced in the first few hundreds of kilometers by the abundant coastal filaments that quickly channel and downwell the coastally produced organic carbon. The vertical mixing fluxes of organic carbon across 100 m shows that this component is important only in the northern subregion characterized by a much deeper MLD, and declines offshore with the decrease of the organic carbon concentration. Sinking fluxes through the 100m depth are not shown as their pattern is mostly proportional to the ~~100m-integrated~~ 100 m-integrated NCP (Figure 6b) with high export in regions of high production and do not add substantial complexity to the discussion. However, it is worth remarking that their intensity is about one order of magnitude higher than that of the vertical advective and vertical mixing fluxes, reaching very intense peaks ($\sim$-40 molC/(m^{2}day)) in the surroundings of the most productive region of Cape Blanc, and high values of about -10 molC/(m^{2}day) in the Mauritanian-Senegalese subregion. The southern sector of the CanUS is therefore dominated by intense sinking fluxes of organic carbon, while both non-sinking vertical components of the export have a very limited role in the organic carbon export in the region ~~below~~ south of Cape Blanc.

The analysis of the spatial pattern of the organic carbon fluxes also remarks the special role of the central zonal band located between the Canary Archipelago and the Cape Verde Islands, characterized by the most intense biological and physical fluxes. This central zonal band is characterized by the strongest heterotrophic activity offshore, a persistent and intense offshore transport, a convergence of the lateral alongshore fluxes in the shelf, strong vertical advective export at depth, intense vertical mixing and a peak of the sinking flux. To highlight how differently the physical fluxes impact the organic carbon budget at different latitudes and to study the interaction between significant zonal bands in the CanUS we divided the region into southern, central and northern subregions (defined as in Figure 3b) and carried out a subregional box budget analysis.

Among the CanUS subregions, the Southern subregion (pink line of Figure 12) is characterized by very high levels of NCP in the euphotic layer also in the open waters (Figure 12a) accompanied by a relatively low impact of the physical fluxes of carbon on the local budget. In fact, despite both the offshore transport and the vertical advective+mixing export below 100 m have high intensities in absolute terms, their divergences are low when compared to the high values of NCP in each box and therefore they do not have a substantial impact on biology (Figure 12b and Figure 12d). On the one side, the little accumulation of organic carbon due to the offshore flux explains the large portion of biologically neutral water column in this region ($\int$NCP$\sim$0, see

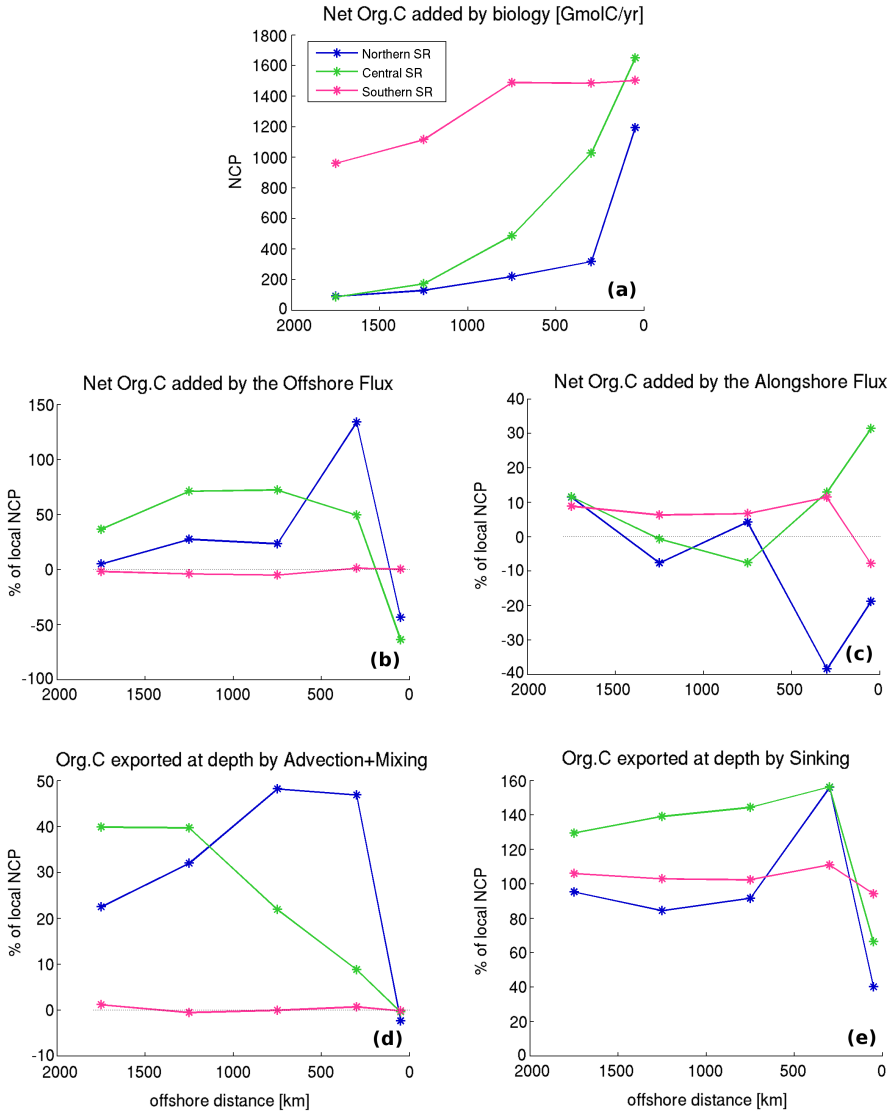

Figure 12. Trends of NCP and impact of the organic carbon fluxes ~~(divergence of the flux / NCP)~~ by subregion and offshore distance in top 100 m as a function of offshore distance. (a) ~~XXX ADD description~~ NCP [GmolC/yr]; (b) Divergence of the offshore transport in % of NCP; (c) Divergence of thealongshore transport in % of NCP; (d) Export below 100m by advection and mixing in % of NCP; (d) Export below 100 m by sinking in % of NCP. Fluxes in the plots are binned at the center of the box of reference (eg, fluxes referring to the 0 km-100 km box are binned to 50 km offshore on the x-axis).~~NCP is integrated through the whole volume of each box. Flux impacts, i.e., the net amount of organic carbon added in each box by the divergence of the flux, are expressed in percent of the local NCP.~~

Figure 6a). On the other side, even though the sinking fluxes (Figure 12e) still export substantial amounts of carbon in this subregion, the low efficiency of the advective+mixing export points to a potentially limited capacity of this subregion to export

at depth dissolved and suspended material (not modeled in our study). The comparatively higher impact of the alongshore flux is explained by the strong coupling of the southern subregion with the equatorial carbon rich area that allows a net influx of organic carbon through the southern boundary.

The impact of the lateral offshore transport in the Northern subregion (blue line of Figure 12) is particularly high in the first 500 km offshore (Figure 12b). This is the result of a combination of both strong export fluxes on the shelf and of the fast decline of NCP in the offshore direction, with a consequent high ratio of the offshore flux divergence to NCP and an important influence of the flux on the local budget. The intense mesoscale activity in this northern subregion, especially in the form of persistent filaments that detach from the coast and quickly ~~channell~~ channel water and tracers offshore typically for some hundreds km, has an important role in this intense nearshore export. The northern subregion is also the most efficient in the vertical advective+mixing export up to 1000 km offshore as a consequence of the deep MLD and the abundant mesoscale coastal filaments, with a consequently high capacity to export light organic carbon species below the euphotic layer. However, both the lateral and the vertical export efficiency decline quickly moving offshore in the northern subregion. This decline is likely due to the low organic carbon concentration of the offshore waters, to the limited offshore extension of the filaments and to the incoming flux of the Azores Current counteracting the offshore transport at the northern edge of the domain.

As anticipated, the most active area in terms of the organic carbon transport and export is the central CanUS subregion (green line of Figure 12), which includes the Cape Verde frontal zone. The central subregion collects the lateral alongshore fluxes from the northern and southern subregions in the nearshore area, with a net increase of the carbon availability in the first coastal box (0 km-100 km range) of more than 1/3 of the local NCP (Figure 12c). The southward flowing Canary Current and northward flowing Mauritanian Current that converge in this zonal band are the main contributors to this organic carbon influx on the coast around Cape Blanc. The carbon collected on the shelf is likely exported offshore together with the locally produced carbon by a very intense zonal flux characterized also by a large divergence that exceeds the values of the northern subregion in the offshore waters (Figure 12b). The carbon accumulation due to the divergence of the offshore transport over the central zonal band is on average as high as 57 % of the local NCP, reaching peaks of more than 70 % of NCP in the 500 km-1500 km range and still accounting for 37 % of NCP in the farthest offshore box (1500 km-2000 km range). Both the mean circulation characterized by the westward flowing currents along the Cape Verde front and the mesoscale activity in the form of the giant Cape Blanc filament are expected to contribute to this intense offshore transport. As a consequence of this increased carbon availability, the central subregion allows very high values of the total vertical export of carbon below the euphotic layer (advective+mixing+sinking transport), which almost doubles the local production. Among these vertical components, the advective+mixing vertical export becomes particularly important in the offshore waters. The alongshore convergence of the organic carbon on the shelf and the high lateral mobility of the organic carbon in the offshore direction of the central subregion not only explain the peak of net water column heterotrophy in the offshore waters around Cape Blanc (see Figure 6a), but they characterize the Cape Verde frontal zone as a key region of the CanUS for the collection and export of the coastally produced organic carbon far into the North Atlantic Gyre.

Further insights in the zonal differences of the organic carbon transport below the euphotic layer are given by the zonally averaged mean vertical profiles of the offshore and vertical advective+mixing fluxes for each subregion (Figure 13). The

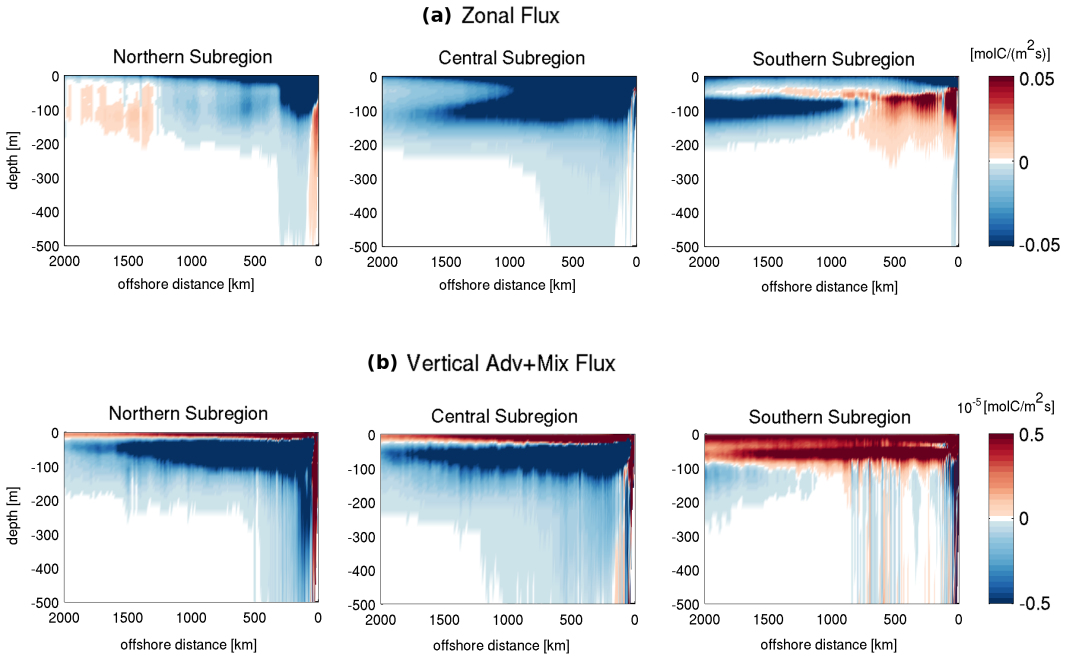

Figure 13. Vertical sections of the organic carbon offshore flux (a) and vertical advective+mixing flux (b), averaged meridionally along lines of equal distance from the coast in each subregion in accordance to the zonal bands defined by the budget analysis boxes. In all the plots the horizontal x-axis represents the distance from the coast (km); the ~~vertcal~~ vertical y-axis represents the depth (m). Subplot (a) Zonal flux: positive means eastward (onshore); Subplot (b) Vertical advective + mixing (eddy-diffusive) flux: positive means upward.

southern subregion is confirmed to be the least efficient in the offshore transport and vertical advective+mixing export also at depth, despite an intensification of the offshore flux below the surface in the farthest region of analysis. This offshore intensification is however probably connected to the intersection of our southern zonal band with the Cape Verde frontal region which crosses the northern boundary of this subregion at about 1000 km offshore. The vertical advective+mixing export in the southern subregion is also remarkably different from the other subregions: not only the shallow MLD limits vertical mixing but the positive signature of the wind stress curl favors upwelling in this subregion. The mean vertical profiles of the zonal flux for the northern subregion shows clearly in the offshore waters below the surface a weak onshore flux that confirms the important influence of the incoming Azores current in the limitation of the offshore transport away from the coast. The deep extension of both the offshore flux and of the vertical advective+mixing downwelling in the first few kilometers from the coast of the northern subregion suggests again the link with the recurrent coastal filaments that characterize this sector of the CanUS and are known to enhance the fluxes through a depth of several hundreds of meters (Arístegui et al., 2009). The central subregion presents also at depth the most intense and persistent offshore flux that reaches 2000 km from the coast in the whole first 200 m layer, remarking the important role of this subregion for the offshore redistribution of the organic carbon. Both offshore and advective+mixing fluxes extend particularly deep into the water column in the first several hundreds of

kilometers from the coast in the central subregion, likely due to both the intense mean circulation and the powerful giant Cape Blanc filament renown for its remarkable offshore extension (Gabric et al., 1993; Fischer et al., 2009). In both the northern and central subregions the offshore gradient of the zonal flux is the cause of the important accumulation of organic carbon that allows an enhanced respiration at depth.

The results of our subregional analysis show how physical forcing, mean and mesoscale circulation drive the lateral and vertical redistribution of the organic carbon in the CanUS, giving rise to a persistent offshore transport of organic carbon that shapesthe $\int$NCP pattern and can reach as far as 2000 km into the North Atlantic Gyre. Further insights into the special role of mesoscale activity in the lateral redistribution of organic carbon in the CanUS and a quantification of this component of the transport will be provided in detail in a dedicated publication.

5 Discussion

~~The results of our modeling study~~

5.1 Implications and comparison with previous work

Our results highlight the importance of the lateral transport of organic carbon from coastal regions of intense production to the oligotrophic open waters and its key role in fueling the offshore heterotrophic activity~~, confirming~~. We thus confirm the predictions of several in situ observations and estimates from multiple independent local surveys ~~(Arístegui et al., 2009; Pelegrí et al., 2005). With our study we provide a detailed quantification of the total lateral transport in the whole CanUS and of its long-range influence.~~

~~The modeled offshore transport of coastal production lies in the range of previous estimates (Duarte and Cebrián, 1996), with about~~ (Arístegui et al., 2009; Pelegrí et al., 2005). Our modeled fraction of the coastal production of organic carbon that is transported offshore beyond 100 km amounts to 18% of ~~the phytoplankton~~ NPP (36 % of NCP) ~~being exported from the shelf to the open sea across the 100km distance line from the coast~~and lies in the range of previous estimates (Duarte and Cebrián, 1996). Our results ~~reveal also~~ also reveal that the offshore transport ~~does not decline to zero in the open ocean, where it still has~~ extends far offshore, having important consequences for the biological activity: the enhancement of the carbon availability due to the offshore influx can still be as ~~big~~ large as 37% of the local net community production between 1500 km and 2000 km offshore. The offshore transport is ~~relevant also~~ particularly relevant below the euphotic layer, especially in the 100m-200m layer, ~~allowing~~ where the lateral transport of the ~~sunk or downwelled organic carbon and reaching far~~ organic carbon can extend even farther into the North Atlantic gyre~~.~~

~~The offshore transport below 200 m is generally very small, and never larger than 12 % of the total transport. However, model limitations in the representation of the offshore transport at depths below the first few hundreds meters should be discussed taking into account three potential and partially contrasting caveats. First, the model does not include the process of sediment resuspension, therefore impeding the formation of deep spots of high POC concentration near the shelves (Inthorn et al., 2006a; Alonso-González et al., 2009) and limiting the bottom transport along the slopes~~

(Inthorn et al., 2006b; Hwang et al., 2008). Second, and with a similar effect, the dynamics of our particulate pools only allows the aggregation of small particles into bigger and heavier ones, while it does not allow disaggregation of heavy particles into lighter ones as a consequence of degradation or partial grazing (Alonso-González et al., 2010), resulting in a one-way path to fast sinking that cannot be reversed. Due to these two factors that preclude the existence of deep maxima of suspended POC, our study may underestimate the lateral transport of organic carbon at depth. Third, sinking velocities in our model are fixed at every depth to relatively small values (maximum of 10 m day^{-1} for large detritus), while sinking velocities have been observed to be able to reach relatively high values, increasing by roughly an order of magnitude between the mesopelagic and bathypelagic regions (Fischer and Karakaş, 2009; Berelson, 2002) with a consequent fast vertical export at depth of the particles by sinking. Heavy particles at depths below 1000 m have been shown to have mean sinking velocities of 100-300 m day^{-1} (Fischer and Karakaş, 2009) and to be often accompanied by a pool of slow sinking material with mean sinking velocities of 1 to a few m day^{-1}, resulting in a bimodal distribution of the sinking speeds (Alonso-González et al., 2010). Viewing these three caveats together, we have two missing processes that would cause the correct offshore transport to be larger than modeled, and one process that would cause the correct offshore transport to be smaller. We cannot assess the implication of this finding in full, but submit that at least with regard to the offshore transport in the upper waters, , i.e., upper 200 m, our model is likely in the right range. We have much less confidence in the offshoretransport below 200 m, where the observed concentrations of organic carbon can be quite high, although the offshore velocities are substantially smallerbeyond 2000 km offshore.

The total This long-range offshore transport that reaches in our model as far as 2000 km from the coast in the central subregion can be explained by two possibleschemes of interplay of biological and physical fluxes. In a first hypothesisof organic matter involves two possible, not mutually exclusive pathways. In the first "direct" pathway, the offshore transport is sustained entirely by the excess organic carbon produced on the African shelf, which then gets advected offshore up to the final boundary of our analysis domain getting only partially remineralized and exported at depth without the addition of "new", i.e., locally formed organic carbon along the way. In a second hypothesisthe second "recycling" pathway, the offshore flux of organic carbon is sustained by the production of organic carbon that happens along the way to the open sea: new and regenerated offshore production substitutes the incoming coastal replaces the incoming organic carbon that gets remineralized and sinks at to depth in a continuous rejuvenation recycling of the organic carbon that is advected offshore. This offshore production would be sustained by nutrients either upwelled near the coast and advected offshore or by nutrients obtained The nutrients required to fuel the production stem from either from the upwelling along the coast and subsequent offshore transport and/or from the local remineralization of the incoming carbonorganic matter. The vertical pumping of the nutrients from the deeper waters offshore would be significant only in regions of positive wind stress curl (in our case only the southern CanUS) or abundant in mesoscale eddies. A simple analysis of the residence times of the modeled organic carbon pools makes us inclined to sustain the second as well as the fact that alongside the organic carbon, also substantial amounts of nutrients are transported offshore favors a dominance of the second "recycling" hypothesis. In fact, a small detritus particle would likely reside in the first resides, on average, only about 200 days in the top 200 m depth layer on average about 200 days due to its sinking speed if we disregard advective and mixing downwelling downwelling and other loss terms such as remineralization; given typical lateral transport

velocities of less than 0.05 m/s when averaged ~~through~~ over the top 200 m~~depth~~, this particle would be able to travel at best only about 800km offshore. This distance ~~must be divided by 10 in the case of~~ is only 80 km for large detritus and ~~doubled~~ 1600 km in the case of phytoplankton~~, making it very~~ . If we further include the loss terms (coagulation and remineralization) of these organic carbon pools, which substantially reduce the life time, it is highly unlikely for the coastally produced organic carbon to reach as far as 2000 km in the open sea. Even though zooplankton is the only organic carbon species that ~~doesn't~~ does not sink in the model, its modest contribution to the offshore fluxes, compared to those of phytoplankton and of the abundant small detritus, cannot justify the magnitude of the observed lateral transport. Further~~analysis such as Lagrangian experiments coupled with the biological fluxes~~ , the inorganic nutrients fluxes (see Appendix B: Supplementary figures, Figure B7) are of sufficient magnitude to refuel new growth of organic matter to replace that part that is lost by sinking. Further analyses including Lagrangian experiments are necessary to gain a quantitative understanding of the succession of transformations happening along the way to the open waters.

~~Meridional~~ The meridional alongshore transport also contributes to the organic carbon redistribution, especially on the shelf~~region~~ , where we find the maximum intensity of the coastal currents. In line with the results of Auger et al. (2016) and Pastor et al. (2013) we find that the area around Cape Blanc, corresponding to the region of convergence of the coastal flows and formation of the Cape Verde frontal zone, is a key region of the CanUS. The relevance of the central Cape Verde frontal zone in the CanUS was discussed in Auger et al. (2016) and Pastor et al. (2013) in terms of chlorophyll and nutrient convergence on the shelf and of their subsequent offshore advection, visible as a persistent bloom in ~~correspondence~~ offshore of the Cape Blanc region. Here we confirm and strengthen ~~this observations~~these results, affirming that this sector of the CanUS has a central role in collecting the organic carbon produced on the shelf and then transporting ~~offshore coastally produced organic carbon, allowing intense water column heterotrophy at depth in its proximity~~it offshore. This offshore flux of carbon against the gradient of productivity extends far away from the coast and feeds the heterotrophic activity of the deep open waters for at least 2000 km of kilometers offshore, generating a long tail of net heterotrophy. Deep offshore transport and subduction in this region are likely enhanced by the persistent ~~giant~~ Cape Blanc filament, which is known from local surveys for being able to transport an estimated 50 % of the coastally produced carbon both in the surface and at depth, ~~reaching an extension of~~ extending several hundreds of km offshore (Gabric et al., 1993; Ohde et al., 2015).

The ~~natural~~ partition of the CanUS into a northern anticyclonic and a southern cyclonic circulation ~~and the subregional differences in both~~ regime and the differences in mesoscale activity and wind stress curl ~~(Arístegui et al., 2009) are reflected into~~ (Arístegui et al., 2009) are well reflected by the differences in the transport and cycling of the organic carbon north and south of the Cape Verde frontal zone. The ~~northern CanUS located above~~ portion of CanUS located north of the Cape Verde ~~frontal zone~~ front can be regarded as the very eastern edge of the North Atlantic Gyre ~~(Pelegrí et al., 2005), which receives from the shelf of this CanUS sector a relevant amount of organic carbon~~(Pelegrí et al., 2005). Several studies highlight the way in which the abundant coastal filaments of this northern CanUS sector substantially enhance the offshore transport and the downwelling of organic carbon in the first hundreds of kilometers from the coast (Álvarez-Salgado et al., 2007; Gabric et al., 1993; Fischer et al., 2009; García-Muñoz et al., 2005; Ohde et al., 2015). These structures together with a strong mean offshore flow explain the intense ~~modeled~~ zonal transport and the vertical downwelling in the shelf region of the northern

CanUS and ~~their sharp decline~~ the sharp decline of these two fluxes in the open waters. The range of influence of the offshore transport in this zonal band ~~may be~~ is further enhanced by ~~multiple eddies spun~~ the eddies spun off by the filaments (Barton et al., 2004), while the negative signature of the wind stress curl maintains the vertical downwelling ~~dominant also offshore. Our model overestimates the MLD depth and therefore potentially the mixing export at depth in this region (see section 3. Evaluation); however the observed MLD pattern still presents a strong meridional gradient with an extremely shallow mixed layer in the southern region below the Cape Verde front and deeper mixed layer in the north, favoring intense mixing~~in the offshore. The strength of ~~both the mixing and the advective vertical transport indicate~~ the vertical transport by downwelling and mixing suggests that the northern subregion is potentially efficient in exporting ~~at~~ to depth the dissolved, suspended and slowly settling material, i.e., the organic carbon species that are ~~also~~ difficult if not impossible to measure with sediment traps, but may still constitute the key component for the closure of the organic carbon budget at depth (Hopkinson and Vallino, 2005; Alonso-González et al., 2010). The ~~southern CanUS sector, located below~~ portion of CanUS located south of the Cape Verde ~~frontal zone,~~ front is instead mostly coupled to the southern equatorial circulation and to a much smaller extent to the Northern Atlantic gyre. Here, the net water column biological activity shows a dominantly neutral water column and little water column heterotrophy, the latter mostly confined to a region between the African coast and the Cape Verde archipelago. The intense near-surface production, the ~~reduced~~ much smaller offshore gradient in productivity ~~moving offshore~~ (NASA-OBPG, 2010) and to some extent the transitory nature of the filaments that form on the shelf at (Arístegui et al., 2009) result in a small impact of the organic carbon lateral fluxes. Sinking dominates the vertical export at these latitudes while mixing and vertical advection are impeded by a shallow MLD and the positive ~~signature of the~~ wind stress curl ~~. In this zonal band, our model shows a weaker than observed circulation and a deeper than observed chlorophyll and NPP maximum (see section 3. Evaluation) which may lead to an underestimation of the lateral transport and therefore of the net heterotrophy of the water column. Both a shoaling of the biological production towards the surface characterized by more intense currents and an intensification of the circulation may in fact result in the strengthening of the lateral zonal and meridional organic carbon fluxes. An increase of the offshore zonal fluxes in the southern subregion could favor a more heterotrophic water column only if accompanied by an increase of the divergence of the flux, resulting in a substantial accumulation of organic carbon compared to the local production. An intensification of the southern circulation and in particular of the Mauritanian current may likely increase the influx of organic carbon from the south into the Cape Verde frontal zone, fueling even further the respiration in this already strongly heterotrophic region.~~ leading to upwelling.

Overall, in ~~great~~ a large part of the CanUS the lateral redistribution of organic carbon from the shelf to the open waters results in a ~~lateral shift of the deep organic carbon sinks from the regions of high organic carbon~~ very substantial lateral shift of the region of remineralization from the region of production. This is in contrast with the representation of the organic carbon pump as a pure vertical process and highlights the fundamental importance of the lateral transport of organic carbon for the maintenance of the biological activity. ~~Despite this~~ However, despite the very large lateral input of organic carbon in the ~~first 100m~~upper 100 m across much of the offshore region of the CanUS, our model does not show evidence for ~~a net heterotrophic activity~~ net heterotrophic conditions in the near-surface waters ~~, therefore suggesting that~~ of these regions. Thus the shallow open sea is everywhere a net source of organic carbon for the deeper layers. ~~Vertical integration through~~

This is the case irrespective of whether the vertical integration is performed over the mean euphotic layer depth (100m), ~~through the punctual~~ over the local euphotic layer depth ~~and through the punctual~~ or over the local MLD (generally shallower than the euphotic layer)~~all agree on~~ . Thus, our model provides strong support for the net autotrophic surface ocean hypothesis (Williams et al., 2013). The spatial pattern of modeled near-surface ~~autotrophic activity~~ autotrophy (Figure 6b~~from Section 4.1) seems to agree with the "Calculated~~) agrees with the calculated global distribution of NCP ~~" from Williams et al. (2013) Figure 1~~from (Williams et al., 2013, Figure 1), once the net heterotrophic regions are substituted by weakly autotrophic low productive waters. The depth at which vertically integrated sinks and sources from top to bottom compensate each other in the model is almost everywhere located at more than 200m depth and can be deeper than 1000 m in regions of nearly neutral water column, confirming the importance of the respiration in deep waters (Del Giorgio and Duarte, 2002).

Both the mean Ekman transport and the turbulent mesoscale activity contribute to the total lateral fluxes of organic carbon connecting coastal sources to deep offshore sinks. The two concur also in determining the vertical downwelling and mixing that increase ~~of the carbon availability at depth. The~~ the organic carbon transport to depth. The magnitude of the relative contribution of these two terms to the organic carbon fluxes and their different role in fueling the heterotrophic activity offshore must be detangled through further analysis.

~~This paper provides a first comprehensive quantification of the lateral and vertical fluxes of organic carbon in the Canary Upwelling System (CanUS) up to 2000km offshore. The net community production vertically-integrated through the whole water column,~~

5.2 Limitations and caveats

We discuss here how our quantification of the offshore transport of organic carbon at the surface and at depth may be affected by a few shortcomings of the model. The first set of shortcomings involve our modeling of the organic matter pool, especially our lack of consideration of the an explicitly modeled DOC pool and the representation of POC at depth. The second set of shortcomings involve a few biases in our modeled physical/biogeochemical fields. We discuss the potential impact of these shortcomings in turn.

Regarding DOC, the pool that matters is that of semi-labile DOC as it has a life time of beyond a few days, implying that it can be transported substantial distances before it gets remineralized. As a result, it has the potential to enhance our modeled lateral export of organic carbon. This is especially the case since DOC is readily produced in the surface ocean and contributes also substantially to the export of organic matter from the near-surface ocean (Hansell, 2002; Arístegui et al., 2002; Hansell et al., 2009; Hansell and Carlson, 2015), in particular in subtropical regions such as the North Atlantic gyre (Torres-Valdés et al., 2009; Roussenov et al., 2006). Even though DOC is not explicitly modeled, the small detritus, with its sinking speed of w_{SD}=1 m day^{-1}, represents essentially a suspended POC pool with some similarity to a semi-refractory DOC, particularly regarding its susceptibility to lateral transport. But differing from DOC, the small detritus coagulates to large detritus resulting in a shorter lifetime than DOC in the surface ocean. At the same time, the rate of production of DOC is likely smaller than that of the small detritus, likely leading to a situation where the small detrital pool likely has a behavior that is rather close to that of DOC. Thus, we would argue that the impact of our shortcoming

of not representing the dynamics of DOC explicitly is smaller than possibly inferred at first sight. In order to explore more quantitatively the potential impacts of our lack of explicit consideration of DOC, we ran a sensitivity study, in which we set the vertical sinking of the small detritus, w_{SD},to zero and reduced the coagulation time scale for small detritus to 40% of its baseline value. No adjustments were made to the parameterization of the large detritus. This sensitivity study needs to be considered as an extreme scenario - i.e., it is meant to explore the potential contribution of DOC rather than an attempt to quantify it in detail. We spun up the model with the new biological parameters from year 24 of the baseline run (6 years of spinup) and used years 30-35 for the analysis, as for the baseline run. The results show, as expected, an intensification of the lateral fluxes of organic carbon in the euphotic layer. The standing stock of suspended POC increases about twofold, largely due to its longer average lifetime in the surface ocean, stimulating the local recycling of organic matter. This increases both primary production and heterotrophic activity in the near-surface layer, leaving the $\int$NCP ~~, reveals a net autotrophy ($\int$NCP>0) of the productive CanUS shelf and a net heterotrophy ($\int$NCP<0) of the offshore waters. However,~~ pattern basically unchanged and preserving the net autotrophy of the ~~shallow heterotrophic layer acts everywhere as an organic carbon source,~~ near-surface waters. In fact, even though the lateral transport of small detritus is much larger in this sensitivity study and reaching further out into the open North Atlantic, the net horizontal divergence of the lateral flux remains roughly the same. Thus, for the key question at hand, i.e., can the offshore transport fuel net heterotrophic conditions in the offshore regions of the Canary CS, the answer essentially remains the same.

Another potential caveat of our study regards the lateral redistribution of the organic carbon at depths larger than the first few hundred meters. On average, our modeled offshore transport below 200 m is very small, and never larger than 12 % of the total transport. However, model limitations in the representation of the offshore transport below this depth should be discussed taking into account three potential and partially contrasting caveats. First, the model does not include the process of sediment resuspension, therefore impeding the formation of high POC concentration spikes near the shelves (Inthorn et al., 2006a; Alonso-González et al., 2009) and limiting the bottom transport along the slopes (Inthorn et al., 2006b; Hwang et al., 2008). Second, and with a similar effect, the dynamics of our particulate pools only allows the aggregation of small particles into bigger and heavier ones, while it does not consider disaggregation of heavy particles into lighter ones as a consequence of degradation or partial grazing (Alonso-González et al., 2010), resulting in a one-way path to fast sinking that cannot be reversed. Due to these two factors that preclude the existence of deep local maxima of suspended POC, our study may underestimate the lateral transport of organic carbon at depth. Third, sinking velocities in our model are fixed at every depth to moderate values (maximum of 10 m day^{-1} for large detritus), while sinking velocities have been observed to be able to reach relatively high values, increasing by roughly an order of magnitude between the mesopelagic and bathypelagic regions (Fischer and Karakaş, 2009; Berelson, 2002) with a consequent fast vertical export at depth of the particles by sinking. Heavy particles at depths below 1000 m have been shown to have mean sinking velocities of 100-300 m day^{-1} (Fischer and Karakaş, 2009) and to be often accompanied by a pool of slow sinking material with mean sinking velocities of 1 to a few m day^{-1}, resulting in a bimodal distribution of the sinking speeds (Alonso-González et al., 2010).

Viewing these three caveats together, we have two missing processes that would cause our model to represent a lower bound estimate, and one process that would cause the correct offshore transport to be smaller. We cannot assess the implication of

this finding in full, but submit that at least with regard to the offshore transport in the upper waters, i.e., ~~is autotrophic. The horizontal displacement of major shallow sources and major deep sinks of organic carbon must be explained by an significant lateral redistribution of the organic carbon~~upper 200 m, our model is likely in the right range, perhaps on the lower side. We have much less confidence in the offshore transport below 200 m, where the observed concentrations of organic carbon can be quite high, although the offshore velocities are substantially smaller.

We also need to assess the potential impact of the physical/biogeochemical biases that we diagnosed in the Evaluation section. In the northern CanS our model overestimates the MLD depth; however our modeled MLD shows a meridional gradient that has the same trend as the observed one, with an extremely shallow mixed layer in the southern region below the Cape Verde front and deeper mixed layer in the north. This suggests that, even though we may potentially overestimate vertical mixing in the northern CanUS, this subregion would still be expected to be the only one in which this process is relevant. In the southern CanUS, our model shows a weaker than observed circulation and a deeper than observed chlorophyll and NPP maximum ,which may lead to an underestimation of the lateral transport and therefore of the net heterotrophy of the water column. Both a shoaling of the biological production towards the surface characterized by more intense currents and an intensification of the circulation can in fact result in the strengthening of the lateral zonal and meridional organic carbon fluxes. However, an increase of the offshore zonal fluxes in the southern subregion could favor a more heterotrophic water column only if accompanied by an increase of the divergence of the flux, resulting in a substantial accumulation of organic carbon compared to the local production. In the meridional direction, an intensification of the alongshore Mauritanian current may instead increase the influx of organic carbon from the south into the Cape Verde frontal zone, fueling even further the deep respiration in the already strongly heterotrophic central CanUS.

To summarize, we believe that the above-discussed caveats do not substantially affect our main findings. If anything they possibly strengthen our conclusion regarding the importance and long-range nature of the offshore transport of organic carbon. In fact our model may, if anything, underestimate the total lateral transport of organic carbon both at the surface and at depth. For this reason we believe that it is of fundamental importance to take into account the three-dimensionality of the marine organic carbon cycle and the essential role of the productive coastal ocean in the global biogeochemical cycles.

~~Long-range lateral~~

6 Conclusions

This paper provides a first comprehensive quantification of the lateral and vertical fluxes of organic carbon in the Canary Upwelling System (CanUS) up to 2000 km offshore.

The long-range lateral fluxes of organic carbon in the euphotic layer (~~0m-100m~~ 0 m-100 m depth) of the CanUS are dominated by the offshore flux that extends on average as far as ~~1500km~~ 1500 km into the North Atlantic Gyre. Along its way, the offshore flux adds to the euphotic layer an amount of organic carbon that corresponds from 8 % to 34 % of the alongshore average NCP, explaining from 62 % to 80 % of the excess vertical export, i.e., the export below the euphotic layer that exceeds the local production, and fueling extra heterotrophic activity at depth. In the ~~100m-200m~~ 100 m-200 m layer the offshore

transport of organic carbon continues to dominate the lateral fluxes, transporting always >8 % of the available organic carbon and intensifies away from the coast with potential repercussions on the biological activity of the North Atlantic Gyre interior.

This massive redistribution of organic carbon from the nearshore to the offshore makes the vertically-integrated net community production, i.e., $\int$NCP, strongly positive in the nearshore regions and strongly negative in the offshore. This implies, when viewed over the whole water column, that the nearshore regions are net autotrophic and the offshore regions are net heterotrophic. However, the upper ocean (down to more than 100 m) acts everywhere as an organic carbon source, i.e., remains autotrophic. Thus, our model demonstrates how critical it is to consider the depth interval over which the trophic state of a system is evaluated.

Strong subregional differences in the fluxes characterize the CanUS. ~~Above~~ North of the Cape Verde frontal zone, coastal production ~~declines quickly offshore and turns into a net water column heterotrophy of the open waters. Here, the sharp peak of negative $\int$NCP is fueled by a~~ quickly declines offshore, while strong offshore transport ~~near the coast likely favored the local abundance of mesoscale filaments~~by filaments fuels strong remineralization in the offshore regions, causing strong heterotrophic conditions downward of 200m. Mixing and vertical downwelling play an important role in the vertical export in this subregion, ~~potentially allowing~~ enhancing the export of ~~light and dissolved organic matter~~ small detrital material below the euphotic layer. ~~Below~~

South of the Cape Verde frontal zone high levels of near-surface production extend far offshore. Despite being the most productive area, the southern subregion ~~is characterized by a modest impact of~~ has a much more modest impact on the offshore flux ~~on the local carbon availability that results in an almost neutral water column~~ and also on the offshore rates of remineralization. This results in a water column that has almost a neutral trophic state ($\int$NCP$\sim$0). Vertical export at depth in this subregion is ~~carried on~~ driven mostly by sinking fluxes due to the shallow MLD and the positive wind stress curl signature.

The central zonal band of the CanUS ~~located above~~ which includes the Cape Verde frontal zone ~~and~~ bridging the northern and southern subregions is characterized by an alongshore convergence of organic carbon on the shelf. The accumulated organic carbon is laterally exported from the shelf by an intense offshore flux that along the way releases on average as much organic carbon as 57 % of the local NCP, fueling the most intense peak of water column heterotrophy of the entire CanUS. The offshore transport is pronounced also at depth especially in the first ~~500km~~ 500 km from the coast, while advective and mixing fluxes have an important role in the vertical export in this subregion. Both the intense offshore transport and downwelling of organic carbon may be enhanced by the ~~giant~~ very large and persistent Cape Blanc filament.

Our study highlights the strength of the coupling between the productive CanUS region and the adjacent oligotrophic open North Atlantic. Lateral fluxes, especially the offshore transport, are influenced by mean circulation, mesoscale activity and physical forcings and have an essential role in the fueling of the ~~open sea heterotrophic activity~~ heterotrophic activity in the open seas. Their impact on the local carbon availability fully explains the complex pattern of net sources and sinks of organic carbon of the CanUS region.

Appendix A: Datasets

a) Forcing datasets

Data source	Ref. time	Resolution	Variables	Reference
Era-Interim	1979-2010	N128 reduced Gaussian grid	freshwater flux, wind stress, net heat flux, net shortwave radiation	Dee et al. (2011)
GLOBALVIEW 2011	1998-2011	1°x 1°grid	atmospheric pCO_2	GLOBALVIEW-CO_2 (2011)

b) Datasets used for corrections to the forcing datasets

Data source	Ref. time	Resolution	Variables	Reference
DFS 5.2	1979-2011	0.7°x 0.7°grid	downward longwave radiation, downward shortwave radiation	Brodeau et al. (2010)
Era-Interim	1979-2011	0.75°x 0.75°grid	downward longwave radiation, downward shortwave radiation	Dee et al. (2011)
Era-Interim	1989-2009	1.5°x 1.5°grid	sea-ice fraction	Dee et al. (2011)
NSIDC Sea Ice Motion Vectors	1979-2006	25 km EASE-Grid	sea-ice drift	Fowler (2003)

Table A1. Description of the datasets used for (a) the model run main forcing, (b) datasets used for calculating stratus cloud an sea ice corrections to the main forcing. DFS: Drakkar Frocing Set; NSIDC: National Snow and Ice Data Center.

Boundary conditions

Data source	Ref. time	Resolution	Variables	Reference
WOA 2013	1955-2012	0.25°x 0.25°grid	temperature, salinity, nitrate	Locarnini et al. (2013), Zweng et al. (2013)
SODA v1.4.2	1958-2001	0.5°x 0.5°grid	momentum components, sea surface height	Carton and Giese (2008)
SeaWiFS	1997-2010	9km grid	sea surface chlorophyll	NASA-OBPG (2010)
GLODAP	-	1°x 1°grid	sea surface alkalinity, sea surface dissolved inorganic carbon	Key et al. (2004)

Table A2. Description of the datasets used for the model run lateral boundary conditions. WOA: World Ocean Atlas; SODA: Simple Ocean Data Assimilation; SeaWiFS: Sea-viewing Wide Field-of-view Sensor; GLODAP: GLobal Ocean Data Analysis Project.

Model evaluation

Data source	Ref. time	Resolution	Variables	Reference
Aviso CMDT Rio05	1993-1999	0.5°x 0.5°grid	sea surface height	Rio and Hernandez (2004)
AVHRR	1981-2014	0.25°x 0.25°grid	sea surface temperature	Reynolds et al. (2007)
CARS	1955-2003	0.5°x 0.5°grid	sea surface salinity	Ridgway et al. (2002)
Argo DT-0.2	1941-2008	2°x 2°grid	mixed layer depth	Montégut et al. (2004)
Drifters	1979-2012	0.5°x 0.5°grid	sea surface height	Lumpkin and Johnson (2013)
SeaWiFS	1997-2010	9km grid	sea surface chlorophyll	NASA-OBPG (2010)
SeaWiFS VGPM	1997-2010	9km grid	extrapolated net primary production (NPP)	Behrenfeld and Falkowski (1997)
SeaWiFS CbPM	1997-2010	9km grid	extrapolated net primary production (NPP)	Westberry et al. (2008)
SeaWiFS POC	1997-2010	9km grid	extrapolated surface particulate organic carbon (POC)	NASA-OB.DAAC (2010)
Modis-Aqua VGPM	2002-2016	9km grid	extrapolated net primary production	Behrenfeld and Falkowski (1997)
WOD09	-	rebinned to 0.5°x 0.5°grid	chlorophyll	Johnson et al. (2009)
AMT	(2004-2014)	in-situ [0m,200m] depth	particulate organic carbon	BODC-NERC (2014)
Geotraces	(2010)	in-situ surface	particulate organic carbon	GEOTRACES (2010)
ANT	(2005)	in-situ [0m,200m] depth	particulate organic carbon	ANT (2005)

Table A3. Description of the datasets used for the model evaluation. CMDT: Combined Mean Dynamic Topography; AVHRR: Advanced Very High Resolution Radiometer; CARS: CSIRO Atlas of Regional Seas; SeaWiFS: Sea-viewing Wide Field-of-view Sensor; WOD09: World Ocean Database 2009.

Appendix B: Supplementary figures

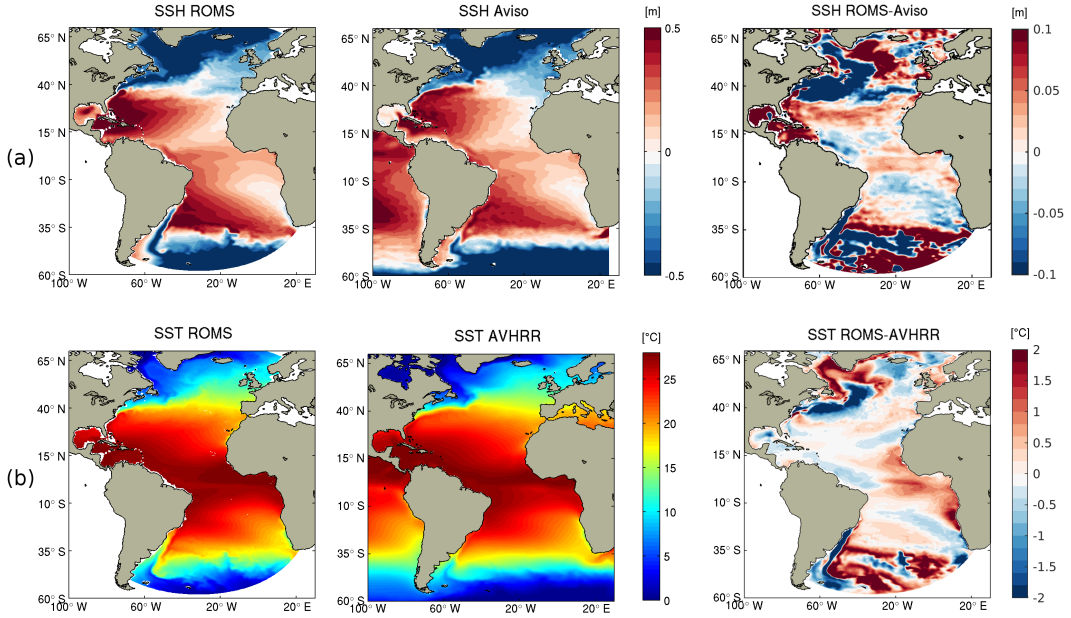

Figure B1. Mean Sea Surface Height SSH (a) and Sea Surface Temperature SST (b) from model and observational data, accompanied by a model-data difference plot in the full Atlantic Telescopic Grid domain. A detailed description of the data used for the evaluation is provided in Appendix A: Datasets, Table A3.

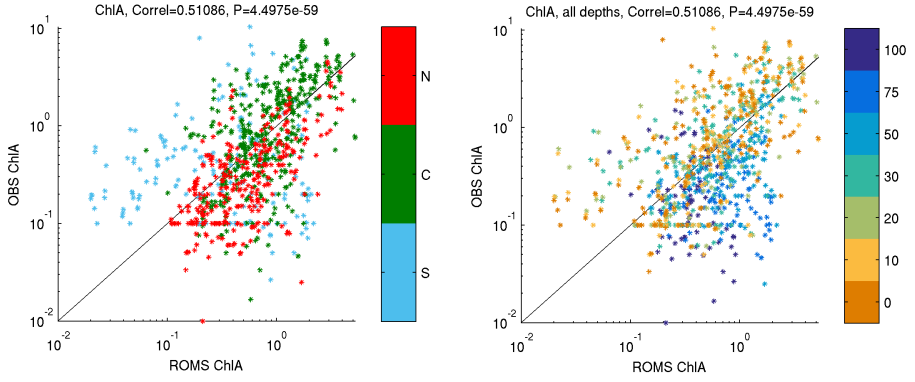

Figure B2. Evaluation of the modeled annual mean Chlorophyll (CHL) by subregion and by depth for the first 500km offshore as defined by the first two budget analysis boxes, see ~~*Figure 4*~~Figure 4. The spread of the dots is maximum for the southern subregion, in which modeled CHL is too low at small depths and too high at large depths. Observational dataset~~used for comparison~~: WOD09, annual mean ~~Chlorophyll~~CHL. A detailed dscription of the ~~data~~ used ~~for the evaluation~~ data is provided in Appendix A: Datasets, Table A3.

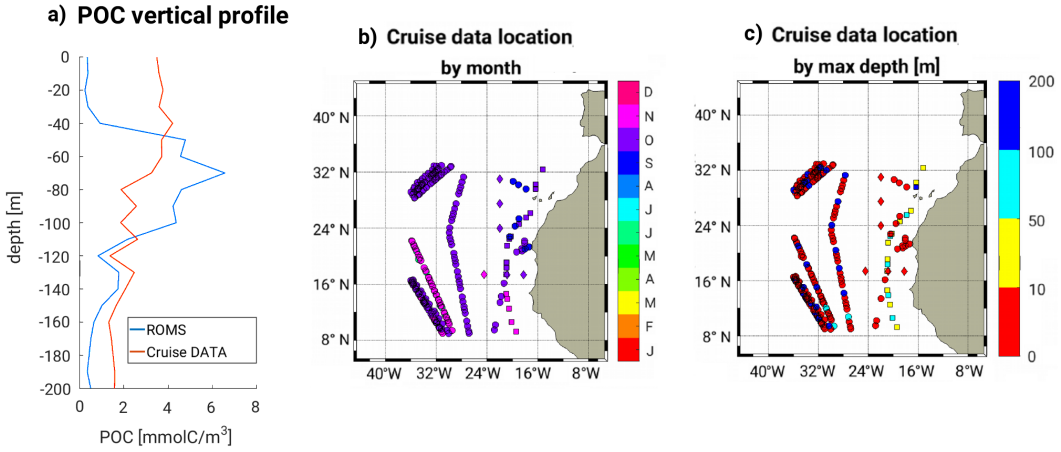

Figure B3. Panel a) Comparison of the modeled mean POC profile with the measured POC mean profile through co-location in space and time of modeled and cruise data POC. Data were re-binned in depth to 10m depth intervals. We used data contained in the first 2000 km from the coast as defined by the Budget Analysis boxes, see Figure 4. Panel b) Location of the cruise data colored by sampling month. Panel c) Location of the cruise data colored by max depth of the samples. A detailed description of the used data is provided in Appendix A: Datasets, Table A3.

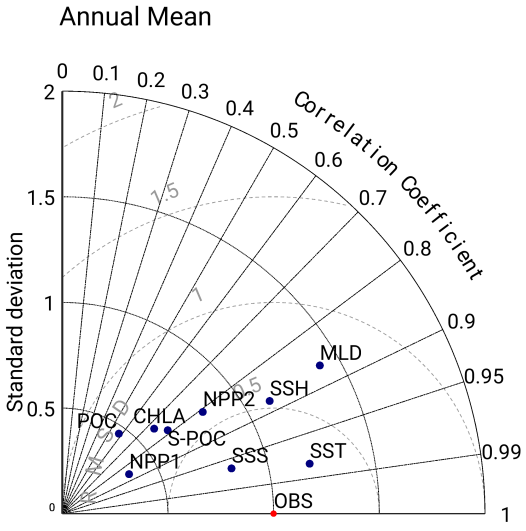

Figure B4. Taylor diagrams for the Canary EBUS region of analysis ([9.5N,32.5N]x[5W,35W]). ~~Subplot (a) Taylor diagram of the~~ climatological annual mean fields~~; Subplot (b) Mean of the four Taylor diagrams obtained for each season from climatological seasonal mean fields~~. Used datasets - Sea Surface Temperature (SST): AVHRR, Sea Surface Salinity (SSS): CARS, Sea Surface Height (SSH): Aviso CMDT Rio05, Mixed Layer Depth (MLD): Argo DT-0.2, Chlorophyll (CHLA): SeaWiFS, Net Primary Production dataset 1 (NPP1): SeaWiFS VGPM, Net Primary Production dataset 2 (NPP2): SeaWiFS CbPM, Surface Particulate Organic Carbon (S-POC): SeaWiFS POC, Particulate Organic Carbon (POC): cruise POC data (AMT, ANT, Geotraces). A detailed description of the data used for the evaluation is provided in Appendix A: Datasets, Table A3.

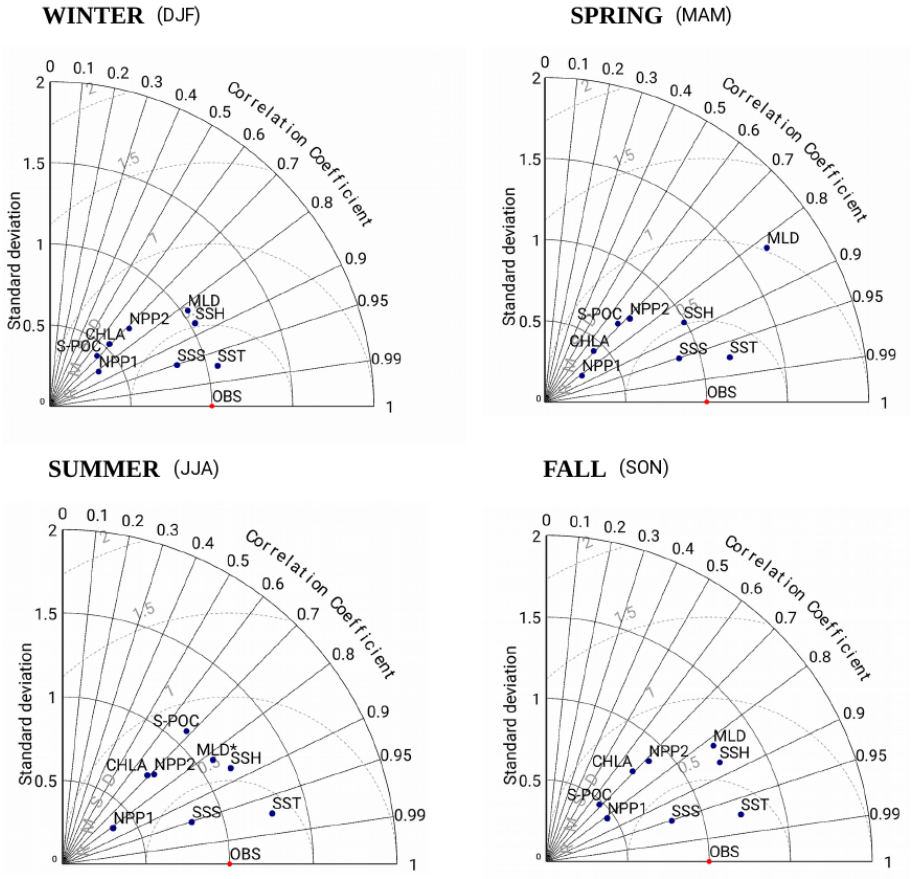

Figure B5. Taylor diagrams for the Canary EBUS region of analysis ([9.5N,32.5N]x[5W,35W]), climatological seasonal mean fields. In the Summer diagram MLD was rescaled to MLD*=MLD/2, the summer MLD_{STD} is therefore 2 times as big as the plotted value, while the correlation remains unchanged. Used datasets - Sea Surface Temperature (SST): AVHRR, Sea Surface Salinity (SSS): CARS, Sea Surface Height (SSH): Aviso CMDT Rio05, Mixed Layer Depth (MLD): Argo DT-0.2, Chlorophyll (CHLA): SeaWiFS, Net Primary Production dataset 1 (NPP1): SeaWiFS VGPM, Net Primary Production dataset 2 (NPP2): SeaWiFS CbPM, Surface Particulate Organic Carbon (S-POC): SeaWiFS POC. A detailed description of the data used for the evaluation is provided in Appendix A: Datasets, Table A3.

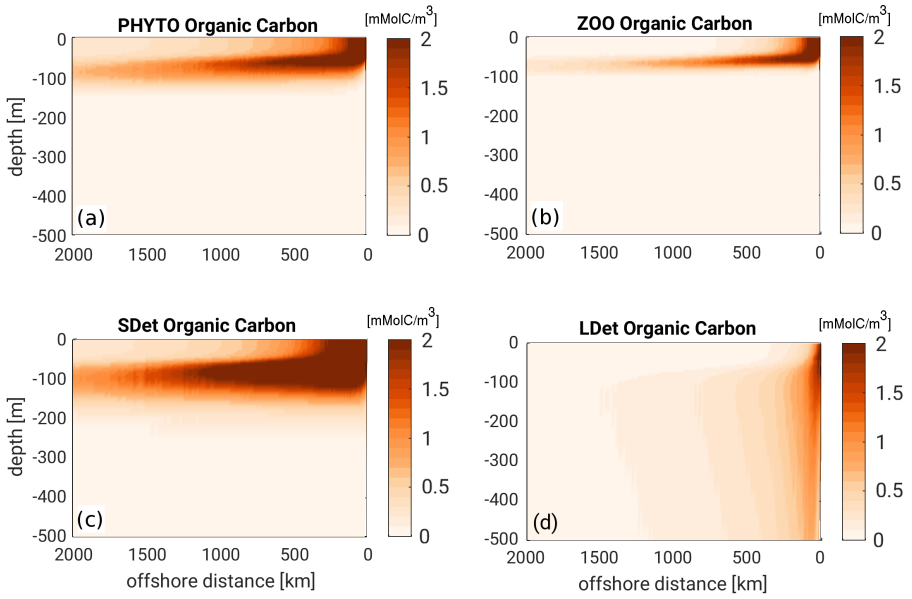

Figure B6. Mean vertical sections of the concentration of the modeled organic carbon (POC) components in the Canary EBUS, averaged meridionally along lines of equal distance from the coast between 9.5°N and 32°N. (a) Phytoplankton (PHYTO); (b) Zooplankton (ZOO); (c) Small detritus (SDet); (d) Large detritus (LDet).

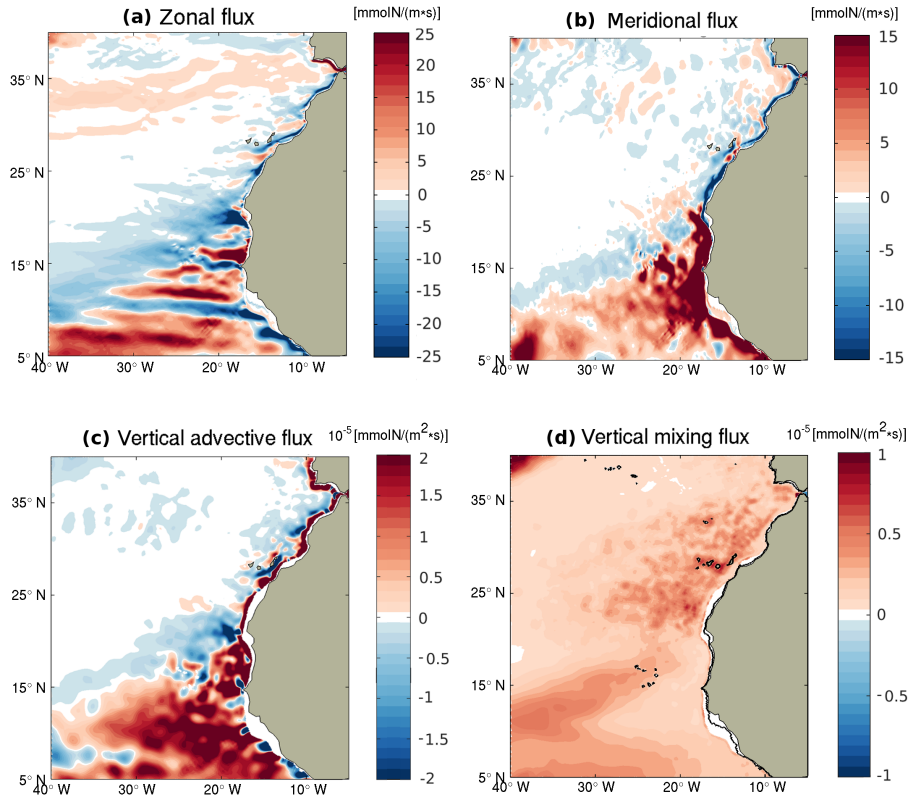

Figure B7. Maps of the inorganic nutrients (total inorganic nitrogen = nitrate + ammonia) flux components in the top 100 m corresponding to the euphotic layer in the CanUS. (a) Zonal flux vertically integrated over the top 100 m with positive values indicating eastward (onshore) transport; (b) as (a), but for the meridional flux with positive values indicating northward transport; (c) vertical advective flux across 100 m with positive values indicating upward transport; (d) as (c) but for vertical mixing. The plotted vertical component was smoothed with a 7x7 grid points 2-dimensional filter.

Author contributions. N.G., Z.L. and E.L. conceived the study. E.L. and M.M. set up the experiment and improved the model. E.L. performed the analysis. E.L. and N.G. wrote the manuscript. All authors contributed to the interpretation of the results and to the manuscript. N.G. and M.M. supervised this study.

"The authors declare that they have no conflict of interest."

Acknowledgements. We would like to thank Martin Frischknecht for his ~~valuable~~ relevant comments on the work and during the preparation of the manuscript, ~~and~~ Cara Nissen and Meike Vogt for their valuable feedback and Damian Loher for the technical support. We thank Referee nr.1 and Dr. Josep Pelegrí for their thoughtful review and their valuable comments that have helped us to improve this manuscript. We also thank the group of the Faculty of Marine Sciences at the University of Las Palmas de Gran Canaria in particular Javier Arístegui for allowing a fruitful exchange of ideas and information and Bàrbara Barceló for her kind support. A special thought goes to the late professor Pablo Sangrà whose generosity and dedication to science will always be a source of inspiration. This research was financially supported by the Swiss Federal Institute of Technology Zürich (ETH Zürich) and the Swiss National Science Foundation (Project CALNEX, grant No.149384). The simulations were performed at the HPC cluster of ETH Zürich, Euler, which is located in the Swiss Supercomputing Center (CSCS) in Lugano and operated by ETH ITS Scientific IT Services in Zürich. Model output is available upon request. Please contact the corresponding author, Elisa Lovecchio (elisa.lovecchio@usys.ethz.ch), in that matter.

References

Alonso-González, I. J., Arístegui, J., Vilas, J. C., and Hernández-Guerra, A.: Latral POC transport and consumption in surface and deep waters of the Canary Current region: a box model, Global Biogeohemical Cycles, 23, GB2007, doi:10.1029/2008GB0, 2009.

Alonso-González, I. J., Arístegui, J., Lee, C., Sanchez-Vidal, A., Calafat, A., Fabrés, J., Sangrà, P., Masquá, P., and Hernández-Guerra, A.: Role of slowly settling particles in the ocean carbon cycle, Geophysical Research Letters, 37, doi:10.1029/2010GL043827, 2010.

Álvarez-Salgado, X. A. and Arístegui, J.: Organic matter dynamics in the Canary Current, in: Oeanographic and biological features in the Canary Current Large Marine Ecosystem, edited by Váldes, L. and Déniz-González, I., chap. 4.3, pp. 115–383, IOC-UNESCO, - Technical Series 115, 2015.

Álvarez-Salgado, X. A., Arístegui, J., Barton, E. D., and Hansell, D. A.: Contribution of upwelling filaments to offshore carbon export in the subtropical Northeast Atlantic Ocean, Limnology and Oceanography, 52, 1287–1292, doi:10.4319/lo.2007.52.3.1287, 2007.

ANT: Particulate organic carbon (POC), Tech. rep., https://seabass.gsfc.nasa.gov/cruise/ant-xxiii-1, (2005), ANT-XXIII-1, SIO Stramsky, (Accessed on 2017 at: $https://seabass.gsfc.nasa.gov/$), 2005.

Arístegui, J., Duarte, C. M., Agustí, S., Doval, M., Álvarez-Salgado, X., and Hansell, D.: Dissolved Organic Carbon Support of Respiration in the Dark Ocean, Science,, 298, 1967, doi:10.1126/science.1076746, 2002.

Arístegui, J., Barton, E. D., Montero, M. F., nos, M. G.-M., and Escánez, J.: Organic carbon distribution and water column respiration in the NW African-Canaries Coastal Transition Zone, Aquatic Microbial Ecology, 33, 289–301, doi:10.3354/ame033289, 2003.

Arístegui, J., Barton, E. D., Álvarez-Salgado, X. A., Santos, M. P., Figueiras, F. G., Kifani, S., Hernández-León, S., Mason, E., Machú, E., and Demarq, H.: Sub-regional ecosystem variability in the Canary Current upwelling, Progress in Oceanography, 83, 33–48, doi:http://dx.doi.org/10.1016/j.pocean.2009.07.031, 2009.

Auger, P. A., Gorgues, T., Machu, E., Aumont, O., and Brehmer, P.: What drives the spatial variability of primary productivity and matter fluxes in the North-West African upwelling system? A modelling approach and box analysis, Biogeociences Discussion, 13, 6419–6440, doi:10.5194/bg-13-6419-2016, http://www.biogeosciences.net/13/6419/2016/, 2016.

Aumont, O., Maier-Reimer, E., Blain, S., and Monfray, P.: An ecosystem model of the global ocean including Fe, Si, P colimitations, Global Biogeochemical Cycles, 17, n/a–n/a, doi:10.1029/2001GB001745, http://dx.doi.org/10.1029/2001GB001745, 1060, 2003.

Barton, E. D., Arístegui, J., Tett, P., and Navarro-Pérez, E.: Variability in the Canary Islands area of filament-eddy exchanges, Progress in Oceanography, 62, 71–94, 2004.

Behrenfeld, M. J. and Falkowski, P. G.: Photosynthetic rates derived from satellite-based chlorophyll concentration, Limnology and Oceanography, 42, 1–20, doi:10.4319/lo.1997.42.1.0001, seaWiFS VGPM available at: http://orca.science.oregonstate.edu/1080.by.2160.monthly.hdf.vgpm.s.chl.a.sst.php, Modis-Aqua VGPM available at: http://orca.science.oregonstate.edu/1080.by.2160.monthly.hdf.vgpm.m.chl.m.sst.php, 1997.

Berelson, W. M.: Particle settling rates increase with depth in the ocean, Deep-Sea Research II: Topical Studies in Oceanography, 49, 237–251, doi:http://dx.doi.org/10.1016/S0967-0645(01)00102-3, 2002.

BODC-NERC, A.: Particulate organic carbon (POC) from Atlantic Meridional Transect (AMT), Tech. rep., Natural Environment Research Council, http://www.amt-uk.org/Home, (2004-2014), AMT 15-24, (Accessed on 2017 at: https://seabass.gsfc.nasa.gov/), 2014.

Brochier, T., Mason, E., Moyano, M., Berraho, A., Colas, F., Sangrà, P., Hernández-León, S., Ettahiri, O., and Lett, C.: Ichtyoplankton transport from the African coast to the Canary Islands, Journal of Marine Systems, 87, 109–122, 2014.

Brodeau, L., Barnier, B., Treguier, A.-M., Penduff, T., and Gulev, S.: An ERA40-based atmospheric forcing for global ocean circulation models, Ocean Modelling, 31, 88–104, doi:http://dx.doi.org/10.1016/j.ocemod.2009.10.005, 2010.

Carr, M.-E.: Estimation of potential productivity in the Eastern Boundary Currents using remote sensing, Deep-Sea Research II: Topical Studies in Oceanography, 49, 59–80, doi:http://dx.doi.org/10.1016/S0967-0645(01)00094-7, 2002.

Carr, M.-E. and Kearns, E. J.: Production regimes in four Eastern Boundary Current Systems, Deep-Sea Research II, 50, 3199–3221, doi:http://dx.doi.org/10.1016/j.dsr2.2003.07.015, 2003.

Carton, J. A. and Giese, B. S.: A Reanalysis of Ocean Climate Using Simple Ocean Data Assimilation (SODA), American Meteorological Society, Monthly Weather Review, 136, 2999–3017, doi:http://dx.doi.org/10.1175/2007MWR1978.1, 2008.

Chavez, F. P. and Messié, M.: A comparison of Eastern Boundary Upwelling Ecosystems, Progress in Oceanography, 83, 80–96, doi:http://dx.doi.org/10.1016/j.pocean.2009.07.032, 2009.

Dai, A., Qian, T., Trenberth, K. E., and Milliman, J. D.: Changes in continental freshwater discharge from 1948-2004, Journal of Climate, American Meteorological Society, 22, 2773–2791, doi:http://dx.doi.org/10.1175/2008JCLI2592.1, dataset: http://www.cgd.ucar.edu/cas/catalog/surface/dai-runoff/ (Accessed 25 May 2016), 2009.

Dee, D. P., Uppala, S. M., Simmons, A. J., P. Berrisford, P. P., Kobayashi, S., Andrae, U., Balmaseda, M. A., G. Balsamo, P. B., P. Bechtold, A. C. M. B., van de Berg, L., Bidlot, J., Bormann, N., Delsol, C., Dragani, R., Fuentes, M., Geer, A. J., Haimberger, L., Healy, S. B., Hersbach, H., Hólm, E. V., Isaksen, L., P. Kallberg, M. K., Matricardi, M., McNally, A. P., B. M. Monge-Sanz, J.-J. M., B.-K. Park, C. P., de Rosnay, P., Tavolato, C., n. Thépaut, J., and Vitart, F.: The ERA-Interim reanalysis: configuration and performance of the data assimilation system, Quarterly Journal of the Royal Meteorolgical Society, 137, 553–597, doi:http://onlinelibrary.wiley.com/doi/10.1002/qj.828/abstract, 2011.

Del Giorgio, P. A. and Duarte, C. M.: Respiration in the open ocean, Nature, 420, 379–384, doi:10.1038/nature01165, 2002.

Duarte, C. M. and Agustí, S.: The CO_2 Balance of Unproductive Aquatic Ecosystems, Science, 281, 234–236, doi:10.1126/science.281.5374.234, http://science.sciencemag.org/content/281/5374/234, 1998.

Duarte, C. M. and Cebrián, J.: The fate of marine autotrophic production, Limnology and Oceanography, 41, 1758–1766, doi:10.4319/lo.1996.41.8.1758, 1996.

Duarte, C. M., de Gioux, A. R., Arrieta, J. M., Delgado-Huertas, A., and Augustí, S.: The Oligotrophic Ocean is Heterotrophic, Annual Review of Marine Science, 5, 551–569, 2013.

Ducklow, H. W. and Doney, S. C.: What is the metabolic state of the oligotrophic ocean? A Debate, Annual Review of Marine Science, 5, 525–533, doi:10.1146/annurev-marine-121211-172331, 2013.

Ducklow, H. W., Steinberg, D. K., and Buesseler, K.: Upper ocean Carbon Export and the Biological Pump, Oceanography, 14, 50–58, doi:http://dx.doi.org/10.5670/oceanog.2001.06, 2001.

Dussin, R., Barnier, B., Brodeau, L., and Molines, J. M.: The Making Of the Drakkar Forcing Set DFS5, Tech. rep., LGGE, Grenoble, France, https://www.drakkar-ocean.eu/publications/reports/report_DFS5v3_April2016.pdf, (Accessed 25 May 2016), 2016.

Falkowski, P. G., Biscaye, P. E., and Sancetta, C.: The lateral flux of biogenic particles from the eastern North American continental margin to the North Atlantic Ocean, Deep-Sea Research II: Topical Studies in Oceanography, 41, 583–601, doi:http://dx.doi.org/10.1016/0967-0645(94)90036-, http://www.sciencedirect.com/science/article/pii/0967064594900361, 1994.

Fischer, G., Reuter, C., Karakas, G., Nowald, N., and Wefer, G.: Offshore advection of particles within the Cape Blanc filament, Mauritania: Results from observational and modelling studies, Progress in Oceanography, 83, 322–330, doi:http://dx.doi.org/10.1016/j.pocean.2009.07.023, 2009.

Fischer, J. and Karakaş, G.: Sinking rates and ballast composition of particles in the Atlantic Ocean: implications for the organic carbon fluxes to the deep ocean, Biogeosciences, 6, 85–102, doi:10.5194/bg-6-85-2009, 2009.

Fowler, C.: Polar Pathfinder Daily 25 km EASE-Grid Sea Ice Motion Vectors (1979-2006), Tech. rep., Boulder, Colorado USA: National Snow and Ice Data Center, http://nsidc.org/data/docs/daac/nsidc0116_icemotion.gd.html, updated 2008 (link accessed Mar 2012), 2003.

Gabric, A. J., Garcia, L., Van Camp, L., Nykjaer, L., Eifler, W., and Schrimpf, W.: Offshore export of shelf production in the Cape Blanc (Mauritania) giant filament as derived from coastal zone color scanner imagery, Journal of Geophysical Research, 98, 4697–4712, doi:10.1029/92JC01714, 1993.

Galbraith, E. D., Gnanadesikan, A., Dunne, J. P., and Hiscock, M. R.: Regional impacts of iron-light colimitation in a global biogeochemical model, Biogeosciences, 7, 1043–1064, doi:10.5194/bg-7-1043-2010, http://www.biogeosciences.net/7/1043/2010/, 2010.

García-Muñoz, M., Arístegui, J., Pelegrí, J. L., Antoranz, A., Ojeda, A., and Torres, M.: Exchange of carbon by an upwelling filament off Cape Ghir (NW Africa), Journal of Marine System, 54, 83–95, doi:http://dx.doi.org/10.1016/j.jmarsys.2004.07.005, 2005.

GEOTRACES: Particulate organic carbon (POC), Tech. rep., http://www.bodc.ac.uk/geotraces/, (2010), RV Knorr KN199-4, (Accessed on 2017 at: https://seabass.gsfc.nasa.gov/), 2010.

GLOBALVIEW-CO_2: Cooperative Atmospheric Data Integration Project – Carbon Dioxide, Tech. rep., NOAA ESRL, Boulder Colorado, https://www.esrl.noaa.gov/gmd/ccgg/globalview/co2/co2_download.html, 2011.

Gruber, N., Frenzel, H., Doney, S. C., Marchesiello, P., McWilliams, J. C., Oram, J. R., Plattner, G. K., and Stolzenbach, K. D.: Eddy-resolving simulation of plankton ecosystem dynamics in the California Current System, Deep Sea Research I: Oceanographic Research Papers, 53, 1483–1516, doi:http://dx.doi.org/10.1016/j.dsr.2006.06.005, 2006.

Gruber, N., Lachkar, Z., Frenzel, H., Marchesiello, P., Münnich, M., McWilliams, J. C., Nagai, T., and Plattner, G.-K.: Eddy-induced reduction of biological production in eastern boundary upwelling systems, Nature Geoscience, 4, 787–792, doi:10.1038/ngeo1273, 2011.

Hansell, D. A.: DOC in the Global Ocean Carbon Cycle, vol. Chap.15, Academic Press - Elsevier, biogeochemistry of marine dissolved organic matter edn., pp.685-714, cp1-cp4, 2002.

Hansell, D. A. and Carlson, C. A.: Biogeochemistry of Marine Dissolved Organic Matter (Second Edition), Academic Press, second edition edn., 2015.

Hansell, D. A., Carlson, C. A., Repeta, D., and Schlitzer, R.: Dissolved Organic Matter in the Ocean: a controversy stimulates new insights, Oceanography, 22, 202 – 211, doi:10.5670/oceanog.2009.109, https://darchive.mblwhoilibrary.org/bitstream/handle/1912/3183/22-4_hansell.pdf?sequence=1, 2009.

Haumann, F. A., Gruber, N., Münnich, M., Frenger, I., and Kern, S.: Sea-ice transport driving Southern Ocean salinity and its recent trends, Nature, 537, 89–92, doi:10.1038/nature19101, 2016.

Hauri, C., Gruber, N., Vogt, M., Doney, S. C., Feely, R. A., Lachkar, Z., Leinweber, A., McDonnell, A. M. P., Munnich, M., and Plattner, G.-K.: Spatiotemporal variability and long-term trends of ocean acidification in the California Current System, Biogeosciences, 10, 193–216, doi:10.5194/bg-10-193-2013, http://www.biogeosciences.net/10/193/2013/, 2013.

Helmke, P., Romero, O., and Fischer, G.: Northwest African upwelling and its effect on offshore organic carbon export to the deep sea, Global Biogeochemical Cycles, 19, GB4015, doi:10.1029/2004GB002265, 2005.

Hopkinson, S. and Vallino, J. J.: Efficient export of carbon to the deep ocean through dissolved organic matter, Nature, 433, 142–145, doi:10.1038/nature03191, 2005.

Hwang, J., Druffel, E. R. M., and Komada, T.: Transport of organic carbon from the California coast to the slope region: A study of Δ^{14}C and Δ^{13} C signatures of organic compound classes, Global Biogeochem. Cycles, 19, doi:10.1029/2004GB002347, 2008.

Inthorn, M., Mohrholz, V., and Zabel, M.: Nepheloid layer distribution in the Benguela upwelling area offshore Namibia, Deep Sea Research I: Oceanographic Research Papers, 53, 1423–1438, doi:http://dx.doi.org/10.1016/j.dsr.2006.06.004, 2006a.

Inthorn, M., Wagner, T., Scheeder, G., and Zabel, M.: Lateral transport controls distribution, quality and burial of organic matter along ocontinental slopes in high-productivity areas, Geology, 34, 205–208, doi:10.1130/G22153.1, 2006b.

Johnson, D. R., Boyer, T. P., Garcia, H. E., Locarnini, R. A., Baranova, O. K., and Zweng, M. M.: World Ocean Database 2009 Documentation, Tech. rep., Edited by Sydney Levitus, NODC Internal Report 20, NOAA Printing Office, Silver Spring, MD, 175 pp., http://www.nodc.noaa.gov/OC5/WOD09/pr_wod09.html, 2009.

Key, R. M., Kozyr, A., Sabine, C. L., Lee, K., Wanninkhof, R., Bullister, J., Feely, R. A., Millero, F., Mordy, C., and Peng, T.-H.: A global ocean carbon climatology: Results from GLODAP, Global Biogeochemical Cycles, 18, GB4031, doi:10.1029/2004GB002247, 2004.

Lachkar, Z. and Gruber, N.: What controls biological production in coastal upwelling systems? Insights from a comparative modeling study, Biogeosciences, 8, 2961–2976, doi:10.5194/bg-8-2961-2011, 2011.

Lachkar, Z. and Gruber, N.: Response of biological production and air–sea CO_2 fluxes to upwelling intensification in the California and Canary Current Systems, Journal of Marine Systems, 109–110, 149 – 160, doi:http://dx.doi.org/10.1016/j.jmarsys.2012.04.003, http://www.sciencedirect.com/science/article/pii/S092479631200108X, large-scale regional comparisons of marine biogeochemistry and ecosystem processes - research approaches and results, 2013.

Landschützer, P., Gruber, N., Bakker, D. C. E., and Schuster, U.: An observation-based global monthly gridded sea surface pCO2 product from 1998 through 2011 and its monthly climatology, Tech. rep., Carbon Dioxide Information Analysis Center, Oak Ridge National Laboratory, US Department of Energy, Oak Ridge, Tennessee, doi:10.3334/CDIAC/OTG.SPCO2_1998_2011_ETH_SOM-FFN, http://cdiac.ornl.gov/ftp/oceans/spco2_1998_2011_ETH_SOM-FFN, 2014.

Large, W. G., McWilliams, J. C., and Doney, S. C.: Oceanic vertical mixing: A review and a model with a nonlocal boundary layer parameterization, Rev. Geophys., 32, 363–403, doi:10.1029/94RG01872, 1994.

Liu, K. K., Atkinson, L., nones, R. A. Q., and Talaue-McManus, L.: Carbon and Nutrient Fluxes in Continental Margins. A Global Synthesis, Global Change - The IGBP Series, Springer-Verlag Berlin Heidelberg, 2010.

Locarnini, R. A., Mishonov, A. V., Antonov, J. I., Boyer, T. P., Garcia, H. E., Baranova, O. K., Zweng, M. M., Paver, C. R., Reagan, J. R., Johnson, D. R., Hamilton, M., and Seidov, D.: World Ocean Atlas 2013, Volume 1: Temperature, Tech. rep., S. Levitus, Ed., A. Mishonov Technical Ed.; NOAA Atlas NESDIS 73, 40 pp, http://data.nodc.noaa.gov/woa/WOA13/DOC/woa13_vol1.pdf, 2013.

Lumpkin, R. and Johnson, G. C.: Global Ocean Surface Velocities from Drifters: Mean, Variance, ENSO Response, and Seasonal Cycle, Journal of Geophysical Research: Oceans, 118, 2992–3006, doi:10.1002/jgrc.20210, 2013.

Mackas, D. L., Strub, P. T., Thomas, A., and Montecino, V.: Eastern Ocean Boundaries: Pan-Regional Overview, book: "The Sea, The Global Coastal Ocean", 14, 2006.

Mason, E., Colas, F., Molemaker, J., Shchepetkin, A. F., Troupin, C., McWilliams, J. C., and Sangrà, P.: Seasonal variability of the Canary Current: A numerical study, Journal of Geophysical Research: Oceans, 116, doi:10.1029/2010JC006665, 2011.

Montégut, C. D. B., Madec, G., Fischer, A. S., Lazar, A., and Iudicone, D.: Mixed layer depth over the global ocean: An examination of profile data and a profile-based climatology, J. Geophys. Res, 109, C12 003, doi:10.1029/2004JC002378, 2004.

Moore, J. K., Doney, S. C., and Lindsay, K.: Upper ocean ecosystem dynamics and iron cycling in a global three-dimensional model, Global Biogeochemical Cycles, 18, doi:10.1029/2004GB002220, http://dx.doi.org/10.1029/2004GB002220, gB4028, 2004.

Nagai, T., Gruber, N., Frenzel, H., Lachkar, Z., McWilliams, J. C., and Plattner, G.-K.: Dominant role of eddies and filaments in the offshore transport of carbon and nutrients in the California Current System, Journal of Geophysical Research, 120, doi:10.1002/2015JC010889, 2015.

NASA-OB.DAAC: SeaWiFS Level-3 Mapped Particulate Organic Carbon Data Version 2014, S19972442010273.3m_mc_chl_chlor_a_9km.nc, NASA Goddard Space Flight Center, Ocean Ecology Laboratory, Ocean Biology Processing Group, http://oceandata.sci.gsfc.nasa.gov, (1997-2010), doi:10.5067/ORBVIEW-2/SEAWIFS/L3M/POC/2014 (Accessed on 2017), 2010.

NASA-OBPG: SeaWiFS Data Level-3 Standard Mapped Image, S19972442010273.3m_mc_chl_chlor_a_9km.nc, NASA Goddard Space Flight Center, Ocean Ecology Laboratory, Ocean Biology Processing Group, http://oceandata.sci.gsfc.nasa.gov(Accessedon2015), (1997-2010), 2010.

Ohde, T., Fiedler, B., and Körtzinger, A.: Spatio-temporal distribution and transport of particulate matter in the eastern tropical North Atlantic observed by Argo floats, Deep-Sea Research I, 102, 26–42, doi:http://dx.doi.org/10.1016/j.dsr.2015.04.007, 2015.

Pastor, M. V., Palter, J. B., Pelegrí, J. L., and Dunne, J. P.: Physical drivers of interannual chlorophyll variability in the eastern subtropical North Atlantic, Journal of Geophysical Research: Oceans, 118, 3871–3886, doi:10.1002/jgrc.20254, http://dx.doi.org/10.1002/jgrc.20254, 2013.

Pelegrí, J., Marrero-Díaz, A., and Ratsimandresey, A.: Nutrient irrigation of the North Atlantic, Progress in Oceanography, 70, 366 – 406, doi:https://doi.org/10.1016/j.pocean.2006.03.018, http://www.sciencedirect.com/science/article/pii/S0079661106000504, 2006.

Pelegrí, J. L. and Benazzouz, A.: Coastal Upwelling off Northwest Africa, in: Oeanographic and biological features in the Canary Current Large Marine Ecosystem, edited by Váldes, L. and Déniz-González, I., chap. 3.4, pp. 115–383, IOC-UNESCO, - Technical Series 115, 2015.

Pelegrí, J. L. and Peña-Izquierdo, J.: Eastern Boudary Currents off Northwest Africa, in: Oeanographic and biological features in the Canary Current Large Marine Ecosystem, edited by Váldes, L. and Déniz-González, I., chap. 3.3, pp. 115–383, IOC-UNESCO, - Technical Series 115, 2015.

Pelegrí, J. L., Arístegui, J., Cana, L., González-Dávila, M., Hernández-Guerra, A., Hernández-León, S., Montero, M. F., Sangrà, P., and Santana-Casiano, M.: Coupling between the open ocean and the coastal upwelling region off northwest Africa: water recirculation and offshore pumping of organic matter, Journal of Marine Systems, 54, 3–37, doi:http://dx.doi.org/10.1016/j.jmarsys.2004.07.003, 2005.

Peliz, A., Santos, A. M. P., Oliveira, P. B., and Dubert, J.: Extreme cross-shelf transport induced by eddy interactions southwest of Iberia in winter 2001, Geophysical Research Letters, 31, L08 301, doi:10.1029/2004GL019618, 2004.

Plattner, G.-K., Gruber, N., Frenzel, H., and McWilliams, J. C.: Decoupling marine export production from new production, Geophysical Research Letters, 32, doi:10.1029/2005GL022660, http://dx.doi.org/10.1029/2005GL022660, l11612, 2005.

Reynolds, R. W., Smith, T. M., Liu, C., Chelton, D. B., Casey, K. S., and Schlax, M. G.: Daily High-Resolution-Blended analyses for sea surface temperature, J. Climate, 20, 5473–5496, doi:http://dx.doi.org/10.1175/2007JCLI1824.1, 2007.

Ridgway, K. R., Dunn, J. R., and Wilkin, J. L.: Ocean interpolation by four-dimensional least squares: Application to the waters around Australia, J. Atmos. Ocean, 19, 1357–1375, doi:http://dx.doi.org/10.1175/1520-0426(2002)019<1357:OIBFDW>2.0.CO;2, 2002.

Rio, M.-H. and Hernandez, F.: A mean dynamic topography computed over the world ocean from altimetry, in situ measurements, and a geoid model, J. Geophys. Res, 109, C12 032, doi:10.1029/2003JC002226, 2004.

Roussenov, V., Williams, R. G., Mahaffey, C., and Wolff, G. A.: Does the transport of dissolved organic nutrients affect export production in the Atlantic Ocean?, Global Biogeochemical Cycles, 20, doi:10.1029/2005GB002510, http://dx.doi.org/10.1029/2005GB002510, gB3002, 2006.

Sangrà, P., Pascual, A., Rodríguez-Santana, Á., F.Machín, Mason, E., McWilliams, J. C., Pelegrí, J. L., Dong, C., Rubio, A., Arístegui, J., Marrero-Díaz, Á., Hernández-Guerra, A., Martínez-Marrero, A., and Auladell, M.: The Canary Eddy Corridor: A major pathway for long-lived eddies in the subtropical North Atlantic, Deep Sea Research I: Oceanographic Research Papers, 56, 2100–2114, doi:http://dx.doi.org/10.1016/j.dsr.2009.08.008, 2009.

Santana-Falcón, Y., Benavides, M., Sangrà, P., Mason, E., Barton, E. D., Orbi, A., and Arístegui, J.: Coastal-offshore exchange of organic matter across the Cape Ghir filament (NW Africa) during moderate upwelling, Journal of Marine Systems, 154, 233–242, doi:http://dx.doi.org/10.1016/j.jmarsys.2015.10.008, 2016.

Sarmiento, J. L. and Gruber, N.: Ocean Biogeochemical Dynamics, Princeton University Press, iSBN: 9781400849079, 2006.

Shchepetkin, A. F. and McWilliams, J. C.: The regional oceanic modeling system (ROMS): a split-explicit, topographic-following-coordinate oceanic model, Ocean Modeling, 9, 347–404, doi:http://dx.doi.org/10.1016/j.ocemod.2004.08.002, 2005.

Shigemitsu, M., Okunishi, T., Nishioka, J., Sumata, H., Hashioka, T., Aita, M. N., Smith, S. L., Yoshie, N., Okada, N., and Yamanaka, Y.: Development of a one-dimensional ecosystem model including the iron cycle applied to the Oyashio region, western subarctic Pacific, Journal of Geophysical Research: Oceans, 117, doi:10.1029/2011JC007689, http://dx.doi.org/10.1029/2011JC007689, c06021, 2012.

Steele, M., Mellor, G. L., and Mcphee, M. G.: Role of the Molecular Sublayer in the Melting or Freezing of Sea Ice, Journal of Physical Oceanography, 19, 139–147, doi:10.1175/1520-0485(1989)019<0139:ROTMSI>2.0.CO;2, http://dx.doi.org/10.1175/1520-0485(1989)019<0139:ROTMSI>2.0.CO;2, 1989.

Torres-Valdés, S., Roussenov, V. M., Sanders, R., Reynolds, S., Pan, X., Mather, R., Landolfi, A., Wolff, G. A., Achterberg, E. P., and Williams, R. G.: Distribution of dissolved organic nutrients and their effect on export production over the Atlantic Ocean, Global Biogeochemical Cycles, 23, doi:10.1029/2008GB003389, http://dx.doi.org/10.1029/2008GB003389, 2009.

Turi, G., Lachkar, Z., and Gruber, N.: Spatiotemporal variability and drivers of pCO_2 and air–sea CO_2 fluxes in the California Current System: an eddy-resolving modeling study, Biogeosciences, 11, 671–690, doi:10.5194/bg-11-671-2014, http://www.biogeosciences.net/11/671/2014/, 2014.

Váldes, L. and Déniz-González, I.: Introduction, in: Oeanographic and biological features in the Canary Current Large Marine Ecosystem, edited by Váldes, L. and Déniz-González, I., chap. 1, pp. 115–383, IOC-UNESCO, - Technical Series 115, 2015.

Walsh, J. J.: Importance of continental margins in the marine biogeochemical cycling of carbon and nitrogen, Nature, 350, 53–55, doi:10.1038/350053a0, 1991.

Westberry, T., Behrenfeld, M. J., Siegel, D. A., and Boss, E.: Carbon-based primary productivity modeling with vertically resolved photoacclimation, Global Biogeochemical Cycles, 22, GB2024, doi:10.1029/2007GB003078, seaWiFS VGPM available at: http://orca.science.oregonstate.edu/1080.by.2160.monthly.hdf.cbpm2.s.php, 2008.

Williams, P. J. L. B., Quay, P. D., Westberry, T. K., and Behrenfeld, M. J.: The Oligotrophic Ocean Is Autotrophic, Annual Review of Marine Science, 5, 535–549, doi:10.1146/annurev-marine-121211-172335, 2013.

Zweng, M., Reagan, J. R., Antonov, J. I., Locarnini, R. A., Mishonov, A. V., Boyer, T. P., Garcia, H. E., Baranova, O. K., Johnson, D. R., and D. Seidov, M. M. B.: World Ocean Atlas 2013, Volume 2: Salinity, Tech. rep., S. Levitus, Ed., A. Mishonov Technical Ed.; NOAA Atlas NESDIS 74, 39 pp, http://data.nodc.noaa.gov/woa/WOA13/DOC/woa13_vol2.pdf, 2013.